2007-07-13

Characterization of a Novel Nuclear Variant of Bmp2 and Coordinate Regulation of Col11a2 and Col27a1 by the Transcription Factor Lc-Maf

Jaime Lynn Mayo
Brigham Young University - Provo

CHARACTERIZATION OF A NOVEL NUCLEAR VARIANT OF BMP2

AND

COORDINATE REGULATION OF *COL11A2* AND *COL27A1* BY THE TRANSCRIPTION FACTOR LC-MAF

by

Jaime L. Mayo

A dissertation submitted to the faculty of

Brigham Young University

in partial fulfillment of the requirements for the degree of

Doctor of Philosophy

Department of Microbiology and Molecular Biology

Brigham Young University

August 2007

BRIGHAM YOUNG UNIVERSITY

GRADUATE COMMITTEE APPROVAL

of a dissertation submitted by

Jaime L. Mayo

This dissertation has been read by each member of the following graduate committee and by majority vote has been found to be satisfactory.

Date	Laura C. Bridgewater, Chair
Date	Jeffery R. Barrow
Date	Michael R. Stark
Date	Brent L. Nielsen
Date	R. Paul Evans

BRIGHAM YOUNG UNIVERSITY

As chair of the candidate's graduate committee, I have read the dissertation of Jaime L. Mayo in its final form and have found that (1) the format, citations and bibliographical style are consistent and acceptable and fulfill university and department style requirements; (2) the illustrative materials including figures, tables, and charts are in place; and (3) the final manuscript is satisfactory to the graduate committee, and the dissertation is ready for submission to the university library.

Date	Laura C. Bridgewater Chair, Graduate Committee

Accepted for the Department

Date	Laura C. Bridgewater Chair, Department of Microbiology and Molecular Biology Graduate Committee

Accepted for the College

Date	Rodney J. Brown Dean, College of Life Science

ABSTRACT

CHARACTERIZATION OF A NOVEL NUCLEAR VARIANT OF BMP2

Jaime L. Mayo

Department of Microbiology and Molecular Biology

Doctor of Philosophy

Bone morphogenetic protein 2 (Bmp2) is a signaling protein that was first detected by its ability to induce cartilage and bone formation. It has since been implicated in broad variety of developmental, patterning, and disease processes. To date, Bmp2 has only been known to function as an extracellular signaling molecule. However, we have obtained clear evidence for a nuclear form of Bmp2. This nuclear variant, nBmp2, contains a bipartite NLS that overlaps the site of proteolytic cleavage. The NLS remains intact and functional when translation of Bmp2 initiates from a downstream alternative start codon. The resulting protein lacks the signal peptide and is therefore translated in the cytoplasm rather than the endoplasmic reticulum, thus avoiding proteolytic processing and secretion. Instead, the uncleaved protein containing the intact NLS is translocated to the nucleus. Preliminary functional analyses in zebrafish indicate that nBmp2 is critical for proper heart development. To determine if this function is conserved in mammals, we have also generated mice harboring a null allele for nBmp2.

ABSTRACT

COORDINATE REGULATION OF *COL11A2* AND *COL27A1* BY THE TRANSCRIPTION FACTOR LC-MAF

Jaime L. Mayo

Department of Microbiology and Molecular Biology

Doctor of Philosophy

During skeletal development, long bones of the body develop from a cartilage template that is progressively replaced by bone. This process of endochondral ossification requires precisely coordinated expression of extracellular matrix proteins such as the cartilage-specific collagens. In this study, enhancer/reporter assays demonstrated that the transcription factor Lc-Maf inhibits the transcriptional activity of a cartilage-specific *Col11a2* enhancer element while a cartilage-specific *COL27A1* enhancer element was strongly activated by Lc-Maf. Site-directed mutagenesis identified the binding region within the *COL27A1* enhancer, and it was found to be unlike any known consensus Maf family binding site. The *in vivo* significance of these results was examined using immunohistochemistry and *in situ* hybridization in mouse limbs undergoing endochondral ossification. Taken together, these results suggest that Lc-Maf participates in the developmental transition from proliferating to hypertrophic chondrocytes during endochondral ossification by coordinately downregulating *Col11a2* and upregulating *Col27a1* collagen gene expression.

ACKNOWLEDGEMENTS

I am grateful for many different people who have been with me on the path to this point; there are too many to name them all individually. Of course, none of this would have been possible without Laura Bridgewater. I would like to thank her for her support, confidence in me, and fearlessness in starting new projects. I also greatly appreciate Jeff Barrow and the major role he played in developing the nBmp2-ko chimeras. Mike Stark, Brent Nielsen, and Paul Evans offered invaluable practical guidance, creative ideas, and moral support. I had many wonderful co-workers along the way, and I thank them for their friendship. Jenny Felin deserves special recognition for her role in the nBmp2 project. I love my husband, Tyler, and am grateful for his wonderful perspective on life, his unyielding faith in me, and his abiding patience.

TABLE OF CONTENTS

LIST OF TABLES

Book I: Characterization of a novel nuclear variant of Bmp2

LIST OF FIGURES

Book I: Characterization of a novel nuclear variant of Bmp2

Book II: Coordinate regulation of *Col11a2* and *Col27a1* by the transcription factor Lc-Maf

BOOK I

CHARACTERIZATION OF A NOVEL NUCLEAR VARIANT OF BMP2

INTRODUCTION

Bmp2

Bone morphogenetic protein 2 (Bmp2) is a member of the transforming growth factor beta (TGFβ) superfamily of secreted signaling molecules. With over 20 members, the BMP subfamily constitutes the largest subfamily in the TGFβ superfamily (Mishina, 2003). BMPs were first detected in the 1960s for their ability to induce ectopic cartilage and bone formation when implanted into rodents (Urist, 1965). Since that time, Bmp2 has been implicated in broad variety of highly conserved cellular and developmental processes. In *Drosophilia*, the Bmp2 homologue Decapentaplegic (Dpp) participates in wing imaginal disc development and axis formation (Raftery and Sutherland, 1999). Similarly, in vertebrates Bmp2 has been shown to play important roles in limb development and specification of left identity during left-right axis formation (Hogan, 1996; Schlange et al., 2002). In addition to these roles, Bmp2 also plays a role in proliferation of spermatogonia (Puglisi et al., 2004). Blockage of Bmp2 signaling in the cranial neural crest prevents cell migration, and mice homozygous for a null Bmp2 allele have lethal defects in the amnion/chorion and heart (Kanzler et al., 2000; Zhang and Bradley, 1996). Bmp2 is known to be expressed in the developing forebrain, gut, pituitary, limb bud, tooth buds, kidney, notochord, axial skeleton, skull sutures, interdigital mesenchyme, and in hair follicles (Drossopoulou et al., 2000; Dudley and Robertson, 1997; Furuta et al., 1997; Kim et al., 1992; Kim et al., 1998; Lyons et al., 1995; Lyons et al., 1990; St-Jacques et al., 1998; Wozney, 1992).

Not surprisingly given its multifunctionality, Bmp2 has also been shown to play a complex role in a variety of cancers. It was shown to stimulate angiogenesis in

developing tumors in mice and to be overexpresssed in a majority of lung carcinomas (Langenfeld et al., 2005; Langenfeld et al., 2003; Langenfeld and Langenfeld, 2004; Raida et al., 2005; Usami et al., 2005). In contrast to these findings, Bmp2 induces apoptosis in human myeloma cells and has also been shown to decrease the proliferation of human prostate cancer cells, gastric cancer cells, and breast cancer cells (Arnold et al., 1999; Kawamura et al., 2000; Tomari et al., 2005; Wen et al., 2004). Also, its loss is associated with increased progression of prostate cancer to a more aggressive phenotype (Horvath et al., 2004).

It was determined in the 1960s that extracts from demineralized bone could induce new bone formation when implanted into ectopic sites in rodents. The proteins responsible for this bone-inducting effect remained unknown until the purification and sequencing of bovine bmp3 (osteogenin) and cloning of human BMP2, 3, and 4 in the late 1980s (Luyten et al., 1989; Wozney et al., 1988). Since that time, much has been revealed about the structure and function of Bmp2. The gene encoding murine Bmp2 spans approximately 11 kb and contains three exons including the noncoding exon 1 and coding exons 2 and 3. Like other TGFβ superfamily ligands, Bmp2 is synthesized as a large preproprotein precursor that consists of a signal peptide that directs translation to the rough endoplasmic reticulum (rER) and consequently the secretory pathway, a propeptide, and a C-terminal mature peptide (Wang et al., 1990). In the *trans*-Golgi apparatus, Bmp2 is cleaved after the proprotein convertase recognition sequence R-E-K-R-$^{\downarrow}$ which is a consensus sequence for a number of proprotein convertases located within secretory pathway compartments (Constam and Robertson, 1999). This cleavage releases the C-terminal mature peptide from the propeptide. The C-terminal peptide then

homodimerizes through disulfide bonds to form the mature secreted growth factor before being secreted from the cell (Chen et al., 2004; Wozney, 1989).

At least two distinct pathways mediate Bmp signaling: the canonical Smad pathway and a mitogen-activated protein kinase (MAPK) pathway. Bmp2, like other members of the TGFβ family, binds to and induces apposition of type I and type II serine/threonine kinase receptors. This causes the type II receptor to phosphorylate serine/threonine residues in the type I receptors. Activated type I receptors phosphorylate, and thereby activate, Smad proteins 1, 5, and 8. These Smads subsequently recruit and bind Smad4 to form heteromeric complexes, which are then translocated to the nucleus and bind DNA directly or interact with DNA binding proteins to regulate the transcription of target genes (Chen et al., 2004; Moustakas and Heldin, 2002). Bmp2 has also been shown to signal through non-Smad pathways involving the activation of JNK and p38 MAPK (Gallea et al., 2001; Guicheux et al., 2003; Lemonnier et al., 2004).

Nuclear proteins

Bmp2 has previously been recognized only as a secreted growth factor. However, we have identified a variant form of Bmp2 that is translated from a downstream alternative start codon and subsequently localized to the nucleus. Although Bmp2 has not previously been found in the nucleus, nuclear forms of several other signaling molecules have been identified. For example, parathyroid hormone-related peptide (PTHrP) is a secreted protein which has an alternate nuclear form. Much like Bmp2, the nuclear form of PTHrP is translated from a downstream alternative start site, enabling it to bypass translation in the ER and eventual secretion (Nguyen et al., 2001). Basic fibroblast growth factor (bFGF) and fibroblast growth factor 3 (FGF3) also have both secreted and

nuclear forms (Amalric et al., 1991; Antoine et al., 1997; Bugler et al., 1991; Kiefer et al., 1994). The nuclear forms of bFGF and FGF3 result when translation occurs upstream of the conventional start codons, resulting in the inclusion of amino acid sequences that direct the finished peptides to the nucleus.

Most nuclear proteins contain nuclear-localizing amino acid sequences called nuclear localization sequences (NLSs) that target the protein to the nucleus. The first of such signal sequences identified was in the simian virus 40 (SV40) large-T antigen (Kalderon et al., 1984a; Kalderon et al., 1984b). That sequence, PKKKRK, and the sequence found in nucleoplasmin, **KR**PAATKKAGQA**KKKK**LD (with basic amino acids key to nuclear localization underlined and in bold), are the prototypes for the monopartite and bipartite nuclear localization signals (NLSs). It is now known that these signals function by binding to a large variety of soluble transport factors called karyopherins that are able to shuttle NLS-containing proteins into the nucleus (Corbett and Silver, 1997).

The machinery responsible for active transport of proteins into the nucleus of cells consists of the nuclear pore complex (NPC) and a subgroup of karyopherins called importins that not only interact with the various NLSs of nuclear proteins but also with the proteins of the NPC (Fried and Kutay, 2003; Macara, 2001; Pemberton and Paschal, 2005). The most common transport system is the importin α/importin β-dependent pathway for nuclear import (Fried and Kutay, 2003; Macara, 2001; Pemberton and Paschal, 2005). In this system, importin α serves as an adapter between the nuclear protein and importin β: it binds directly to the NLS and then to importin β through a characteristic importin β-binding- (IBB-) domain. This complex of nuclear

protein/importin α/importin β translocates through the NPC and then dissociates in the nucleus. While this is the most commonly used and best characterized transport system, a number of other mechanisms exist. For example, transportin is a transport receptor that does not require an adapter molecule to bind to the nuclear proteins. Interestingly, another transport receptor that can function independently of an adapter molecule is importin β itself. It has been shown to be responsible for the importin α-independent nuclear import of proteins such as PTHrP (Lam et al., 2002), cyclin B1 (Moore et al., 1999), the transcription factors c-Jun, c-Fos and CREB (Forwood et al., 2001), and the zinc finger transcription factor Snail (Yamasaki et al., 2005). The HIV-1 Rev protein can be localized to the nucleus by multiple importins: importin β (independently of importin α), transportin, importin 5, and importin 7 (Arnold et al., 2006).

Herein we report the existence of a previously unidentified variant of Bmp2, nuclear Bmp2 (nBmp2). We have demonstrated that nBmp2 is directed to the nucleus through a bipartite NLS that spans the site of proteolytic cleavage. This bipartite NLS is able to localize Bmp2 to the nucleus when translation initiates from an alternative, downstream start codon. The resulting protein lacks the signal peptide and is therefore translated in the cytoplasm rather than the rER, thus avoiding proteolytic processing and secretion and gaining access to the karyopherins responsible for nuclear import. In order to determine the function of nBmp2 in an animal model, a targeting vector was created to inhibit nuclear localization but allow for normal secretion and function of Bmp2. Chimeric mice carrying this defective allele have been generated, and the processes of breeding to homozygosity is underway. Preliminary results in zebrafish strongly suggest a critical role for nBmp2 in heart development.

METHODS

GFP fusion constructs

When we first became interested in a putative nuclear form of Bmp2, we analyzed its amino acid sequence using the PSORT II prediction program (Prediction of Protein Sorting Signals and Localization Sites in Amino Acid Sequences) to search for possible NLSs. Three were identified: NLSa, NLSb, and NLSc. To determine the functionality of each of the putative NLSs identified by PSORT II, each was fused to the C-terminal end of GFP to determine whether they were capable of directing GFP to the nucleus. The pCMV/GFP-NLSa, pCMV/GFP-NLSb, and pCMV/GFP-NLSc constructs were generated by annealing complementary oligonucleotides encoding NLSa (PELGRKK), NLSb (PLHKREK), and NLSc (PLHKREKRQAKHKQRKRLKS) with additional nucleotides to create *Not*I or *Pst*I ends, allowing ligation into an appropriate site in the pCMV/myc/ER/GFP vector. In addition, pCMV/GFP-NLSa/b was generated by inserting NLSa N-terminal of GFP and NLSb C-terminal of GFP in order to mimic the way NLSa and NLSb bracket the free propeptide that is released upon proteolytic cleavage of the Bmp2 preproprotein (Fig. 1). pCMV/myc/ER/GFP was used as a control in transfection experiments, with an inserted stop codon immediately after GFP.

An expression vector for wtBmp2 was generated by synthesizing cDNA from mRNA extracted from rat chondrosarcoma (RCS) cells using the Qiagen OneStep RT-PCR kit (Qiagen,Valencia, CA) according to manufacturer's instructions. Primers were used for PCR amplification that included a *Bam*HI site and a *Xba*I site to allow ligation into the expression vector pcDNA3.1. This plasmid was used as a template for the production of the Bmp2/GFP fusion constructs using a GFP Fusion TOPO TA

Expression Kit (Invitrogen Corporation, Carlsbad, CA) according to the manufacturer's instructions.

Site-directed mutagenesis

The Stratagene QuikChange II Site-Directed Mutagenesis Kit was used to mutate specific nucleotides in the Bmp2/GFP and Bmp2 expression vectors. The manufacturer's protocol was followed with the following specifications: 20 ng of template DNA and 125 ng of each primer were used during the thermal cycling portion. The template DNA was then fragmented by incubating the reaction mixture with 1 µL *Dpn*I at 37°C for 1 hour. The mutagenesis primers used to study the bipartite NLS are as follows with the altered nucleotides bold and underlined:

NtermKm F:GGACATCCACTCCAC**GCA**CGAGAAAAGCGTCAAGCC

NtermKm R:GGCTTGACGCTTTTCTCG**TGC**GTGGAGTGGATGTCC

KRm F:GGACATCCACTCCAC**GCAGC**AGAAAAGCGTCAAGCC

KRm R:GGCTTGACGCTTTTCT**GCTGC**GTGGAGTGGATGTCC

RKRm1 F:GCCAAACACAAACAG**GCGG**AGCGTCTTAAGTCCAGCTGCAAAAG

RKRm1 R:CTTTTGCAGCTGGACTTAAGACGCT**CCGC**CTGTTTGTGTTTGGC

RKRm2 F:GCCAAACACAAACAG**GCGGCGGC**TCTTAAGTCCAGCTGCAAAAG

RKRm2 R:CTTTTGCAGCTGGACTTAAGA**GCCGCCGC**CTGTTTGTGTTTGGC

RKR Km F: CACAAACAG**GCGGCGGC**TCTT**GCG**TCCAGCTGCAAGAG

RKR Km R: CTCTTGCAGCTGGA**CGC**AAGA**GCCGCCGC**CTGTTTGTG

All oligonucleotides were synthesized by Invitrogen Life Technologies. All constructs were verified by DNA sequencing (DNA Sequencing Center, Brigham Young University).

Transient transfection, fixing, and analysis

All tissue culture cells were maintained in Dulbecco's Modified Eagle's Medium (DMEM) supplemented with penicillin (50U/ml), streptomycin (50μg/ml), L-glutamine (2 mM), and 10% fetal bovine serum at 37°C under 5% CO_2. The cells were passaged every 3-4 days. For transient DNA transfections, 5×10^4 cells were seeded into each well of a 4-chambered Lab-Tek II Chamber Slide System glass slide (ISC Bioexpress). After 24 hours, the cells were transfected using the *Trans*IT-Jurkat Transfection Reagent (Mirus, Madison WI) according to manufacturer's directions, with a total of 500 ng DNA and 1.5 μL Jurkat reagent for each well. The transfected cells were incubated for approximately 24 hours at which time the media was replaced. After another 24 hours, the cells were washed in Phosphate Buffered Saline (PBS) and fixed using 4% paraformaldehyde in PBS (PFA/PBS) for 30 minutes. After fixing, the slide was washed three times in PBS and the nuclei were stained with a 1:1000-1:1500 dilution of TO-PRO-3 iodide (Invitrogen Corporation, Carlsbad, CA) according to manufacturer's protocol. Cells were mounted in Fluoromount-G (Southern Biotech, Birmingham, AL) and coverslipped (Fisher, Santa Clara, CA).

The cells were analyzed using an Olympus IX81 laser confocal microscope at 60× magnification, with excitation wavelengths of 488 nm for GFP and 633 nm for TO-PRO-3. The percentage of transfected cells exhibiting nuclear localization was determined by

counting approximately 100 transfected cells per well. Each experiment was repeated at least three times and the average of the three experiments is reported.

Immunocytochemistry

To visualize the localization of endogenous Bmp2, immunohistochemistry was performed on the following cultured tissue lines: RCS, BALB/3T3 fibroblasts, 10T1/2 mesenchyme cells, 231 breast cancer cells, 435 breast cancer cells, MCF-7 breast cancer cells, Hep-G2 liver cancer cells, HT29 colon cancer cells, and a primary culture of mouse embryonic fibroblasts (MEFs). Either 50,000 or 25,000 cells were seeded into each well of a 4-chambered Lab-Tek II Chamber Slide System glass slide (ISC Bioexpress) and grown for 2 days. The media was then removed, and the cells were rinsed twice with 0.4 mL PBS. The cells were fixed with 200 μL of 4% PFA/PBS in each well for 20-30 minutes with gentle agitation. After the incubation, the slides were rinsed three times with 0.4 mL PBS, twice for 5 minutes and once for 20 minutes. The well dividers were then removed and the cells were incubated for 40 minutes in 300 μL blocking solution: 1% BSA and 0.3% Triton X-100 in PBS. This solution was removed and 300 μL of the primary antibody solution was added: 0.1% BSA, 0.3% Triton X-100, and 1:50 dilution of a goat polyclonal anti-Bmp2 antibody (Santa Cruz Biologicals, Santa Cruz, CA) or a rabbit polyclonal anti-Bmp2 antibody (AbCam, Cambridge, MA). The slides were incubated in this solution at room temperature for 2 hours and then placed at 4°C in a humid chamber overnight. The following day, the slides were rinsed three times for 5 minutes each in PBS and then incubated for 30-45 minutes in the secondary antibody solution: 0.1% BSA, 0.3% Triton X-100, and 6 μg/mL donkey anti-goat 488-labeled

secondary antibody or a goat anti-rabbit 488-labeled secondary antibody (Molecular Probes). After this incubation the slides were again rinsed three times for 5 minutes each in PBS. The nuclei were stained with TO-PRO-3 iodide, rinsed, coverslipped, and examined using a laser confocal microscope as detailed above. As a negative control, cells were incubated as detailed above without primary antibody.

Western blot analysis on nuclear extracts

To determine the size of nBmp2, western blots were performed on nuclear extracts from either non-transfected cultured cells or cultured cells that were transfected with an HA-tagged nBmp2 expression vector (HA-ERmBmp2). The *Trans*IT-Jurkat Transfection Reagent (Mirus, Madison, WI) was used to transfect the cells according to manufacturer's directions. Specifically, 1600 μL of Opti-MEM was combined with 50 μL Jurkat reagent for 10 minutes at room temperature before 16 μg of the HA-ERmBmp2 expression plasmid was added. This mixture was incubated for 15 minutes at room temperature then added to one 75-cm^2 tissue culture flask of cells with fresh complete media. The cells were allowed to grow for 24 hours with the transfection reagent before the media was replaced with new complete media and grown for 24 more hours.

Nuclear proteins were isolated using the Cellytic Nuclear Extraction Kit (Sigma, Saint Louis, MO) according to manufacturer's instructions. Specifically, the cells were rinsed twice in cold PBS, collected, and centrifuged in a tabletop centrifuge at 4°C for 5 minutes at 2000 rpm. The cells were lysed in 500 μL hypotonic lysis buffer (provided by manufacturer) for 15 minutes on ice before centrifuging again in a tabletop centrifuge at 4°C for 5 minutes at 2000 rpm. After decanting and resuspending the cell pellet in 200

μL lysis buffer, the cells were disrupted with a 27-gauge needle and syringe. The nuclei were subsequently collected by centrifuging at 4°C for 20 minutes at 8500 rpm. Nuclear proteins were extracted by adding 150 μL extraction buffer (supplied by manufacturer) and incubating at 4°C for 30 minutes in a rotisserie shaker. Supernatants containing the nuclear proteins were flash-frozen in liquid N_2 and stored at -80°C.

Nuclear proteins were fractionated by SDS-PAGE using 10% gels and transferred to Westran Clear Signal PVDF transfer membranes (Schleicher and Schuell, Keene, NH) overnight at 30 volts using Tris glycine buffer (25 mM Tris, 192 mM glycine, 20% methanol, pH 8.3). The membranes were rinsed with TBS-t (0.05 M Tris-HCl, pH 7.5, 0.2 M NaCl, 0.1% Tween-20) and blocked in 2.5% non-fat dry milk (Bio-Rad, Hercules, CA) in TBS-t for 1 hour with gentle agitation on an orbital shaker. The membrane with the nuclear proteins from non-transfected cells was then incubated with a 1:250 dilution of goat anti-Bmp2 antibody (Santa Cruz Biotechnology, Inc., Santa Cruz, CA) while the membrane with the nuclear proteins from the HA-ERmBmp2-transfected cells was incubated with a 1:250 dilution of rabbit anti-HA antibody (Santa Cruz Biotechnology, Inc., Santa Cruz, CA) for 1 hour in 2.5% non-fat dry milk. After a 20-minute wash and two 5-minute washes with agitation in TBS-t, the membranes were incubated in the appropriate HRP-conjugated secondary antibodies (Santa Cruz Biotechnology, Inc., Santa Cruz, CA) for1 hour in 2.5% non-fat dry milk. The washes were performed again as described. To visualize the proteins, the Immobilon Western Chemilumiescent HRP Substrate (Millipore, Billerica, MA) was used according to manufacture's protocol.

In vitro transcription translation and *in vitro* digestion assay

Bmp2 protein was synthesized *in vitro* with the incorporation of [^{35}S]methionine employing the TNT Coupled Wheat Germ Extract System (Promega, Madison, WI) according to manufacturer's instruction using an expression vector containing the rat Bmp2 cDNA. Ten units of furin (New England BioLabs, Ipswich, MA) or furin plus 2 μM α_1-PDX (Affinity BioReagents, Golden, CO) was preincubated in 100 mM HEPES, 0.5% Triton X-100, 1 mM $CaCl_2$ and 1 mM β-mercaptoethanol for 30 minutes at room temperature. The synthesized and labeled Bmp2 proprotein was then added, and the reaction was allowed to proceed for 1 hour or 3 hours at 30°C before products were separated by SDS-PAGE and visualized by autoradiography.

The TNT Coupled Wheat Germ Extract System (Promega, Madison, WI) was also used to transcribe and translate the ATG mutant constructs for the alternative start codon experiments and for the zebrafish bmp4/morpholino translation experiments.

Immunoprecipitation/Western blot of wild-type and RKRm Bmp2

To determine if mutating the RKR portion of the bipartite NLS would affect the processing and secretion of Bmp2, RCS cells were transfected with either the HA-tagged wtBmp2 (HA-wtBmp2) or RKRm (HA-RKRmBmp2) expression plasmids and allowed to grow for two days before the HA-tagged proteins were immunoprecipitated from the media and subjected to immunoblotting. To do this, two 25-cm^2 tissue culture flasks were seeded with 7.8 ×10^5 RCS cells. The following day, 5 μg of either the HA-wtBmp2 or HA-RKRmBmp2 expression plasmids was transfected into the cells using the *Trans*IT-Jurkat Transfection Reagent (Mirus, Madison, WI) according to manufacturer's protocol.

Specifically, 625 µL of Opti-MEM was combined with 16.7 µL Jurkat reagent for 10 minutes at room temperature before the plasmid DNA was added. This mixture was incubated for 15 minutes at room temperature then added to the cells with fresh complete media. The cells were allowed to grow for 24 hours with the transfection reagent before the media was replaced with new complete media and grown for 24 more hours.

After the cells had grown for 48 hours from the start of transfection, 1.5 mL of media was removed from each flask and 2 µL of the protease Leupeptin was added to each sample. The media was centrifuged for 10 minutes at 10,000 rpm to remove cellular debris. The HA-tagged proteins were precipitated using EZview Red Anti-HA Affinity Gel (Sigma, Saint Louis, MO) according to manufacturer's protocol as follows. For immunoprecipitation, 40 µL of the affinity gel was added to a clean microcentrifuge tube on ice and equilibrated by adding 750 µL of PBS, mixing, and centrifuging for 30 seconds at 8,200 × g. The PBS was aspirated and the wash was repeated. The media from the flasks of transfected cells was then added to the affinity gel and incubated at 4°C for 2 hours with rotation. After the incubation, the affinity gel and bound HA-tagged proteins were pelleted by centrifuging for 30 seconds at 8,200 × g and the media aspirated. The gel was washed three times for 5 minutes each with 750 µL PBS. The HA-tagged proteins were removed from the resin by adding 40 µL Laemmli buffer with 5% β-mercaptoethanol and boiling for 5 minutes.

The samples were immediately fractionated by SDS-PAGE using a 10% gel and transferred to a Westran Clear Signal PVDF transfer membrane (Schleicher and Schuell, Keene, NH) overnight at 30 volts using Tris glycine buffer as detailed above. The membranes were rinsed with TBS-t and blocked in 2.5% non-fat dry milk (Bio-Rad,

Hercules, CA) in TBS-t for 1 hour with gentle agitation on an orbital shaker. After a 20-minute wash and two 5-minute washes with agitation in TBS-t, the membrane was incubated with 0.7 μg/mL HRP-conjugated anti-HA antibody for 1 hour in 2.5% non-fat dry milk. The washes were performed again as described. To visualize the HA-tagged proteins, the ECL Western blotting reagent (Amersham Biosciences, Piscataway, NJ) was used according to manufacturer's protocol.

Microarray and Real-Time PCR

A microarray was performed through Assuragen to identify genes that might be responsive to nBmp2. We used real-time PCR to verify the results. To collect mRNA for the microarray and for real-time PCR, RCS cells were transfected with an expression vector for nuclear Bmp2. This construct, ERmutBmp2, lacked the sequence coding for the signal peptide and would thus be translated in the cytosol and subsequently localized to the nucleus. As a control, cells were also transfected with the empty pcDNA3.1 vector. For real-time PCR, another flask of cells was transfected with a nuclear GFP expression vector to use as a control (NLScGFP). The RNA was extracted from these cells using the NucleoSpin RNA II Kit (Clontech, Mountain View, CA) according to manufacturer's protocol. Specifically, the cells were incubated with trypsin, collected in 15-mL conical vials, and centrifuged for 9 minutes at 800 RPM. The media was aspirated and the cells were resuspended in 350 μL of the provided Buffer RA1 and 3.5 μL of β-mercaptoethanol. The sample was passed through a syringe fitted with a 20-gauge needle six times to completely homogenize the cells and shear genomic DNA. To the lysate, 350 μL of 70% ethanol was added and mixed well. The sample was loaded onto a NucleoSpin

column and centrifuged at 8000 × g for 30 seconds. The flow-through was discarded and 350 μL of the provided Buffer MDB was added before centrifuging at 11000 × g for 1 minute. The flow-through was again discarded and 95 μL of DNase I Reaction Mixture was added and incubated for 15 minutes at room temperature before adding 200 μL of the provided Buffer RA2 and centrifuging at 8000 × g for 30 seconds. The flow through was again discarded and 600 μL of the provided Buffer RA3 was added to the column and centrifuged again at 8000 × g for 30 seconds. The flow through was discarded and the column was again washed with Buffer RA3, this time with 250 μL and centrifuging at 11000 × g for 2 minutes. The RNA was eluted in two steps into two 1.5-mL microcentrifuge tubes, each with 40 μL of nuclease-free water and centrifuging at 11000 × g for 1 minute.

For the microarray analysis, three biological replicates of RNA from ERmutBmp2-transfected cells and three biological replicates of RNA from the vector-transfected cells were shipped to Assuragen according to their instructions. RNA was analyzed on Affymetrix Rat Expression Arrays 230 2.0. Differentially expressed genes were selected using two-tailed student t statistics comparing expression values from the ERmutBmp2-transfected samples and the replicate data from the vector-transfected controls. A p-value of <0.05 and a fold-change of >1.5 fold in either direction were considered significant.

To verify the microarray results, real-time PCR was performed on a number of genes that were indicated as being differentially expressed and perhaps regulated by nBmp2. For these assays, RNA from nuclear GFP-transfected cells was included to control for genes that may be responding to overexpression of any nuclear protein,

perhaps as a stress response. The extracted RNA was reverse transcribed into cDNA using the iScript cDNA Synthesis Kit (Bio-Rad, Hercules, CA) according to manufacturer's protocol. Specifically, the following components were combined in a PCR tube: 4 μL 5 × iScript Reaction Mix, 1 μL iScript Reverse Transcriptase, 600-900 μg RNA template, and nuclease-free water to a total volume of 20 μL. The reaction components were mixed, placed in a thermocycler and subjected to the following program: 5 minutes at 25°C, 30 minutes at 42°C, and 5 minutes at 85°C.

For the real-time PCR reaction, the iTaq SYBR Green Supermix with ROX (Bio-Rad, Hercules, CA) was initially used, but we later switched to the LightCycler 480 SYBR Green I Master (Roche, Indianapolis, IN) not only because it was designed for the machine we were using but also because it had higher sensitivity. For the Roche kit, each reaction contained 300 ng of cDNA template, 10 μL of the Master Mix, 0.5 μL of 10 μM forward and reverse primer, and water up to 20 μL. The reactions were placed into wells of a 96-well plate, sealed shut using Optically Clear Thermalseal (ISC BioExpress, Kaysville, UT), and centrifuged.

Raw real-time PCR results were expressed as Cp ("crossing point") values and were analyzed using the - ΔΔCp method as follows: the Cp value for each sample was normalized by subtracting the corresponding 18S rRNA average Cp value from each reaction (e.g. the 18S Cp values for the ERmutBmp2 template were averaged and subtracted from all wells using the ERmutBmp2 cDNA as template). To calculate differences in gene expression between ERmutBmp2-transfected cells and vector-transfected controls, normalized ERmutBmp2 Cp values were then subtracted from the control Cp values, resulting in a ΔΔCp value. Fold difference in Cp values between

ERmutBmp2-transfected cells and vector-transfected controls was calculated by raising 2 to the –ΔΔCp. To calculate the fold differences in the RNA levels, the fold differences in the Cp values from 2-4 experiments were averaged, then the average fold difference in Cp values of the vector-transfected controls was divided by the average fold difference in Cp values for the ERmutBmp2-transfected cells.

Construction of the nBmp2 knock-out targeting vector

The nuclear Bmp2-knockout targeting vector was constructed using recombineering (recombination-mediated genetic engineering) (Copeland et al., 2001). This technique uses a modified *E. coli* strain containing defective λ prophage recombination genes (strain SW102). A temperature-sensitive repressor controls the expression of the λ recombination genes *exo*, *bet*, and *gam*, allowing for induction of recombination to occur upon heating the cells. *exo* encodes a 5′-3′ exonuclease that acts on the 5′ ends of linear double-strand DNA (dsDNA) to produce 3′ single-strand DNA (ssDNA) overhangs. *bet* encodes a pairing protein, Beta, that binds to the 3′ end of the ssDNA overhangs and promotes annealing to its complementary DNA strands on the target DNA. The Gam protein inhibits the RecBCD exonuclease of the host *E. coli* allowing the linear dsDNA to remain stable.

Primers

PCR and sequencing primers used for construction the nuclear Bmp2 knockout vector are listed below:

5′ Bmp2 Forward, gaatgcggccgcCTGTCTCGAGAATGAGC;

5′ Bmp2 Reverse, gctaaagcttGAAGGCTGAGGCAAGGCTG;

3′ Bmp2 Forward, gaataagcttCACAGCAGGCCCCATGTGAC;

3′ Bmp2 Reverse, ggtcactagtGCTCAGCATGTCAGCACCCAG;

5′ Neo Forward, gttaggtaccGATCTGATAGAAAACGTCTCGC;

5′ Neo Reverse, gttagtcgacGGGTGCTTTGGAGAATAGAG;

3′ Neo Forward, gaccgaattcCGCAGCAAAATTGAGCATATG;

3′ Neo Reverse, gaacgaattcCATTGGTAAGTCCTTTGGTCCAAC;

3′ Neo sequencing, GACGAGTTCTTCTGAGGGGATC;

PGK-EM7 Forward,

aagacagaataaaacgcacgggtgttgggtcgtttgttcggtcgagctcgcgaaTCTACCGGGTAGGGGAGG;

PGK-EM7 Reverse,

aacctgcgtgcaatccatcttgttcaatggccgatcccatattggctgcacggatGGTTTAGTTCCTCACCTTGTC;

galK Forward,

aaaggacatccgctccacaaacgagaaaagcgtcaagccaaacacaaacagCCTGTTGACAATTAATCATCGGCA;

galK Reverse,

acatcactgaagtccacatacaaagggtgtctcttgcagctggacttgagTCAGCACTGTCCTGCTCCTT;

NLS sequencing, GGTCTTTGCACCAAGATGAAC;

Minitargvec Reverse, TCCAACTGGGGTTTGCTTAG;

Genotyping Forward, GGCCATTTAGAGGAGAACC;

Genotyping Reverse, CATGCCTTAGGGATTTTGGA.

Homology to the sequence being amplified is capitalized while sequence containing restriction endonuclease recognition site and/or homology arms is lowercase. The primers to amplify homology arms amplified the following size fragments: 5′ Bmp2

homology arm: 329 bp; 3′ Bmp2 homology arm: 329 bp; 5′ Neo insertion arm: 327 bp; 3′ Neo insertion arm: 341 bp.

Plasmid Construction

Neo mini-targeting vector

The ACN selection cassette was used in the targeting vector because this cassette not only contains the necessary neomycin resistance (*Neo*) gene, but also it contains the *Cre* recombinase gene. Cre is the 38-kDa product of the *Cre* (cyclization recombination) gene of bacteriophage P1 and is a site-specific DNA recombinase. Cre recognizes a 34-bp site on the P1 genome called loxP (locus of X-over of P1) and efficiently catalyzes reciprocal conservative DNA recombination between pairs of loxP sites. The *Neo* cassettes used in targeting vectors are generally flanked ("floxed") by loxP sites and the generated mice are then bred with a strain of mice that express Cre to remove the cassette. However, the ACN cassette contains the *Cre* gene and a testis-specific promoter (tACE from the gene encoding angiotensin-converting enzyme 27) that drives its expression in the male germline. Consequently, there is no need for extra breeding steps when the generated mice contain this cassette.

In order to make the ACN selection cassette functional for selection in bacterial cells as well as in eukaryotic cells so that it could be used in the recombineering technique, the eukaryotic Pol II promoter that drove expression of *Neo* was replaced by the combined eukaryotic PGK and bacterial EM7 promoters described by Liu et al. (Liu et al., 2003). PCR amplification (Invitrogen PLATINUM *Taq* DNA polymerase) of the PGK-EM7 promoters was performed using reaction mixtures containing 5 μL 10x PCR buffer minus Mg, 1 μL of 10 mM dNTP mixture, 1.5 μL of 50 mM $MgCl_2$, 1 μL of 10

μM forward primer, 1 μL of 10 μM reverse primer, 1 μL of 50 ng/μL PL451, 0.3 μL of 5 U/μL PLATINUM *Taq* DNA Polymerase and 40.2 μL of water. Four reactions were performed to acquire adequate amounts of the desired product. The PCR products were purified via a 1% agarose gel followed by extraction from the gel using the Qiagen Qiaex II kit (Qiagen, Qiagen,Valencia, CA) according to manufacturer's instructions. The samples were pooled and ethanol precipitated using 0.2 M NaCl and 10 mM $MgCl_2$. SW102 cells already containing pACN were induced for recombination at 42°C for 15 minutes in a water bath to induce the λ recombination proteins and electroporated with 100 ng of the purified PGK-EM7 promoters.

Insertion of the promoters introduced an additional *Spe*I recognition site into pACN, so correctly recombined plasmids were identified via digestion with *Spe*I. Since one successful homologous recombination event could render the cell kanamycin resistant and pACN is a multi-copy plasmid, it was not surprising that all plasmid extractions consisted of mixed populations of recombined and non-recombined plasmids. To remedy this, SW102 cells were transformed with mixed plasmid extractions that contained both correctly-recombined PGK-EM7/pACN plasmid and the non-recombined pACN plasmid. Plasmid DNA was extracted from several of these colonies and digested with *Spe*I to reveal which plasmid extractions were pure populations of the desired pACN/PGK-EM7 plasmid.

DNA sequences homologous to specific regions of genomic *Bmp2* were amplified and ligated into pACN/PGK-EM7 (the 5′ Neo and 3′ Neo homology arms) and into PL253 (the 5′ Bmp2 and 3′ Bmp2) in order to complete construction of the *Neo* mini-targeting vector and the *Bmp2* retrieval vector, respectively. Amplification of these

homology arms was performed with the following settings: 94°C for 2 minutes, then 2 cycles of 94°C for 15 sec, lowest T_m of the primer pair (from the portion that binds to the region of Bmp2) for 30 sec and 72°C for 25 sec. This was followed by 33 cycles of 94°C for 15 sec, lowest T_m of the primer pair (including the initial non-binding region used to insert restriction endonuclease recognition sites) for 30 sec and 72°C for 25 sec. The 5′ Neo and 3′ Neo homology arms were amplified (Invitrogen *Taq* DNA Polymerase kit) using reaction mixtures containing 5 µL 10x PCR buffer minus Mg, 1 µL of 10 mM dNTP mixture, 1.5 µL of 50 mM $MgCl_2$, 1 µL of 10 µM forward primer, 1 µL of 10 µM reverse primer, 2 µL of 50 ng/µL BAC DNA (RP23-384M14 from BAC-PAC), 0.3 µL of either 5 U/µL *Taq* DNA Polymerase (5′ Neo arm) or 2.5 U/µL PLATINUM *Pfx* (3′ Neo arm) and 38.1 µL of water. The 5′ Bmp2 and 3′ Bmp2 homology arms were amplified (Invitrogen PLATINUM *Pfx* DNA Polymerase kit) using reaction mixtures containing 5 µL 10x *Pfx* Amplification Buffer, 1.5 µL of 10 mM dNTP, 1 µL 50 µM $MgSO_4$, 1 µL of 10 µM forward primer, 1 µL of 10 µM reverse primer, 2 µL of 50 ng/µL BAC DNA, 0.4 µL 2.5 U/µL PLATINUM *Pfx* DNA Polymerase and 39.1 µL of water. To check the PCR reactions, 5 µL of the 50-µL PCR reaction mixtures were separated on a 1% agarose gel. The remainder of each reaction was purified using the Qiagen QIAquick PCR Purification Kit (Qiagen,Valencia, CA) according to manufacturer's instructions before digesting with the appropriate restriction enzymes. The digested PCR fragments were purified again with the PCR purification kit and were ready to be ligated.

Several steps were used to generate the *Neo* mini-targeting vector. Ligation of the 3′ Neo arm was accomplished using the Fermentas Rapid DNA Ligation Kit, by mixing 100 ng of pACN/PGK-EM7 digested with *Eco*RI, 14 ng of the 3′ Neo arm digested with

*Eco*RI , 4 µL of 5x Rapid Ligation Buffer, 1 µL of 5 U/µL T4 DNA ligase and water up to 20 µL. After 15 minutes, 5 µL of the ligation mixture was used to transform cells. Plasmid DNA was extracted (Qiagen miniprep kit) from overnight cultures of individual colonies and digested with *Eco*RI to identify plasmids with inserts. Those plasmid preparations with inserts were then sequenced to identify correctly-orientated 3′ Neo homology arms. Once the desired plasmid preparation was identified, it was digested with *Kpn*I and *Sal*I in a step-wise manner with a purification step between each digest (via the Qiagen QIAquick PCR Purification Kit). After the final digest, the vector was dephosphorylated by adding 2 µL of 20 U/ µL Calf Intestinal Alkaline Phosphatase (Promega) and 3 µL of 10 × Alkaline Phosphatase Reaction Buffer in a final volume of 30 µL. Ligation of the 5′ Neo arm was accomplished using the Fermentas Rapid DNA Ligation Kit by mixing 100 ng of the *Kpn*I/*Sal*I-digested and dephosphorylated pACN/PGK-EM7, 14 ng of the 5′ Neo arm digested with *Kpn*I and *Sal*I, 4 µL of 5x Rapid Ligation Buffer, 1 µL of 5 U/µL T4 DNA ligase and water up to 20 µL. After 15 minutes, 5 µL of the ligation mixture was used to transform cells. Plasmid DNA was extracted (Qiagen miniprep kit) from overnight cultures of individual colonies and digested with *Kpn*I and *Sal*I to identify correctly-ligated and completed *Neo* mini-targeting vectors.

The homology arms used to generate the *Neo* mini-targeting vector targeted the *Neo* mini-targeting cassette into the 3′UTR of Bmp2, downstream of all known posttranscriptional regulatory regions within the 3′UTR (Fritz et al., 2006; Fritz et al., 2004).

Bmp2 retrieval vector

Amplification and purification of the homology arms used for construction of the *Bmp2* retrieval vector are described above. The retrieval vector was constructed using the same Fermentas Rapid DNA Ligation Kit by mixing 100 ng of PL253 (Liu et al., 2003) digested with *Not*I and *Spe*I, 6 ng of the 5′ Bmp2 arm digested with *Not*I and *Hin*dIII, 6 ng of the 3′ Bmp2 arm digested with *Hin*dIII and *Spe*I), 4 µL of 5x rapid ligation buffer, 1 µL of 5 U/µL T4 DNA ligase and water up to 20 µL. After 15 minutes, 5 µL of the ligation mixture was used to transform cells. Plasmid DNA was extracted (Qiagen miniprep kit) from overnight cultures of individual colonies and digested with *Not*I and *Spe*I to identify correctly-ligated and completed *Bmp2* retrieval vectors.

Transformation of BAC into Recombinogenic Strains

E. coli strains containing the BAC with the *Bmp2* gene (RP23-384M14 from BAC-PAC) were grown overnight in 5 mL of LB broth with chloramphenicol. Cells were transferred to a centrifuge tube and pelleted for 5 minutes at 5,000 RPM, the supernatant removed, and the pellet dissolved in 250 µL buffer P1 (Qiagen miniprep kit) before being transferred to an eppendorf tube. The cells were lysed by adding 250 µL P2 buffer, mixing by inversion and incubating for 5 minutes at room temperature. The reaction was neutralized by adding 350 µL N3 buffer, mixing by inversion and incubating on ice for 5 minutes. The supernatant was cleared by two rounds of centrifugation at 13200 rpm for 5 minutes in a tabletop centrifuge, transferring to a clean tube between centrifugation steps. BAC DNA was precipitated by adding 750 µL isopropanol and incubating on ice for 10 minutes before being pelleted by centrifugation for 10 minutes at 13000 rpm. The pellet

was washed with 70% ethanol and air-dried before dissolving in 50 μL TE. For electroporation, 1 μg was used.

To make the SW102 cells electrocompetent, they were grown in a 5 mL of LB broth with tetracycline at 32°C overnight with shaking. The next day the cells were collected by centrifuging at 5000 rpm for 5 minutes at 0°C. Cell pellets were resuspended in 1 mL ice-cold water. Cells were transferred to a pre-chilled 1.7-mL eppendorf tube and centrifuged using a benchtop centrifuge for 15-20 sec at room temperature. The tubes were placed on ice, and the supernatants were aspirated. This washing step was repeated two more times. Finally, the cell pellet was resuspended in 40 μL ice-cold water and 1 μg of BAC DNA was added and mixed before transferring to a pre-chilled electroporation cuvette (0.1-cm gap). Electroporation was performed using a BIO-RAD electroporator under the following conditions: 1.8 kV, 25 μF with the pulse controller set at 200 Ω. The time constant was usually between 3.8 and 4.8. Following electroporation, 1 mL of LB was added to each cuvette and the cells were transferred to a 14-mL round-bottom culture tube and incubated with shaking for 1 hour at 32°C. SW102 cells containing the BAC were selected for by growing on LB plates with both chloramphenicol (for the BAC) and tetracycline (for the SW102 cells).

Mutating the bipartite NLS of Bmp2

In order to mutate the bipartite NLS of Bmp2, the *galK* positive/negative selection system was used to first replace the target amino acids with the *galK* gene, and then replace the *galK* gene with the desired mutation (**KR**EKRQAKHKQ**RKR**L**K**S was changed to **KR**EKRQAKHKQ**AAA**L**K**S) as described in Warming et al (Warming et al., 2005). The SW102 strain used for recombineering contains a fully functional galactose

operon except the galactokinase gene (*galK*) has been deleted. The galK function can be added in *trans*, so the ability to grow on galactose as the sole carbon source can be selected. Conveniently, galK can also be selected against by using 2-deoxy-galactose (DOG); when phosphorylated by galK, DOG becomes cytotoxic. To mutate the **RKR** portion of the NLS to **AAA**, the *galK* gene was amplified using primers that contain 50 bp of homology to the area directly surrounding the codons that code for the **RKR**. SW102 cells containing the BAC were induced for recombination and electroporated with the *galK* amplicon, and recombinant bacteria were able to grow on minimal media with galactose as its only carbon source.

In detail, *em7-galK* was PCR amplified from 2 ng p*galK* (Warming et al., 2005) as template with the following cycle parameters: 94°C for 2 min, then 35 cycles of 94°C for 15 sec, 60°C for 30 sec, and 68°C for 1.2 min. PCR was carried out (Invitrogen PLATINUM *Pfx* DNA Polymerase kit) with reaction mixtures containing 5 µL 10x *Pfx* Amplification Buffer, 1.5 µL of 10 mM dNTP, 1 µL 50 µM $MgSO_4$, 1 µL of 10 µM forward primer, 1 µL of 10 µM reverse primer, 1 µL of 2 ng/µL p*galK* DNA, 0.4 µL 2.5 U/µL PLATINUM *Pfx* DNA Polymerase and 39.1 µL of water. After the PCR was complete, 10 U of *Dpn*I was added to the reaction and incubated at 37°C for 1 hour to remove template DNA. After digestion, the reaction was separated overnight on a 1% agarose gel. After extraction from the gel using the Qiagen Qiaex II kit according to manufacturer's instructions, the samples were pooled and ethanol precipitated using 0.2 M NaCl and 10 mM $MgCl_2$.

Meanwhile, SW102 cells containing the BAC were inoculated into 5 mL of LB broth and grown at 32°C overnight with tetracycline. The next day, 500 µL of the

overnight culture was inoculated into 25 mL of LB with tetracycline and grown until OD_{600} = 0.550. Half of the culture was kept at 32°C, while the other half was induced for recombination by incubating for 15 minutes at 42°C. To make the cells electrocompetent, both flasks were transferred to an ice bath and incubated for 15 minutes before pelleting at 4000 rpm for 5 minutes at 0°C. The cells were then resuspended in 1 mL ice-cold water and transferred to cold eppendorf tubes and washed as described above. Electroporation was carried out using 330 ng of the purified *galK* gene. After a 1-hour recovery in 1 mL of LB, the bacteria were washed twice in 1×M9 salts as follows: the cells were pelleted in an eppendorf tube at 13200 rpm for 15 sec. and the supernatant was removed with a pipette. The pellet was gently resuspended in 1 mL 1×M9 salts and pelleted again. The cells were washed and resuspended in 1×M9 once more before plating 200 µL onto M63 minimal media plates (appendix). After a 3-day incubation at 32°C, several colonies were streaked for isolation onto MacConkey indicator plates containing chloramphenicol and tetracycline to reveal colonies capable of fermenting galactose. The next day, several of the bright pink colonies were grown overnight in culture. After extracting BAC DNA, PCR was used to determine if *galK* had recombined into the desired location using primers that flank the NLS. If *galK* has inserted at the NLS, the amplicon would be ~2.6 kb; if *galK* had not inserted into the proper location, the amplicon would only be ~1.4 kb. All bright pink colonies contained successful recombinants of *galK* into the desired location of *Bmp2*.

Double-stranded oligos were used to replace *galK* with the desired mutation (**KR**EKRQAKHKQ**RKR**L**K**S to **KR**EKRQAKHKQ**AAA**L**K**S). These oligos were 100-bp long and contained nucleotides coding for the desired NLS mutations (three Ala

codons) along with homology to the surrounding sequence in *Bmp2.* They were purchased (Invitrogen, Carlsbad, CA), resuspended in TNE, boiled for 10 minutes, and then slowly cooled to room temperature for 2 hours before EtOH-precipitating in the presence of 0.2 M NaCl and 10 mM $MgCl_2$. The oligos were resuspended in water. Cells containing the *galK* BAC were grown and induced as described above and electroporated with 300 ng of the double-stranded oligos. This time the cells were recovered in 10 mL LB in a 50 mL Erlenmeyer flask for 4.5 hours to allow ample time to obtain cells containing the targeted BAC only. After this recovery period, the cells were pelleted, washed twice in 1×M9 salts, and resuspended in 1 mL of 1×M9 before plating 200 μL of both the induced and uninduced onto M63 minimal plates containing glycerol and 2-deoxy-D-galactose. The 2-deoxy-D-galactose is cytotoxic to cells that still contained the *galK* gene, while those cells that had substituted the NLS mutation for the *galK* gene were able to grow.

Retrieving NLSmBmp2 from the BAC

The *Bmp2* retrieval vector described above was used to subclone the *NLSmBmp2* gene from the BAC into pBluescript modified to contain a thymidine kinase (*MC1TK*) gene. To prepare the retrieval vector for gap-repair (retrieval), 250 ng was digested with 20 units *Hin*dIII in 35 μL volume for 2 hours. The digestion reaction was run overnight on a 1% agarose gel at 35 volts. The linearized plasmid was then excised from the gel and purified using the Qiagen Qiaex II DNA extraction kit according to manufacturer's instructions.

SW102 cells containing the *NLSmBmp2* BAC were grown in 5 mL of LB broth containing chloramphenicol and tetracycline at 32°C overnight with shaking. The next

day, 1.0 mL of the overnight culture was transferred to 20 mL of LB containing chloramphenicol and tetracycline and incubated at 32°C with shaking until OD_{600} = 0.5. Next, 10 mL of the cells were transferred to a new flask and shaken in a 42°C water bath for 15 minutes to induce recombination while the remaining 10 mL of cells continued to be incubated at 32°C. Both flasks of cells were promptly placed into an ice bath and shaken to ensure rapid dropping of the temperature.

The cells were made electro-competent as described above. The cell pellet was resuspended in 40 µL ice-cold water before 2 µL (40 ng) of the purified, linearized plasmid was added. The cells were then electroporated and plated on LB + ampicillin plates.

Targeting with the* Neo *cassette

The *NLSmBmp2* retrieved plasmid was transferred into fresh (never been induced) SW102 cells using 5 ng of DNA and plating 100 µL of the transformation reaction. Overnight cultures were examined with a *Bgl*II digest and "genotyped" (see below) to verify that they contained the correct plasmid. These cells were grown, induced for recombination, and made electrocompetent as described above. The cells were electroporated with 500 ng of the *Neo* mini-targeting cassette. This cassette was PCR-amplified from the *Neo* mini-targeting vector using the 5′ Neo Forward and the Minitargvec Reverse primers and prepared for recombination as follows. After PCR, the mini-targeting vector template was removed with *Dpn*I, and the cassette was electrophoretically separated. The cassette was extracted from the gel using the Qiagen Qiaex II gel extraction kit and EtOH-precipitated before using for electroporation. Several PCR reactions were performed and pooled after extracting from the gel and

before precipitating to obtain a high concentration of the *Neo* mini-targeting cassette. After electroporation and a 1-hour recovery, the cells were grown on plates containing 25 ng/μL kanamyacin. Only three colonies grew, and only two of those colonies were able to grow in culture overnight in the presence of 20 ng/μL kanamycin. Both of these colonies contained a mixture of recombined and un-recombined plasmids, as verified through a *Bgl*II digest and a *Cla*I digest.

To separate recombined clones from the un-recombined, the mixed plasmid preparation was re-transformed into SW102 cells. No colonies were obtained until 10 ng of DNA was used and the entire reaction was plated onto kanamycin plates. Nine colonies were examined with a *Bgl*II digest, and six of them had only the desired, targeted plasmid. This was confirmed by performing two more analytical digests, one with *Xba*I and one with *Pst*I and "genotyping" (see below) the plasmid to verify the presence of the NLS mutation.

Gene Targeting in Mouse ES cells

To generate targeted mouse ES cells, two reactions of 7×10^6 129XI/SvJ-derived AV3 ES cells were electroporated at 250 V with 40 μg of the *Not*I-linearized nBmp2-ko targeting vector each. After electroporation the cuvettes were placed on ice for 20 minutes. As a negative control, 7×10^6 AV3 ES cells were also treated with the electroporation procedure. The contents of each cuvette was then plated onto two 10-cm dishes with mitomycinC-treated (mitoC-treated) *Neo*^{r} mouse embryonic fibroblasts (MEFSs) and grown in complete media for 24 hours, at which time the media was

removed and replaced with media containing 300 μg/mL of G418 and 2 μM FIAU (appendix). The media was changed every other day.

Within 7-9 days, all the neomycin-sensitive (*Neo*^{s}) colonies had cleared and the *Neo*^{r} colonies could be picked. Healthy-looking, refractile colonies were picked with a pipette and placed into wells of a 48-well plate containing 100 μL typsin/EDTA in each well. Once 48 colonies had been picked, the plate was placed at 37°C for 10 minutes. Then, 100 μL ES media (appendix) (with G418 but not FIAU from this point on) was added to all the wells to inactivate the trypsin. The cells in each well were dispersed with a multi-channel pipetman and transferred to a 48-well plate of mitoC-treated *Neo*^{r} MEFSs. Enough colonies to fill two 48-well plates of mitoC-treated *Neo*^{r} MEFSs were picked from each plate. The media was changed every other day until the wells needed to be replica-plated, which took anywhere from 1 day to 1 week depending on the well.

To replica plate, the media was removed and the desired wells were washed with PBS before adding 100 μL trypsin/EDTA and incubating at 37°C for 10 minutes. Then, 100 μL of ES media was added to the wells and the cells were dispersed with a pipteman. The contents of the well was then split 1:1 into wells of a 48-well plate with mitoC-treated MEFs (the master plate) and the remaining 100 μL to a 48-well plate without MEFs (the DNA plate), both with ES media.

When the master plate had grown to confluency, the wells were rinsed with PBS, incubated with 100 μL trypsin/EDTA at 37°C for 10 minutes, and dispersed with 100 μL ES media before adding 200 μL of 2 × freezing media (appendix) to the wells and swirling to mix. The plate was then wrapped in parafilm and placed in a Styrofoam box at

-80°C. Alternatively, if wells remained that were not ready to freeze, the wells needing to be frozen were transferred to a new 48-well plate and labeled before freezing.

When wells of the DNA plate had grown to maximum confluency they were lysed with 300 µL Lysis Buffer and 1 mg/mL Proteinase K overnight at 37°C. To purify the DNA, the lysate was transferred to an eppendorf tube the following day and an equal volume of phenol:chloroform:isoamyl alcohol (24:24:1) was added. The tubes were shaken for approximately 1 minute and then centrifuged for 4 minutes. The aqueous layer was transferred to a new tube containing 1.2 mL of isopropanol and the tubes were shaken again. The DNA was spooled with a fired capillary tube, dipped into 80% EtOH, and placed into a new eppendorf tube. After the EtOH had evaporated, 50 µL TE was added and the DNA was allowed to dissolve for several hours before removing the fired glass capillary tube. The DNA was incubated at 37°C overnight to completely dissolve.

Additionally, collaboration with Dr. Mario Capecchi at the University of Utah is underway to generate nBmp2-ko mice by microinjecting targeted ES cells into blastula-stage host embryos. For this technique, the targeting vector was electroporated into mouse 129/Bl6 G4-56 ES cells and DNA was isolated as explained above and analyzed by Southern blot as detailed below.

Southern Blot Analysis

Successfully targeted loci should contain an additional *Drd*I site such that upon digestion and Southern blot analysis, a 6.1-kb band would be apparent rather than the wt-13.6 kb band (Fig. 12). Once the DNA had completely dissolved, a digestion reaction was set up with 25 µL of ES DNA, 19 µL water, 5 µL of 10 × buffer 4, and 1 µL (5 units)

*Drd*I (New England Biolabs, Ipswich, MA). The reaction was incubated overnight at 37°C. The following morning, an additional 1 μL of *Drd*I was added to the reaction and allowed to incubate for at least 1 hour more. The digested DNA was then separated on a 0.7% TAE agarose gel at approximately 60 V for 4-5 hours. After electrophoresis, the DNA was depurinated by soaking the gel in 0.2 N HCl for 30 minutes, rinsed in water, and then denatured by soaking the gel for 30 minutes in 1.5 M NaCl/0.5 N NaOH. After these treatments, the gel was neutralized by soaking in 1.5 M NaCl /0.5 M Tris-HCl, pH 7.0 for 45 minutes.

After these treatments, the DNA was transferred to a nylon membrane using the capillary transfer method. The membrane was pre-wet in water and then soaked in 10 × SSC (1.5 M NaCl, 0.15 M NaCitrate ,pH 7.0) for 5 minutes. The transfer was set up as follows, from bottom to top: a large sponge soaking in 10 × SSC, 2 pieces of Whatman paper, the gel, the membrane, 2 more pieces of Whatman paper cut to the size of the gel, 6 cm of paper towels cut to the size of the gel, and a weight. The transfer proceeded overnight. The following day, the membrane was rinsed in 5 × SSC for 5 minutes and then baked at 80°C for 2 hours before a pre-hybridization incubation with Hybrisol (Chemicon, Temecula, CA) for 1 hour at 42°C.

The 3′ flanking Bmp2 southern probe was made by PCR amplification of a region outside of the targeting vector but contained within the fragment created by *Drd*I digestion. The primers used were Bmp2southFor: gccctctcgagCTCAATAGCTCTGGGCCTTG and Bmp2southRev: ttatagcggccgcATCTCAGCATGGAGCCTGTC. These primers amplified a 720-bp region and contained a *Xho*I and a *Not*I restriction site that were used to clone the amplicon into

pBS SK^+. Before labeling, these enzymes were also used to remove the probe from the plasmid backbone. The digestion reaction was separated by gel electrophoresis and the probe was gel-purified using the Qiagne Qiaex II gel extraction kit. The Roche hexanucleotide labeling mix was used to label the probe according to manufacturer's protocol (Roche, Indianapolis, IN). Briefly, 80 ng of the purified, linearized DNA in 9 μL total volume was boiled for 10 minutes and then placed into an ice water bath for an additional 10 minutes. Once cooled, 3 μL 0.5 mM dNTP mix (minus dCTP) and 2 μL Hexanucleotide mix were added to the reaction, followed by the addition of 50 μCi α-^{32}P dCTP and 1 μL Klenow fragment. The reaction was then incubated for 40 to 90 minutes before stopping the reaction with the addition of 2 μL 0.2 M EDTA.

Next, the unincorporated labeled nucleotides were purified from the labeled probe using Roche Quick Spin columns as follows. The buffer in the columns was drained by gravity flow before centrifugation at 1100 × g for 2 minutes in a swinging-bucket rotor. The labeling reaction was brought up to a total volume of 60 μL with water and added to the column. The labeled probe was eluted by centrifugation at 1100 × g for 4 minutes and then a 2 μL sample was counted with a scintillation counter. The appropriate volume of labeled probe was boiled for 10 minutes, placed on ice for 5 minutes, and then added to the hybridization canister already containing the membrane(s) and Hybrisol. A total of 2-8 $\times 10^6$ cpm/mL was used for the Southern blots.

After an overnight hybridization, the membranes were washed at 55°C as follows: 5 minutes and then 30 minutes in 2 × SSC, 2% SDS followed by two 15-minute washes in 1 × SSC, 2% SDS. The membrane(s) were then sandwiched between layers of plastic wrap and placed in an audoradiography cassette with film.

Thawing targeted ES cells

For the AV3 cells here at BYU, when the DNA from the 48-well plates had been screened for recombinant clones, the plates containing the targeted clones were thawed by floating them in a 37°C water bath. When thawed, 500 μL ES media, containing G418, was added to the appropriate well and gently mixed. This cell suspension was centrifuged and the media was aspirated before resuspending in fresh ES media containing G418. The cells were plated onto a 3.5-cm dish containing Mito-C treated *Neo*^{r} MEFs. When confluent, this dish was split onto a 6-cm dish and a 3.5-cm dish of Mito-C treated *Neo*^{r} MEFs, plus a 3.5-cm dish without MEFs for DNA isolation to verify the colony by repeating the Southern analysis. When confluent, the 6-cm dish and the 3.5-cm dish were split onto 6 6-cm dishes. Once the cells had reached confluency on these plates, the cells were divided into 30 cryogenic vials and stored in a liquid N_2 tank. When the DNA plate was confluent, the DNA was isolated and analyzed via Southern hybridization as described above.

Morulae Aggregation

Pregnant Mare Serum (PMS) and human chorionic gonadotropin (hCG) was administered to three- to four-week-old CD1 female mice to induce superovulation before mating with CD1 males. After two-and-one-half days (embryonic day 2.5 or E2.5) the morulae were collected by removing the oviducts of the superovulated females and flushing them under a dissecting microscope with a filed 30-guage needle and M2 media (recipe in appendix). The morulae were then transferred through a series of acid tyrode washes (Millipore, Billerica, MA) with a mouthpipette in order to remove the zona

pellucida. Each dezoned morulae was then neutralized in M2 media and placed into a divot in a previously-prepared tissue culture dish to await addition of ES cells.

Three days prior to the preparation of the morulae, targeted frozen transgenic stem cells were thawed and cultured in 20% ES cell media for two days. The day before aggregation, the cells were seeded into a new 3.5-cm dish and allowed to grow overnight. On the day of aggregation, the cells were subjected to a light trypsin treatment in order to allow removal from the dish while maintaining a degree of cohesion between cells. Clusters of 4 to 12 ES cells were added to each divot containing a prepared morula. After incubating overnight at 37°C, the ES cells and the morulae that had merged were implanted into a pseudo-impregnated female. These Swiss Webster (SW) surrogate mothers were mated with vasectomized SW males two-and-one-half days previous to implantation in order to induce a state of pseudo-pregnancy. Chimeric embryos were surgically implanted into uterine horns of the pseudo-pregnant females.

Generation of nBmp2-ko mice

It was determined that the AV3 ES cells used for gene targeting here at BYU were not suitable for use in the morulae aggregation procedure. Consequently, we collaborated with Dr. Mario Capecchi at the University of Utah to target 129/Bl6 G4-56 ES cells and use them for microinjection into Bl6 host embryos in order to generate chimeric mice. Fifteen chimeras were born, all of which were substantially (over 80%) composed of cells that derived from the targeted ES cells. When the chimeric mice have reached sexual maturity, the males will be intercrossed with Bl6 females. The chimeric animals are composed of cells both from the F1 host embryos from a Bl6 × CBA cross

and the agouti ES cells. Thus, the resulting embryos will be fertilized from sperm derived from either the host embryo or the targeted stem cell line. As the stem cells are heterozygous for the Bmp2 allele, 50% of the progeny will carry the modified Bmp2 allele whereas 50% will be wild type. Since black G4 ES cells were used for targeting, the black pups should also be checked. Excision of the *Neo* cassette will take place in the heterozygous males as the testes specific promoter is activated and the Cre recombinase is expressed. Intercrossing heterozygous mice will generate mice homozygous for the nBmp2-ko allele at 25% frequency.

Genotyping

A PCR/restriction digest assay will be used to genotype the nBmp2-ko mice. PCR on genomic DNA using the NLSmutgenotypingFor (GGCCCATTTAGAGGAGAACC) and NLSmutgenotypingRev (CATGCCTTAGGGATTTTGGA) primers will generate a 390 bp amplicon. Amplicons containing the **KR**EKRQAKHKQ**RKR**L**K**S to **KR**EKRQAKHKQ**AAA**L**K**S mutation will contain a *Cfr*12I restriction site and will be subsequently cut into 209-bp and 180-bp fragments. The following parameters have worked well for this assay in genotyping ES cells.

The 390-bp genotyping amplicon was amplified (Invitrogen PLATINUM *Pfx* DNA Polymerase kit) using reaction mixtures containing 5 µL 10x *Pfx* Amplification Buffer, 1.5 µL of 10 mM dNTP mix, 1 µL 50 µM $MgSO_4$, 1 µL of 10 µM NLSmutgenotypingFor primer, 1 µL of 10 µM NLSmutgenotypingRev primer, 2 µL of purified genomic DNA, 0.5 µL 2.5 U/µL PLATINUM *Pfx* DNA Polymerase and 38 µL of nanopure water. The following cycling parameters were followed: 94°C for 5 minutes,

then 34 cycles of 94°C for 25 sec, 55°C for 30 sec, and 68°C for 30 sec. After completion of the PCR reaction, 1 μL (10 units) of *Cfr*12I (Fermentas, Hanover, MD) was added directly to the reaction and incubated at 37°C for 1 hour. Following this digestion reaction, the DNA was fractionated on a 1% agarose TBE gel. Using the O'GeneRuler 50 bp DNA Ladder (Fermentas, Hanover, MD) as a reference makes it easy to distinguish between the mutant 209/180-bp band and the wild-type 390-bp band.

Zebrafish

We chose to use morpholinos to block translation of nBmp2. When base paired at the translational start site, morpholinos prevent initiation of translation. When annealed to mRNA more than 30 bases downstream of the start site, however, the morpholinos are displaced by the ribosome and have no effect on translation (Gene Tools, LLC Targeting Guidelines, http://www.gene-tools.com/node/18). This means that a morpholino targeted to the downstream alternative start codon of Bmp2 will decrease production of the cytoplasmically-translated nuclear variant without affecting translation at the upstream start codon that produces secreted Bmp2.

All experiments were performed in wild-type zebrafish embryos (Tubingen AB) raised at the University of Utah Centralized Zebrafish Animal Resource Center (CZAR) and in collaboration with Dr. Richard Dorsky. We designed a morpholino antisense oligonucleotide (MO, Gene Tools, LLC) directed against the sequence around the putative alternative start codon of zebrafish bmp4 to block translation of zebrafish nbmp4 (nBmp4-MO): 5′-TGGGACGCCTTTGCAGGCCAAACAT-3′. A standard control MO was also used for injections: 5′-CCTCTTACCTCAGTTACAATTTATA-3′. The MOs were

resuspended in Danieau's buffer (58 mM NaCl, 0.7 mM KCl, 0.4 M $MgSO_4$, 0.6 mM $Ca(NO_3)_2$, 0.5 mM HEPES, pH 7.6) and diluted to 2 mg/mL for injections. The MOs were injected at the single-cell stage and embryos were allowed to develop until hatching. Phenotypes were examined throughout development using a dissecting microscope.

In vitro transcription/translation of zebrafish bmp4

To test the specificity of our morpholino, nBmp4-MO, *in vitro* we constructed zebrafish bmp4 expression vectors and used them for *in vitro* transcription/translation experiments. To construct these plasmids, RNA was extracted from wild-type zebrafish by homogenizing embryos in TRIzol (Invitrogen, Carlsbad, CA) with 10-15 passes through a 22-guage needle. A chloroform extraction was performed by adding an equal volume of chloroform, vortexing briefly, incubating at room temperature for 10 minutes, and centrifuging at 11500 × g for 15 minutes at 4°C. The aqueous layer was put in a new tube and an equal volume of isoproanol was added. After a 10 minute room-temperature incubation, the RNA was collected by centrifugation at 11500 rcf for 10 minutes at 4°C. After washing with 75% EtOH, the RNA was further purified by using the Qiagen RNeasy Kit according to the manufacturer's protocol.

To construct the expression vectors, the iScript cDNA Synthesis Kit (Bio-Rad, Hercules, CA) was used for reverse transcription of bmp4 according to manufacturer's protocol. The cDNA was used for PCR amplification of full-length bmp4 and a nuclear-only version of bmp4 that started at the downstream ATG. Primers were used that would include a *Bam*HI and a *Xho*I restriction site at either end of the amplicons for cloning into $pCS2p^+$ (Richard Dorsky, University of Utah).

Zebrafish bmp4 protein was synthesized *in vitro* with the incorporation of [^{35}S]methionine employing the TNT Coupled Wheat Germ Extract System (Promega, Madison, WI) according to manufacturer's instruction. To test the specificity of the nBmp4-MO, 10 μg was included in some reactions. In order to visualize the products, 7 μL of the reaction was boiled for 5 minutes with 20 μL 2× Laemmli Sample Buffer and 5% β-mercaptoethanol before separating by SDS-PAGE and visualizing by autoradiography.

RESULTS

Nuclear Localization of putative NLS/GFP fusion constructs

We first gained interest in nuclear Bmp2 when it emerged as a possible DNA-binding protein from two separate experiments routinely performed in our lab to identify possible transcription factors for cartilage-specific collagen genes: the yeast one-hybrid screen and DNA affinity chromatography followed by mass spectrometry. Having this secreted protein identified as a possible DNA-binding protein in two separate assays led us to analyze its amino acid sequence in search of NLSs. Indeed, analysis of the Bmp2 amino acid sequence using the PSORT II program identified three potential NLSs. NLSa (PELGRKK) and NLSb (PLHKREK) are monopartite signals located within the propeptide region, NLSa at the N-terminal end and NLSb at the C-terminal end. NLSc (**KR**EKRQAKHKQ**RKR**L**K**S) is a bipartite NLS that spans the site of proteolytic cleavage between the propeptide and mature peptide (Fig. 1).

To test the functionality of each of the putative NLSs identified by PSORT II, each was fused to the C-terminal end of green fluorescent protein (GFP) to determine

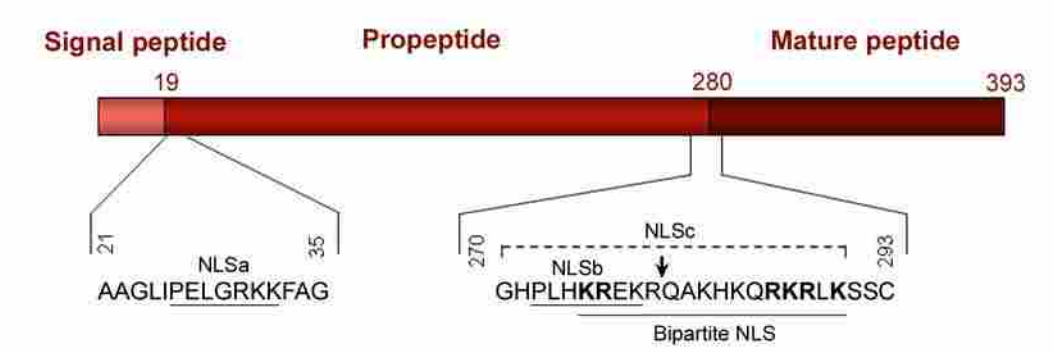

Figure 1. Schematic of the Bmp2 preproprotein. Map of the rat Bmp2 preproprotein showing the signal peptide, propeptide, and mature chain. The amino acid sequence and location of each predicted NLS is underlined, and the site of proteolytic cleavage is marked by an arrow. Critical amino acids in the bipartite NLS are shown in bold.

whether the NLS could direct GFP to the nucleus. The fusion constructs were transiently transfected into rat chondrosarcoma (RCS) cells, and cells were stained with the DNA-specific stain TO-PRO-3 iodide to visualize nuclei. Neither NLSa (PELGRKK) nor NLSb (PLHKREK) produced nuclear localization of GFP. Rather, GFP (a 26-kDa protein) fused to the short NLSs was distributed throughout both the cytoplasm and the nucleus as would be expected for a protein that is small enough (<30-40 kDa) to diffuse through nuclear pores (Adam, 2001; Cubitt et al., 1995) (Fig. 2A).

Because the two short putative NLSs bracket the free propeptide that would be released upon proteolytic cleavage of the Bmp2 proprotein, we investigated whether the two NLSs might cooperate to transport the free propeptide to the nucleus. We built a construct in which the N-terminal putative NLSa was fused to the N-terminus of GFP and the C-terminal putative NLSb was fused to the C-terminus of GFP. Transient transfection of this construct into RCS cells revealed that even together, the two short NLSs failed to produce nuclear localization of GFP (Fig. 2A).

Finally, the putative bipartite NLSc, also containing three of the amino acids of NLSb -PLHKREKRQAKHKQRKRLKS, was fused to the C-terminus of GFP. Transient transfection of this expression plasmid into RCS cells produced clear and unmistakable nuclear localization of GFP, indicating that the predicted bipartite NLSc is indeed functional (Fig. 2A).

To determine whether the intact bipartite NLS was functional in the context of the entire Bmp2 proprotein we built another fusion construct, this time designed to express the entire Bmp2 proprotein, including the signal peptide, with GFP fused to its C-terminus. Transient transfection of this wtBmp2/GFP plasmid into RCS cells produced

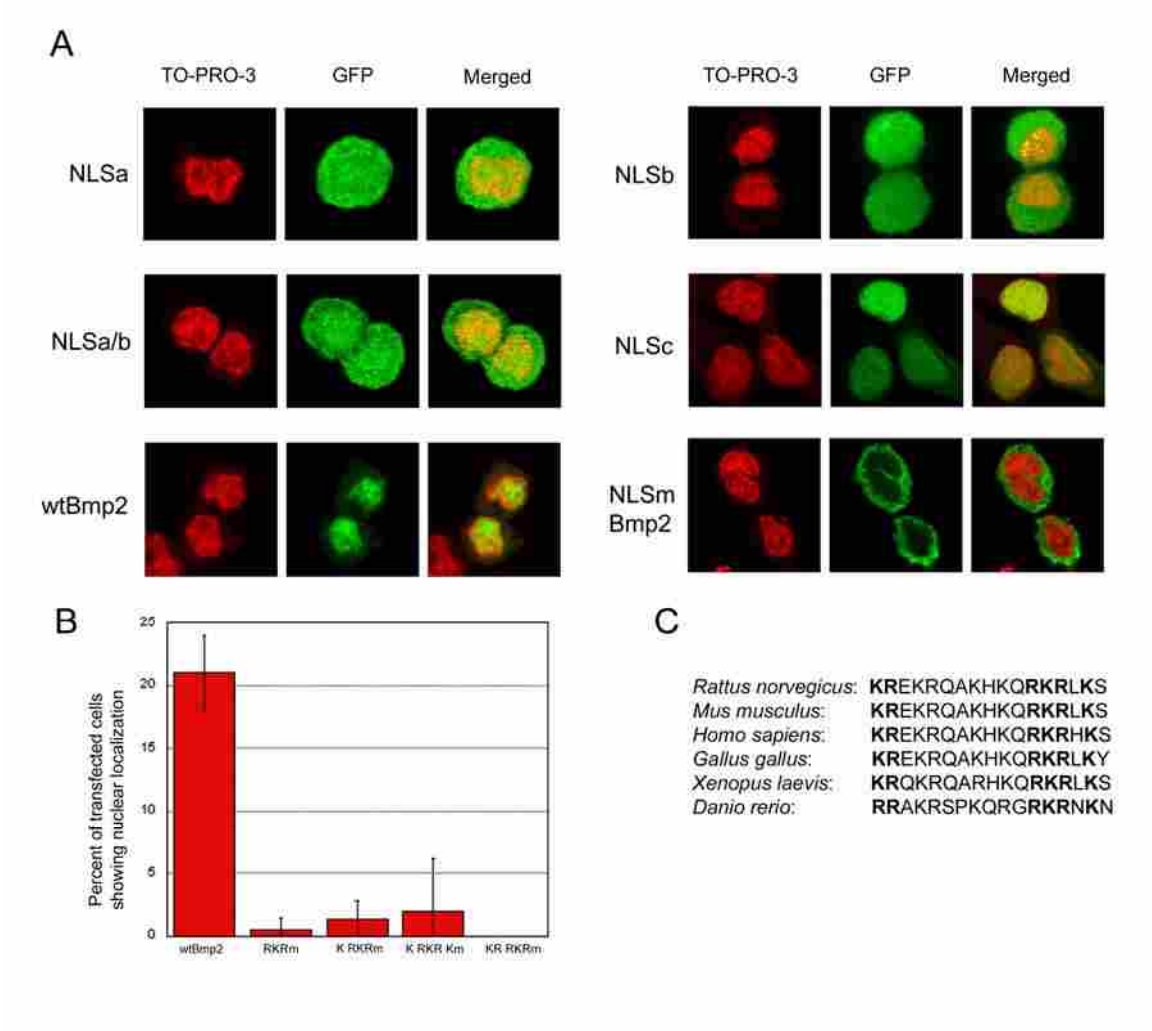

Figure 2. Bmp2 contains a functional bipartite NLS that overlaps the site of proteolytic processing. (A) To test the ability of each predicted NLS to direct GFP to the nucleus, GFP/NLS fusion constructs were built. These expression vectors were transfected into RCS cells, and GFP localization (green) was visualized using laser confocal microscopy. Nuclei were stained with TO-PRO-3 (red). Neither NLSa nor NLSb directed nuclear localization, even when one was fused to each end of GFP (NLSa/b). Instead, GFP diffused throughout the cytoplasm and nucleus. The bipartite NLSc, in contrast, directed strong nuclear localization. To determine whether the bipartite NLSc is functional within Bmp2, GFP was fused to the C-terminus of the full-length Bmp2 preproprotein (wtBmp2/GFP). In a parallel fusion construct, the bipartite NLSc was mutated (NLSmBmp2/GFP) (**KR**EKRQAKHKQ**RKR**L**K**S was changed to **AA**EKRQAKHKQ**AAA**L**K**S). Representative images are shown. **(B)** The wild-type fusion construct produced nuclear localization of Bmp2/GFP in 21% ± 3% of transfected cells, while a series of mutations within the bipartite NLSc eliminated nuclear localization. **(C)** Alignment of Bmp2 bipartite NLSc sequences from six different species. The conserved six basic amino acids that characterize this sequence as a bipartite NLS are in bold. *Danio rerio* bmp4 was used for alignment.

striking and unambiguous nuclear localization of the fusion protein in approximately 21% ± 3% of transfected cells, sometimes with areas of high concentration within the nucleus (Fig. 2A). A control expression plasmid expressing GFP only produced diffuse GFP in both the cytoplasm and nucleus of all transfected cells as previously observed by others (Cubitt et al., 1995), verifying that the Bmp2 portion of the fusion protein was required for nuclear localization.

The bipartite NLS is necessary for nuclear localization of Bmp2/GFP

A series of mutations was introduced into the bipartite NLS within the Bmp2/GFP fusion construct to investigate whether the bipartite NLS is the only sequence involved in the nuclear translocation of proBmp2 (**KR**EKRQAKHKQ**RKR**L**K**S changed to **KR**EKRQAKHKQ**AAA**L**K**S, **AR**EKRQAKHKQ**AAA**L**K**S, **AR**EKRQAKHKQ**AAA**L**A**S, and **AA**EKRQAKHKQ**AAA**L**K**S) (Table 1). When transfected into RCS cells, the NLSmtBmp2/GFP fusion constructs all produced 0% nuclear localization of Bmp2/GFP, confirming that the bipartite NLS is sufficient and necessary for nuclear localization and that no other sequence elements can compensate for the absence of the bipartite signal (Fig. 2B). Alignment of the Bmp2 amino acid sequence from six different species including *Rattus norvegicus, Mus musculus, Homo sapiens, Gallus gallus, Xenopus laevis,* and *Danio rerio* revealed that the bipartite NLS is highly conserved (Fig. 2C).

Plasmid Name	Description
1. NLSaGFP	putative NLSa cloned C-terminal to GFP in pCMV/GFP
2. NLSbGFP	putative NLSb cloned C-terminal to GFP in pCMV/GFP
3. NLSa/bGFP	putative NLSa and b cloned to bracket GFP in pCMV/GFP
4. NLScGFP	putative NLSc cloned C-terminal to GFP in pCMV/GFP
5. wtBmp2/GFP	wtBmp2 cDNA cloned N-terminal to GFP in pcDNA3.1/CT-GFP-TOPO
6. KRmBmp2/GFP	**KR**EKRQAKHKQ**RKR**L**K**S mutated to **AA**EKRQAKHKQ**RKR**L**K**S
7. RKRmBmp2/GFP	**KR**EKRQAKHKQ**RKR**L**K**S mutated to **KR**EKRQAKHKQ**AAA**L**K**S
8. K RKRmBmp2/GFP	**KR**EKRQAKHKQ**RKR**L**K**S mutated to **AR**EKRQAKHKQ**AAA**L**K**S
9. K RKR KmBmp2 /GFP	**KR**EKRQAKHKQ**RKR**L**K**S mutated to **AR**EKRQAKHKQ**AAA**L**A**S
10. KR RKRmBmp2 /GFP	**KR**EKRQAKHKQ**RKR**L**K**S mutated to **AA**EKRQAKHKQ**AAA**L**K**S
11. mtBmp2/GFP	**KR**EKRQAKHKQ**RKR**L**K**S mutated to **KR**EK**G**QAKHKQ**RKR**L**K**S
12. HA-wtBmp2	wtBmp2 cDNA cloned N-terminal to GFP in pcDNA3.1/CT-GFP-TOPO
13. HA-RKRmBmp2	Bmp2 cDNA containing the RKR to AAA mutation with an HA tag at the C-terminal end
14. ERmBmp2	Bmp2 in pcDNA3.1 with the signal peptide removed, producing only nBmp2
15. pcDNA3.1	vector used for expression of Bmp2; often used as a negative control
16. Neo mini-targeting vector	contains the neomycin resistant cassette inserted into the nBmp2-ko targeting vector
17. Bmp2 retrieval vector	contains MC1TK and Bmp2 homology arms for subcloning Bmp2 from the BAC using recombineering
18. pACN	contains a PolII promoter driving neo expression and a testes-specific promoter driving Cre expression
19. pACN/PGK-EM7	the PolII promoter has been substituted with the combined PGK-EM7 promoter
20. RP23-384M14	the BAC that contains mouse *Bmp2* from the Black 6 strain
21. NLSmBmp2 BAC	*Bmp2* NLS mutated to **KR**EKRQAKHKQ**AAA**L**K**S in the BAC
22. NLSmBmp2 retrieved plasmid	*NLSmBmp2* subcloned from the BAC into the Bmp2 retrieval vector
23. nBmp2-ko targeting vector	finished vector containing *NLSmBmp2*, the Neo cassette, and the MC1TK coding sequence

Table 1. DNA constructs used in Book I.

Endogenous Bmp2 localizes to the nucleus

To determine if endogenous Bmp2 localized to the nucleus of cultured cells, immunocytochemistry was performed on RCS, BALB/3T3 fibroblasts, 10T1/2 mesenchyme cells, 231 breast cancer cells, 435 breast cancer cells, MCF-7 breast cancer cells, Hep-G2 liver cancer cells, HT29 colon cancer cells, and a primary culture of mouse embryonic fibroblasts (MEFs). Two different anti-Bmp2 antibodies (BMP-2 (N-14):sc-6895, Santa Cruz Biotechnology, Santa Cruz, CA, and Bmp2, ab14933, Abcam, Cambridge, MA) were used to perform the immunocytochemistry and to verify that the results were not an antibody-specific artifact. These experiments revealed that endogenous Bmp2 was in fact localized to the nucleus in a number of tissue culture lines and in a primary cell culture (Fig. 3A and B). Interestingly, the degree of nuclear localization of Bmp2 was not the same in each cell line; most of the tissue lines had distinct nuclear localizations while others, such as RCS cells, did not.

Western blot analysis reveals endogenous Bmp2 in nuclear extracts from cultured cells

To determine the size of nBmp2, nuclear proteins were extracted from non-transfected cell lines and analyzed by western blotting using an anti-Bmp2 antibody. In parallel, nuclear proteins were extracted from cells transfected with an HA-tagged nBmp2 expression vector (ERmBmp2-HA) and were analyzed by western blotting using an anti-HA antibody. Both the anti-Bmp2 and anti-HA antibodies recognized a band that corresponds to the theoretical size of nBmp2, 38.6 kDa (Fig. 4).

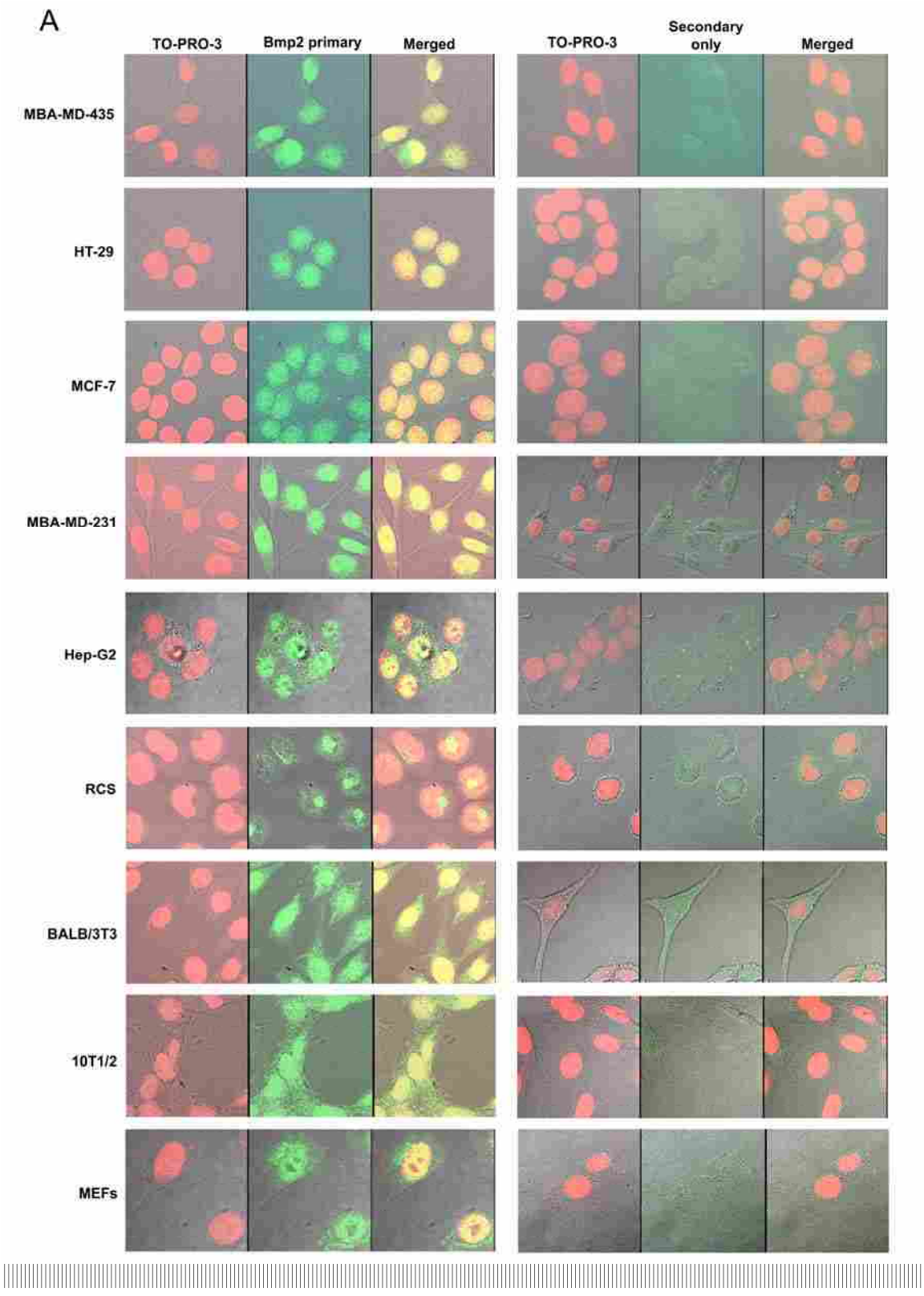
A
TO-PRO-3
Bmp2 primary
Merged
TO-PRO-3
Secondary only
Merged
MBA-MD-435
HT-29
MCF-7
MBA-MD-231
Hep-G2
RCS
BALB/3T3
10T1/2
MEFs

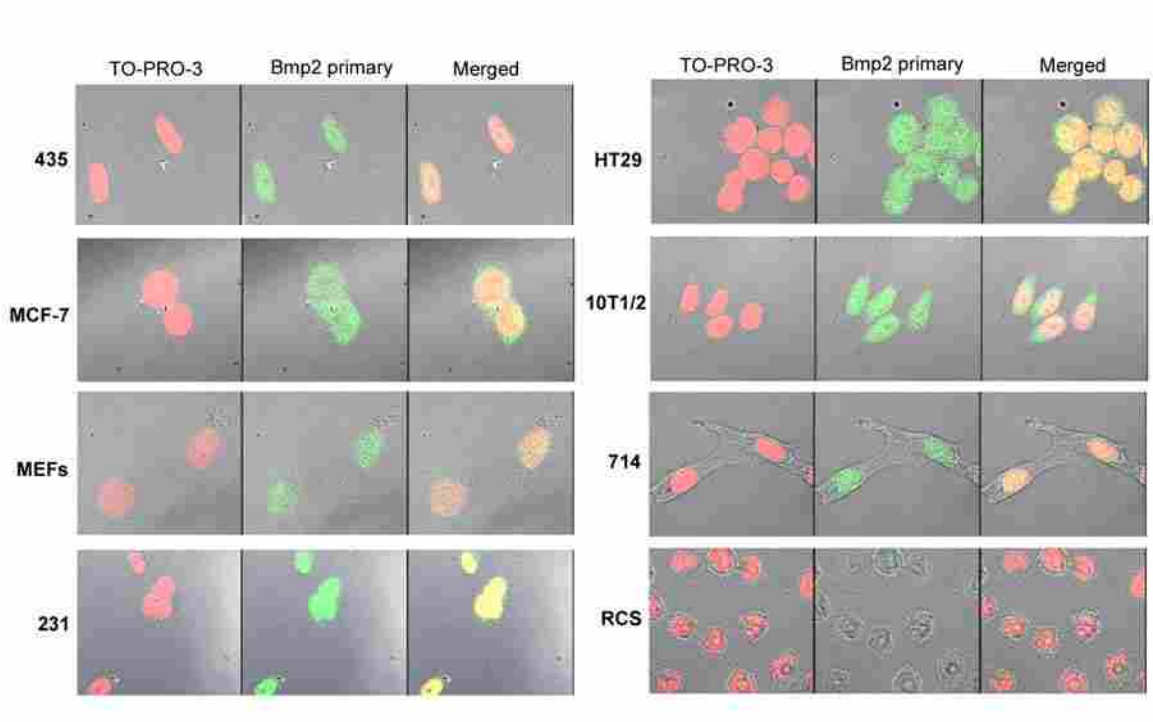

Figure 3. Immunocytochemistry reveals endogenous Bmp2 in the nuclei of cultured cell lines. (A) Non-transfected cells were cultured on slides and immunostained using the anti-Bmp2 antibody (BMP-2 (N-14):sc-6895, Santa Cruz Biotechnology) (green). Nuclei were stained with TO-PRO-3 (red), and cells were examined by laser confocal microscopy. Many cell cultures contained cells with strong nuclear localization of Bmp2. Staining with only the secondary antibody gave no signal, as indicated by the panels on the right-hand side of the figure. **(B)** To rule out the possibility of an antibody-specific artifact, the immunofluorescence staining was repeated using a second anti-Bmp2 antibody (Bmp2, ab14933, Abcam), and similar results were obtained.

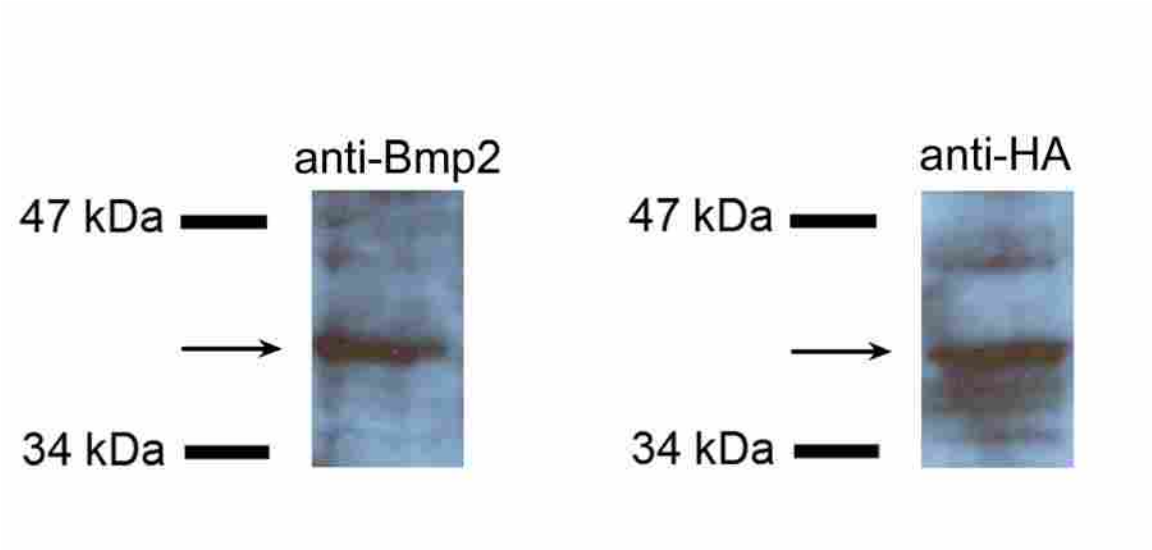

Figure 4. Western blot analysis reveals endogenous Bmp2 in nuclear extracts from cultured cells. (A) Nuclear proteins were extracted from non-transfected cell lines and analyzed by western blotting using an anti-Bmp2 antibody. **(B)** In parallel, nuclear proteins were also extracted from cells transfected with ERmBmp2-HA and were analyzed by western blot using an anti-HA antibody in order to reveal the size of nBmp2. Both the anti-Bmp2 and anti-HA antibodies recognized a band that corresponds to the theoretical size of nBmp2, 38.6 kDa.

Modulation of proteolytic processing does not alter nuclear localization of Bmp2

The cleavage site of Bmp2, R-E-K-R-$^{\downarrow}$, is a consensus site for furin as well as for several related members of the proprotein convertase family (Granjeiro et al., 2005; Thomas, 2002). Furin has been shown to proteolytically activate Bmp4, the Bmp family member most closely related to Bmp2 (Mishina, 2003), but this protease has not previously been shown to activate Bmp2 (Cui et al., 1998). To determine whether furin can cleave Bmp2, we used an *in vitro* protein cleavage assay. We synthesized full length Bmp2 from cDNA *in vitro* with the incorporation of ^{35}S methionine. When separated by SDS-PAGE, the primary protein product was a 43-kDa peptide as expected (Fig. 5A, lane 1). Incubation of the radiolabeled Bmp2 proprotein with 10 units of furin for 1 or 3 hours caused a new peptide to appear at 31 kDa, the predicted molecular weight of the free propeptide following proteolytic cleavage of Bmp2 (Fig. 5A, lanes 2 and 3) (the mature Bmp2 peptide, with a predicted molecular weight of approximately 13 kDa, was not visible because of background radioactivity in that region of the electrophoretic gel). When furin was preincubated with the serine protease inhibitor α_1-PDX, which is a mutated form of α_1-antitrypsin and highly selective in its inhibition of furin (Anderson et al., 1993; Jean et al., 1998), formation of the 31-kDa peptide was not observed, indicating the ability of α_1-PDX to prevent cleavage of Bmp2 by furin (Fig. 5A, lane 4).

In order to examine whether furin plays a role in regulating Bmp2 nuclear localization *in vivo*, we utilized an α_1-PDX expression plasmid that was a kind gift from Dr. Gary Thomas at the Oregon Health Sciences University in Portland, Oregon. We cotransfected this plasmid with the wtBmp2/GFP fusion plasmid into RCS cells to determine whether inhibition of furin activity could increase nuclear localization of the

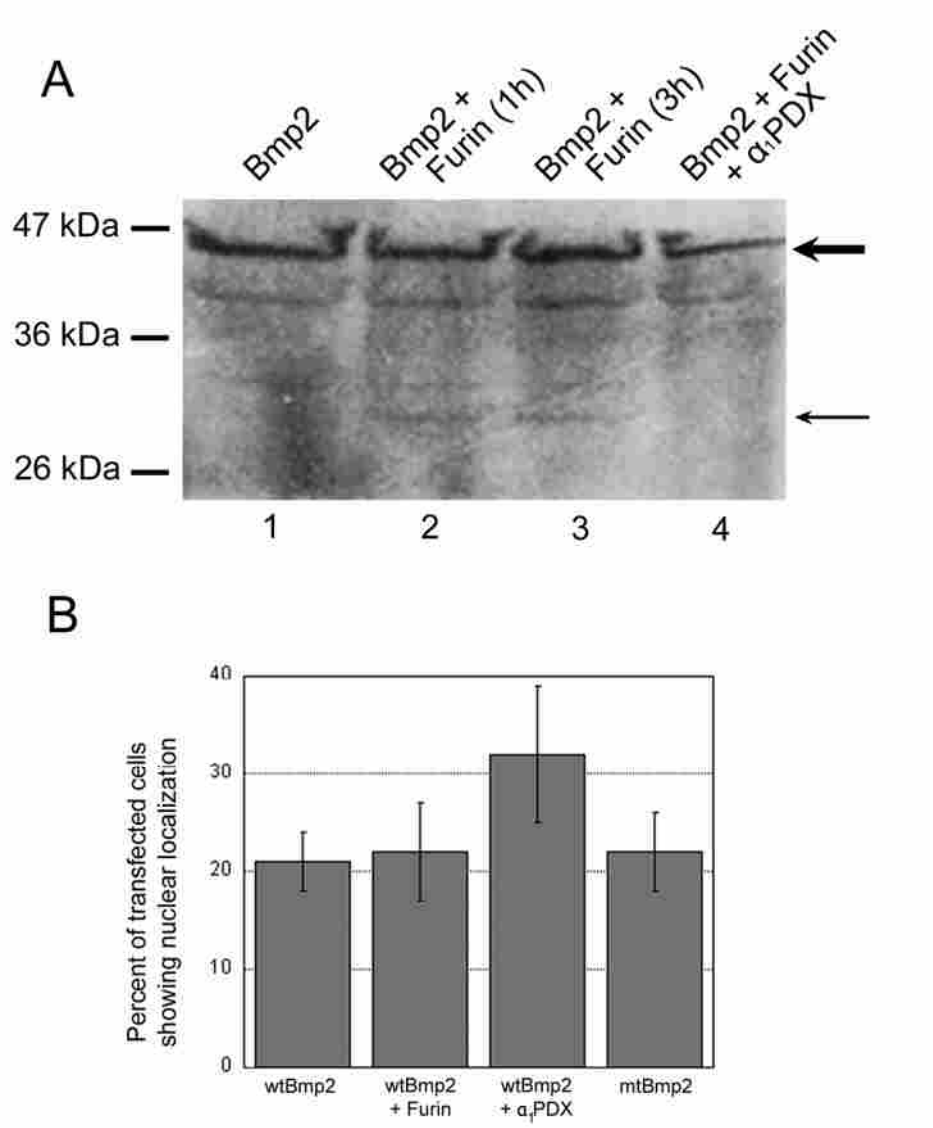

Figure 5. Inhibition of Bmp2 proprotein processing does not increase nuclear localization. (A) *In vitro* synthesis of radiolabeled Bmp2 preproprotein produced the expected 43-kDa protein (lane 1, large arrow). Incubation of this protein with recombinant furin for 1 or 3 hours generated a new protein band at 31 kDa, the predicted size of the combined free Bmp2 signal peptide and propeptide following proteolytic cleavage (lanes 2 and 3, small arrow). Preincubation of the furin with α_1PDX, a serine protease inhibitor that blocks furin activity, prevented the formation of this band (lane 4). **(B)** Furin and α_1PDX expression plasmids were each cotransfected with the wtBmp2/GFP fusion plasmid into RCS cells. Increasing furin expression did not significantly decrease nuclear localization of Bmp2/GFP ($p = 0.810$), nor did inhibiting furin activity with α_1PDX significantly increase nuclear localization ($p = 0.145$). Mutation of the Bmp2 cleavage site to make it unrecognizable by furin or any related proprotein convertase (mtBmp2/GFP) also failed to significantly increase nuclear localization of Bmp2/GFP ($p = 0.652$).

wtBmp2/GFP fusion protein. Transfection of the wtBmp2/GFP expression plasmid alone resulted in nuclear localization of the fusion protein in 21% ± 3% of transfected cells. Co-transfection with the α_1-PDX expression increased nuclear localization of the wtBmp2/GFP fusion protein to 32% ±7%, but the increase was not statistically significant ($p = 0.145$) (Fig. 5B). We also used a furin expression vector in a cotransfection with the wtBmp2/GFP fusion construct to investigate whether overexpression of furin could decrease the percentage of cells showing nuclear localization of Bmp2. This resulted in 22% ± 5% of transfected cells showing nuclear localization, an insignificant increase ($p = 0.810$) (Fig 5B).

Since it is possible that other serine proteases besides furin are involved in the proteolytic activation of Bmp2, we constructed a cleavage mutant of Bmp2 that contained a disrupted consensus proteolytic cleavage site (mtBmp2/GFP) but with the essential amino acids in the bipartite NLS intact (KREK**R**QAKHKQRKRLKS was changed to KREK**G**QAKHKQRKRLKS). This mutant could not be proteolytically processed by any member of the proprotein convertase family. This cleavage mutant still produced nuclear localization in 22% ± 4% of transfected cells, statistically similar to the nuclear localization observed in wtBmp2/GFP (0.652) (Fig. 5B). In summary, neither furin overexpression, furin inhibition, nor inactivation of the cleavage recognition sequence produced any significant difference in the nuclear localization of Bmp2/GFP. These results suggest that regulation of proteolytic processing of Bmp2 is probably not the mechanism by which the uncleaved nuclear variant of Bmp2 is produced.

Translation from an alternative, downstream start codon leads to nuclear localization of Bmp2

The results of the cleavage experiments led us to hypothesize that Bmp2 nuclear localization is achieved not through regulating Bmp2 proprotein processing but rather through avoiding the secretory pathway altogether by gaining access to the cytosol for translation. If translated via free ribosomes in the cytosol, Bmp2 would avoid contact with proprotein convertases located in the rER and Golgi, and the Bmp2 bipartite NLS could then be utilized for translocation to the nucleus. It would be possible for Bmp2 to gain access to the cytosol if translation of nBmp2 occurred at an alternative start codon downstream of the signal peptide, thereby allowing it to bypass the rER.

To investigate the possibility of an alternative Bmp2 translational start site downstream of the signal peptide, we examined the nucleotide sequence and found an in-frame ATG surrounded by a partial Kozak sequence starting at nucleotide 236. We used the NetStart 1.0 Prediction program (http://www.cbs.dtu.dk/services/NetStart/) to determine the likelihood that ATG-236 is a functional initiation codon. The program rated ATG-236 with a score of 0.724, second only to the conventional initiator codon at 0.848 (Fig. 6A). In support of our hypothesis that ATG-236 is an alternative start codon, *in vitro* transcribed and translated wtBmp2 in the presence of ^{35}S-methionine produced two major products: the full-length expected band at 43 kDa as well as a minor 37-kDa band that is the predicted size of a protein generated from initiation at ATG-236 (Fig. 5A, lanes 1-4).

To determine if translation initiating from ATG-236 is responsible for the 37-kDa product, the putative alternative start codon (ATG-236) was converted to AAG to prevent

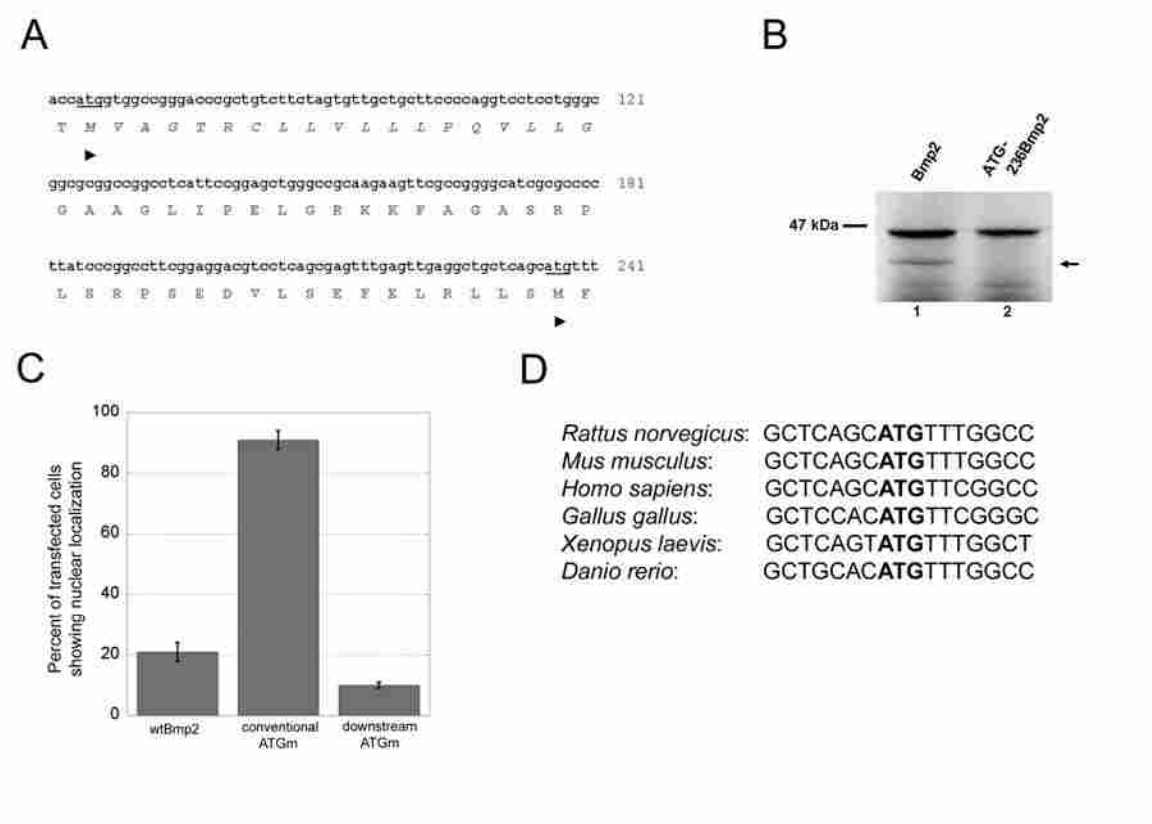

Figure 6. Translation of Bmp2 from an alternative start codon downstream of the signal peptide produces the uncleaved nuclear variant of Bmp2. (A) The N-terminus of the rat Bmp2 protein with corresponding DNA sequence is shown. The conventional start codon 1, as well as the predicted downstream alternative start codon, are marked (►). Amino acids of the signal peptide are shown in italics. **(B)** *In vitro* synthesis of Bmp2 produced the expected 43-kDa protein as well as some lower molecular weight proteins (lane 1). Substitution of the predicted alternative start codon 58 (position 236 in the mRNA) with a non-initiator AAG codon eliminated one of the smaller proteins, indicating that this protein had been initiated at codon 58 (arrow). **(C)** Bmp2/GFP fusion constructs containing ATG to AAG substitutions in either the conventional start codon 1 or the alternative start codon 58 were transfected into RCS cells to examine the effects of these mutations on nuclear localization of Bmp2. Mutation of the conventional start codon (conventional ATGm) to force utilization of the downstream alternative start codon increased nuclear localization dramatically ($p < 0.001$), and mutation of the alternative start codon (downstream ATGm) decreased nuclear localization by half ($p = 0.014$). **(D)** Alignment of the Bmp2 alternative start codon from six different species. The conserved alternative start codons are indicated in bold. *Danio rerio* bmp4 was used for alignment.

its utilization (ATG-236Bmp2). The construct was then transcribed and translated *in vitro* in the presence of [^{35}S]methionine. Mutation of the putative alternative start site ATG-236 abolished the 37-kDa protein product generated from wtBmp2, indicating that ATG-236 is the start site from which translation of the 37-kDa protein is initiated (Fig. 6B).

To study the significance of the alternative translation initiation codons *in vivo*, we mutated the conventional start codon, ATG-65, and the alternative start codon, ATG-236, in the context of the wtBmp2/GFP fusion construct and transfected them into RCS cells. The subcellular localization of GFP was analyzed by fluorescent laser confocal microscopy as described. Mutation of ATG-65 to prevent its utilization and encourage use of any downstream initiation codons, dramatically increased nuclear localization of transfected cells to 91 ± 3% (Fig. 6C). In contrast, mutation of the alternative start codon ATG-236 reduced nuclear localization to only 10% ± 1% of transfected cells (Fig. 6C). These results demonstrate the importance of the alternative start codon ATG-236 for synthesis of the nuclear form of Bmp2 in cultured cells. Alignment of the Bmp2 amino acid sequence from six different species including *R. norvegicus, M. musculus, H. sapiens, G. gallus, X. laevis,* and *D. rerio* revealed that the alternative downstream ATG is highly conserved (Fig. 6D).

Mutating the Bmp2 bipartite NLS does not affect secretion

Having verified the existence of nBmp2 and identified a mechanism for its localization to the nucleus, we were interested in uncovering the function of nBmp2. We determined to generate mice that lack nBmp2 but still produce secreted Bmp2. Previous experiments demonstrated that the bipartite NLS (**KR**EKRQAKHKQ**RKR**L**K**S), which

spans the cleavage site, was responsible for nuclear transport of Bmp2, and thus the amino acid alterations to generate mice lacking nBmp2 should be within this sequence. Altering this sequence was complicated by the fact that the **RKR**-**K** portion of the NLS is within the secreted region of Bmp2; also, the **KR** portion of the NLS overlaps the recognition sequence for the proprotein convertases responsible for cleaving the Bmp2 proprotein. Changing these amino acids had the potential to alter the function of secreted Bmp2 or to prevent processing of Bmp2, in essence creating a Bmp2 knockout mouse.

Previous experiments determined that mutating the **RKR** portion of the NLS would prevent nuclear localization and data reported elsewhere suggested that this mutation would also have minimal effect on the function of secreted Bmp2 (Hillger et al., 2005; Ohkawara et al., 2002). We wanted to determine if mutating the **RKR** portion of the Bmp2 bipartite NLS would affect the processing and secretion of Bmp2. To do this, RCS cells were transfected with either the HA-tagged wtBmp2 (HA-wtBmp2) or RKRm (HA-RKRmBmp2) expression plasmids and allowed to grow for two days before the HA-tagged proteins were immunoprecipitated from the media and subjected to immunoblotting. Both immunoprecipitation/immunoblotting reactions resulted in protein bands slightly lower than the 20-kDa ladder band, indicating that mutating the RKR portion of the bipartite NLS to AAA does not affect proper processing and secretion of Bmp2 (Fig. 7A). Further supporting this visual analysis, the UN-SCAN-IT software program was used to quantitate the relative intensity of the two bands; it determined that the intensity of the band from HA-wtBmp2 transfected cells to be 7042 relative intensity units while the intensity of the band from the HA-RKRmBmp2 transfected cells to be similar at 7011 relative intensity units compared to background levels (Fig. 7B).

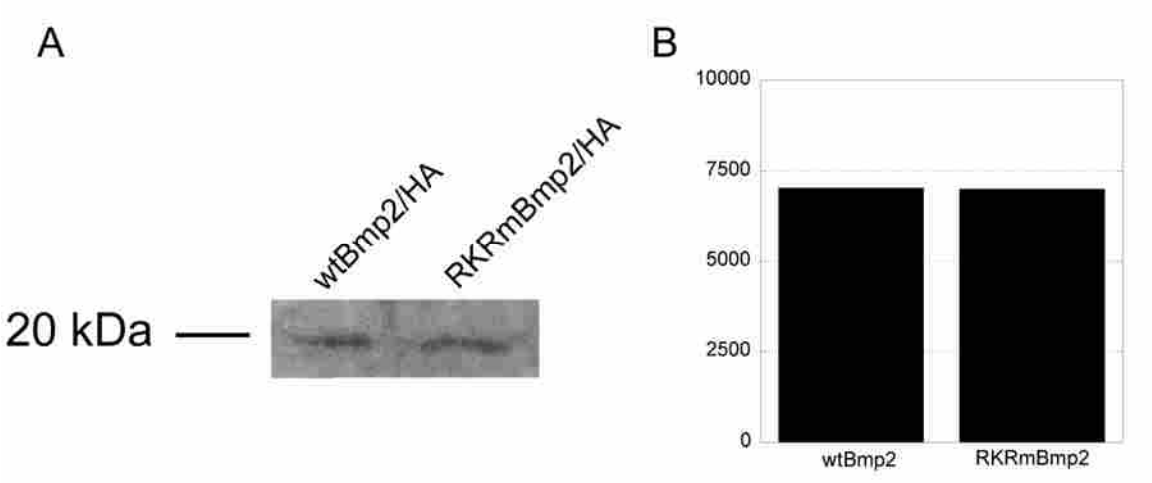

Figure 7. Mutation of the RKR portion of the bipartite NLS does not inhibit secretion of Bmp2. (A) To determine whether mutation of the RKR portion of the bipartite NLS (**KR**EKRQAKHKQ**RKR**L**K**S to **KR**EKRQAKHKQ**AAA**L**K**S) affected cleavage and secretion of Bmp2, the media from RCS cells transfected with either HA-tagged wtBmp2 or HA-tagged RKRmBmp2 was collected. The tagged proteins were immunoprecipitated and analyzed via western blotting using an anti-HA antibody. **(B)** To quantify the band intensities from the western blot, the image was scanned and analyzed by the UN-SCAN-IT program. The intensity of the band from the HA-wtBmp2 transfected cells was 7042 relative intensity units while the intensity of the band from the HA-RKRmBmp2 transfected cells was similar at 7011 relative intensity units.

Microarray and Real-Time PCR

To learn more about the function of nBmp2 in the nucleus, we determined to perform microarray analysis. To do this, we generated a plasmid that exclusively expresses nBmp2 by removing the signal peptide. mRNA was isolated from RCS cells transfected with this plasmid (ERmBmp2) and from RCS cells transfected with the empty expression vector (pcDNA3.1) for comparison. Three biological replicates were used for the gene expression analysis by Assuragen on Affymetrix Rat 230 2.0 genomic arrays. In addition, two of the biological replicates were also re-analyzed by GenUs Biosystems on GE CodeLink Arrays. These analyses indicated that there were over 300 genes that had a p-value of <0.05 and a fold-change of >1.5 fold in either direction and were considered significant. The genes with altered expression clustered largely as genes involved with nervous system development and function, lipid metabolism, immune system functioning, and cancer (Table 2).

Unfortunately, a large proportion of these genes had such low initial expression levels that even after activation, but especially after inhibition, real-time PCR could not be performed on them accurately. As an additional control in our real-time PCR experiments, we used RNA from cells transfected with an expression vector for nuclear GFP. This proved to be a good control, as a few of the genes that were expressed at levels high enough for real-time PCR analysis had differential expression when nuclear GFP was overexpressed. However, of the few genes with expression levels high enough for real-time PCR, two genes, forming binding protein (Fnbp1) and neuron-glia-CAM-related cell adhesion molecule (NrCam), appeared to respond specifically to overexpression of nBmp2. Fnbp1 was down-regulated while NrCam was up-regulated.

Genbank Accession	Official Symbol	Fold Change	Gene Name
NERVOUS SYSTEM			
NM_012825	Aqp4	6.40	aquaporin 4
NM_145777	Olfm3	6.04	olfactomedin 3
NM_199499	Lgi4	5.06	Leucine-rich repeat LGI family, member 4
NM_172324	Elav13	3.23	ELAV (embryonic lethal, abnormal vision, Drosophila)-like 3 (Hu antigen C)
NM_017251	Gjb1	3.20	gap junction membrane channel protein beta 1
NM_017263	Gria4	3.13	Glutamate receptor, ionotropic, 4
NM_012508	Atp2b2	2.80	ATPase, Ca++ transporting, plasma membrane 2
NM_017323	Tr4	2.74	TR4 orphan receptor
NM_012838	Cstb	2.42	cystatin B
NM_022285	Hapln2	2.27	Hyaluronan and proteoglycan link protein 2
NM_130822	Lphn3	2.24	latrophilin 3
NM_012896	Adora3	2.22	adenosine A3 receptor
NM_199397	Panx1	2.16	Pannexin 1
NM_032462	Csen	2.12	calsenilin, presenilin binding protein, EF hand transcription factor
NM_012563	Gad2	-2.08	glutamate decarboxylase 2
NM_017027	Mpz	-2.17	myelin protein zero
NM_012528	Chrnb1	-2.38	Cholinergic receptor, nicotinic, beta polypeptide 1 (muscle)
NM_130816	Fgf11	-2.38	fibroblast growth factor 11
NM_012643	Ret	-2.50	ret proto-oncogene
NM_053601	Nnat	-2.86	neuronatin
NM_012997	P2rx1	-2.94	purinergic receptor P2X, ligand-gated ion channel, 1
NM_138914	Fnbp1	-2.94	formin binding protein 1
NM_053399	Nrtn	-3.03	neurturin
NM_001033680	Syt1	-3.03	Synaptotagmin 1
NM_017001	Epo	-3.13	erythropoietin
NM_133651	Cav	-3.57	caveolin
NM_016989	Adcyap1	-3.57	Adenylate cyclase activating polypeptide 1
NM_031066	Fez1	-3.70	fasciculation and elongation protein zeta 1 (zygin I)
NM_019145	Chrng	-4.35	cholinergic receptor, nicotinic, gamma polypeptide
NM_013104	Igfbp6	-5.00	insulin-like growth factor binding protein 6
NM_031588	Nrg1	-5.00	neuregulin 1
NM_021869	Stx7	-20.00	syntaxin 7
NM_017218	Erbb3	-33.33	avian erythroblastosis oncogene B 3
NM_057184	Chrna6	-50.00	cholinergic receptor, nicotinic, alpha polypeptide 6
LIPID METABOLISM			
AJ225633	Vigilin	1525.59*	High density lipoprotein binding protein
NM_012907	Apobec1	3.96	apolipoprotein B editing complex 1
NM_021596	Dbil5	3.23	diazepam binding inhibitor-like 5
AAZ80296	Serinc2	2.92	serine incorporator 2
NM_022627	Prkab2	2.23	Protein kinase, AMP-activated, beta 2 non-catalytic subunit
NM_173116	Sgpl1	-2.13	sphingosine phosphate lyase 1
NM_031627	Nr1h3	-2.27	nuclear receptor subfamily 1, group H, member 3
NM_031635	Fut2	-2.50	fucosyltransferase 2 (secretor status included)
NM_057186	Hadhsc	-2.70	L-3-hydroxyacyl-Coenzyme A dehydrogenase, short chain
NM_080576	Apoa5	-3.13	apolipoprotein A-V
NM_133651	Cav	-3.57	caveolin
NM_053922	Acacb	-4.17	acetyl-Coenzyme A carboxylase beta
*Vigilin mRNA was virtually undetectable in control samples, accounting for the dramatic fold-increase			
IMMUNE SYSTEM			
NM_017317	Rab27a	3.77	RAB27A, member RAS oncogene family
NM_031044	Hnmt	2.13	histamine N-methyltransferase
NM_032462	Csen	2.12	calsenilin, presenilin binding protein, EF hand transcription factor
NM_016995	C4bpb	2.06	complement component 4 binding protein, beta
NM_013169	Cd3d	2.04	CD3 antigen delta polypeptide
NM_153466	Gzmg	-2.13	granzyme G
NM_001033913	Gimap5	-3.23	GTPase, IMAP family member 5
NM_012645	RT1-Aw2	-3.33	RT1 class Ib, locus Aw2
NM_017330	Prf1	-4.00	perforin 1 (pore forming protein)
NM_001079898	RatNP-3b	-4.35	defensin RatNP-3 precursor
CANCER			
NM_053927	Epb4.1l3	2.82	erythrocyte protein band 4.1-like 3
NM_130741	Lcn2	2.51	lipocalin 2
NM_012838	Cstb	2.42	cystatin B
NM_031632	Casp9	2.06	caspase 9
NM_130816	Fgf11	-2.38	fibroblast growth factor 11
NM_012927	Cdh6	-2.50	Cadherin 6
NM_012643	Ret	-2.50	ret proto-oncogene
NM_012561	Fst	-3.03	follistatin
NM_022603	Fgfbp1	-3.57	fibroblast growth factor binding protein 1
NM_133651	Cav	-3.57	caveolin
NM_017218	Erbb3	-33.33	avian erythroblastosis oncogene B 3

Table 2. Selected genes showing greater than 2-fold change in gene expression in response to nBmp2.

Construction of the nBmp2 knock-out targeting vector

The nuclear Bmp2-knockout targeting vector was constructed using recombineering (recombination-mediated genetic engineering) (Copeland, Jenkins et al. 2001). This technique uses a modified *E. coli* strain containing defective λ prophage recombination genes (strain SW102). A temperature-sensitive repressor controls the expression of the λ recombination genes allowing for induction of recombination to occur upon heating the cells. The steps taken to construct the targeting vector included mutating the bipartite NLS of *Bmp2* in the BAC, subcloning the mutated *Bmp2* gene in to a plasmid, and targeting this *NLSmBmp2* with a modified ACN Neo selection cassette (Fig. 8).

***Mutating the bipartite NLS of* Bmp2**

In order to mutate the bipartite NLS of Bmp2, the *galK* positive/negative selection was used to first replace the target amino acids with the *galK* gene, and then replace the *galK* gene with the desired mutation (**KR**EKRQAKHKQ**RKR**L**K**S was changed to **KR**EKRQAKHKQ**AAA**L**K**S) as described in Warming et al. PCR on BAC DNA with the inserted *galK* was used to determine if *galK* had recombined into the desired location. If *galK* had inserted at the NLS, the amplicon would be ~2.6 kb; if *galK* had not inserted into the proper location, the amplicon would only be ~1.4 kb. The PCR assay revealed that all colonies had successful recombination of *galK* into the desired location (Fig. 9A).

The next step was to use double-stranded oligos to replace *galK* with the desired mutation. These oligos were 100-bp long and contained nucleotides coding for the desired NLS mutations (three Ala codons) along with homology to the surrounding sequence in *Bmp2.* The PCR method described above was used to determine if the *galK*

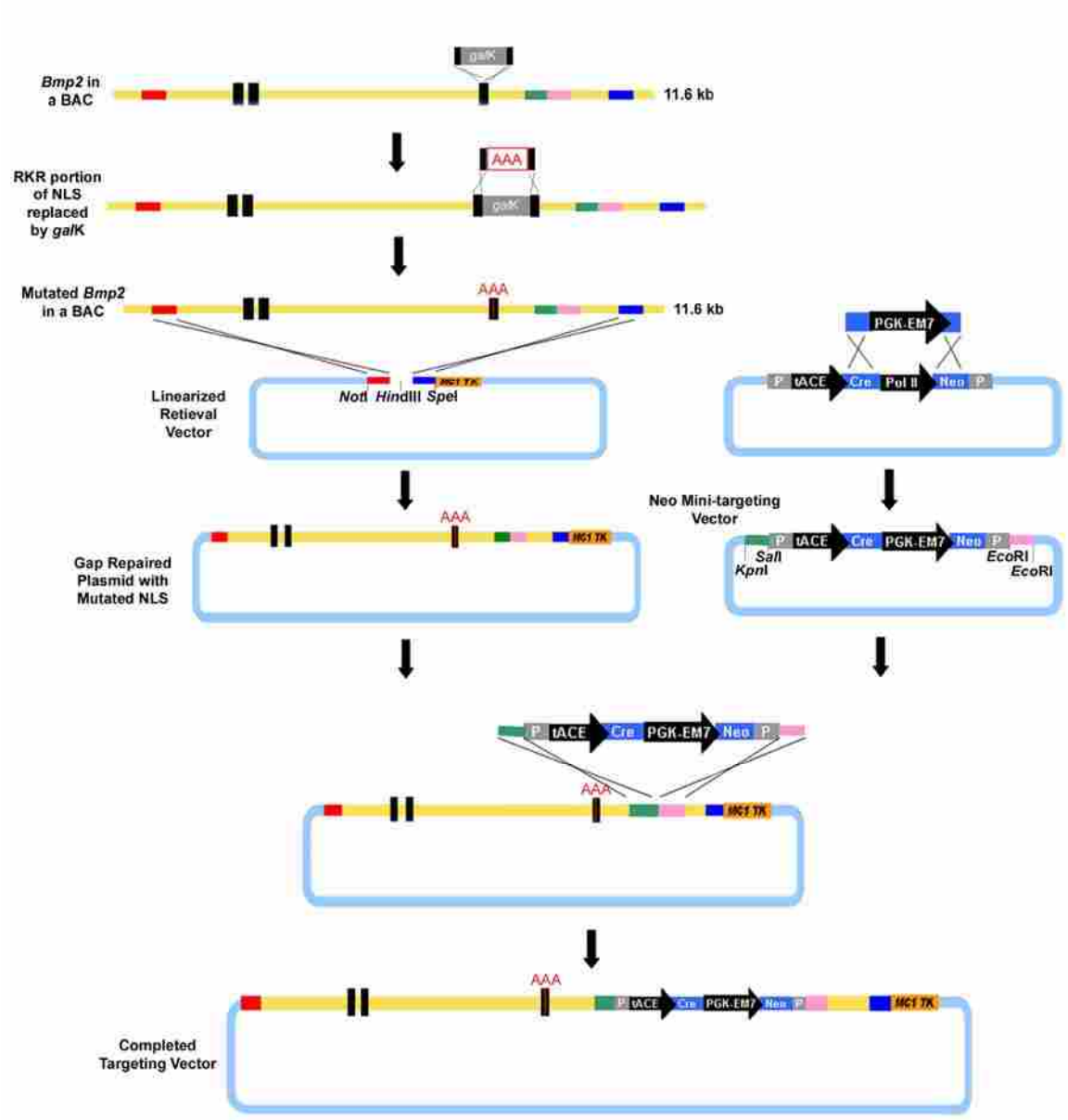

Figure 8. Construction of the nBmp2-ko targeting vector using recombineering. The bipartite NLS of *Bmp2* in the BAC RP23-384M14 was mutated by using the *gal*K positive/negative selection scheme. The *gal*K amplicon included 50-bp homology arms homologous to the areas surrounding the codons that code for the RKR portion of the NLS (indicated by black bars) and was electroporated into induced SW102 cells already containing the BAC. Once correctly-targeted clones were identified, the *gal*K gene was replaced with codons for three Ala residues via recombineering. Cells still containing the *gal*K gene were selected against by using 2-deoxy-galactose. Using recombineering, the *Bmp2* gene that carried the mutated NLS was subcloned into a plasmid containing *MC1TK* using recombineering. The 300-bp homology arms used for this step are indicated as red and blue boxes. The final step replaced the *PolII* promoter from the ACN *Neo* cassette with a dual prokaryotic-eukaryotic promoter *PGK-EM7* so the *Neo* gene

would also be expressed in *E. coli*. This Neo mini-targeting vector was then recombined into the *Bmp2* gene using homology arms indicated with green and pink boxes to produce the completed targeting vector.

gene had successfully been replaced during recombineering. Of the 10 colonies that were grown in overnight culture from this plate, all no longer contained the *galK* gene (Fig. 9B). All 10 also contained the desired NLSm sequence as determined by sequencing (Fig. 9C).

Retrieving NLSm* Bmp2 *from the BAC

In order to subclone the mutated Bmp2 gene from the BAC into a plasmid, cells containing the NLSm BAC were grown, induced for recombination, and electroporated with 40 ng of the linearized Bmp2 retrieval vector containing the appropriate homology arms and *MC1TK*. The following day, the ratio of colonies on the induced plate compared to the control (uninduced) plate was large, indicating that recombination had occurred as expected. Plasmid DNA was extracted from overnight cultures of individual colonies from the induced plate and digested with *Bgl*II to identify correctly-recombined plasmids. Of the eight colonies examined, three contained the appropriate bands for the NLSm *Bmp2* retrieved plasmid: 5137 bp, 3575 bp, 2603 bp, 1927 bp, 1853 bp, 986 bp, 425 bp, and 390 bp (Fig. 10). Sequencing of the NLS region verified that these plasmids were indeed correct.

Targeting with* Neo *cassette

The final step in constructing the nBmp2-ko targeting vector was to insert the neomycin selection cassette into the Bmp2 gene in the area that would be the 3′UTR of Bmp2 after transcription. Cells containing the retrieved NLSm Bmp2 plasmid were grown, induced for recombination, and electroporated with the *Neo* mini-targeting cassette. Only three colonies grew, and only two of those colonies were able to grow in culture overnight in the presence of 20 ng/μL kanamycin. After extracting the plasmids

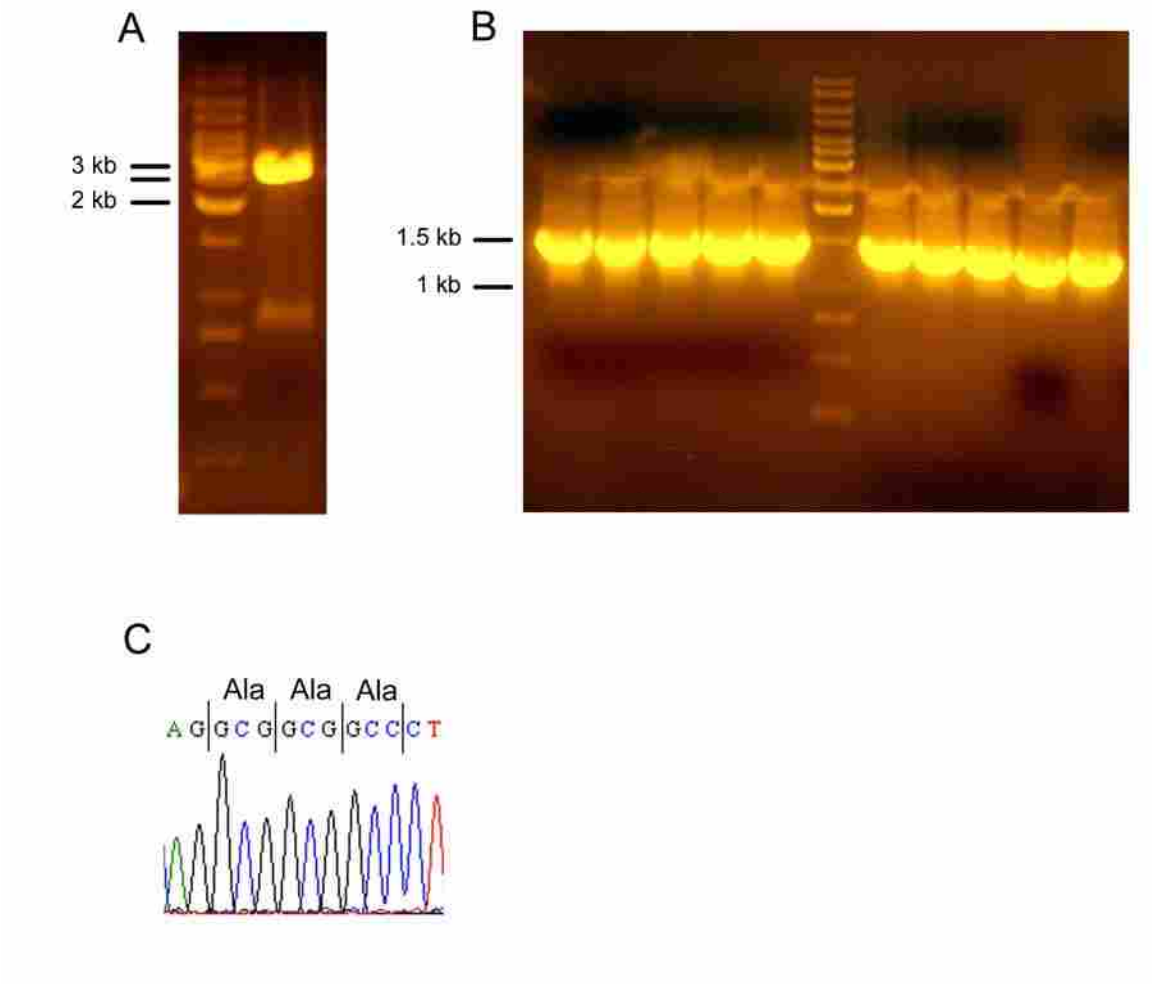

Figure 9. The bipartite NLS of Bmp2 in BAC RP23-384M14 was mutated. Recombineering was used to replace the nucleotides coding for the RKR portion of the bipartite NLS with the *galk* gene, and then to replace the *galk* gene with the nucleotides coding for the three Ala residues (**KR**EKRQAKHKQ**RKR**L**K**S to **KR**EKRQAKHKQ**AAA**L**K**S). **(A, B)** Using primers that flank the bipartite NLS, PCR was used to determine if the *galk* gene was present within that region. **(A)** *galk* had successfully recombined into the bipartite NLS, yielding a 2.6 kb amplicon. **(B)** After the recombineering reaction to replace the *galk* gene with the desired mutation had been performed, PCR was again used to verify that *galk* was no longer present, as indicated by the presence of the 1.4 kb band. **(C)** Sequencing verified that the nucleotides coding for RKR had in fact been exchanged for nucleotides coding for AAA.

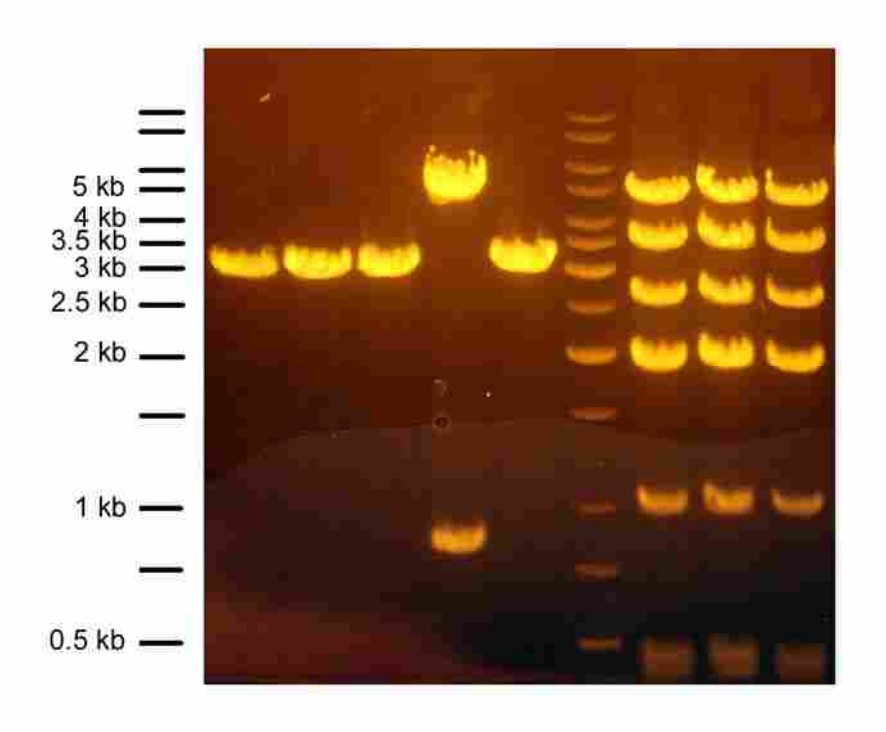

Figure 10. NLSmBmp2 was subcloned from the BAC into a plasmid. After the recombineering reaction to subclone the mutated Bmp2 from the BAC into the retrieval vector containing the *MC1TK* gene, eight plasmid preparations were digested with *Bgl*II. NLSmBmp2 was successfully recombined into the retrieval vector in three of the plasmid preparations as indicated by the presence of the following bands: 5137 bp, 3575bp, 2603 bp, 1927 bp, 1853 bp, 986 bp, 452 bp, and 390 bp.

from the colonies, they were digested with *Bgl*II. A correctly-targeted plasmid would give the following bands: 5137 bp, 4472 bp, 3575 bp, 1927 bp, 1853 bp, 1742 bp, 986 bp, 425 bp, and 390 bp. The NLSm Bmp2 retrieved plasmid would not have the 4472-bp band nor the 1742-bp band but an additional band of 2603 bp (Fig. 11C). Digestion of both of the colonies revealed that they contained a mixture of recombined and un-recombined plasmids since all bands were present (Fig. 11A). To verify this result, the colonies were also digested with *Cla*I. A correctly-targeted plasmid would give the following bands: 10021 bp, 3713 bp, 3213 bp, 1961 bp, and 1599 bp. The untargeted *NLSmBmp2* retrieved plasmid would only have a 10021-bp band and a 6815-bp band (Fig. 11C). Again, digestion of both of the colonies revealed that they contained a mixture of recombined and un-recombined plasmids since all bands were present (Fig. 11A).

To separate recombined clones from the un-recombined, the mixed plasmid preparations were re-transformed into SW102 cells. No colonies were obtained until 10 ng of DNA was used and the entire reaction was plated onto kanamycin plates. Nine colonies were examined with a *Bgl*II digest, and six of them had only the desired, targeted plasmid. This was confirmed by performing two more analytical digests, one with *Xba*I and one with *Pst*I and genotyping the plasmid as described (Fig. 11B).

Southern blot analysis identifies correctly targeted ES cells

The completed nBmp2-ko targeting vector was linearized and electroporated into AV3 ES cells. After selection with G418 and FIAU, the resistant colonies were analyzed by Southern hybridization to identify targeted clones. Successfully targeted loci would

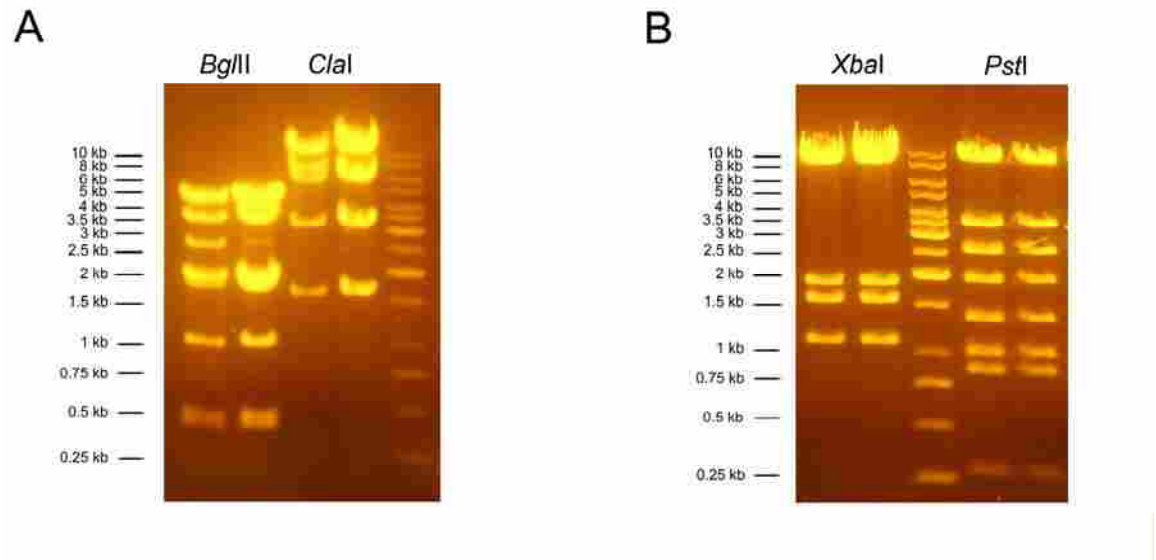

C

*Bgl*II		*Cla*I		*Xba*I		*Pst*I	
Targeted	Untargeted	Targeted	Untargeted	Targeted	Untargeted	Targeted	Untargeted
5137 bp	5137 bp	10021 bp	10021 bp	8269 bp	8269 bp	8980 bp	8980 bp
4472 bp			6815 bp	7706 bp		3513 bp	3513 bp
3575 bp	3575 bp	5674 bp			4095 bp	2545 bp	
	2603 bp	3213 bp		1850 bp	1850 bp		2105 bp
1927 bp	1927 bp	1599 bp		1576 bp	1576 bp	1897 bp	
1853 bp	1853 bp			1106 bp	1106 bp	1365 bp	1365 bp
1742 bp						998 bp	
986 bp	986 bp					840 bp	840 bp
425 bp	425 bp					276 bp	
390 bp	390 bp					93 bp	93 bp

Figure 11. Completion of the nBmp2-ko targeting vector. The final step in construction of the nBmp2-ko targeting vector was to target the neomycin selection cassette into the area that would be the 3'UTR of Bmp2 after transcription. **(A)** After the recombination reaction, plasmid DNA was extracted and digested with either *Bgl*II or *Cla*I. These digests revealed that the plasmid preparation contained a mixture of targeted and untargeted plasmids since bands specific to either plasmid were present (see table in (C)). **(B)** The mixed plasmid preparations were re-transformed, plasmid DNA was extracted, and this time the plasmid DNA was also digested with *Xba*I and *Pst*I, which revealed that the desired, targeted plasmid had been isolated (see table in (C)). **(C)** Table indicating the bands that would be present from the targeted or untargeted plasmids after each digestion.

now contain an additional *Drd*I site such that upon digestion and Southern blot analysis, a 6.1-kb band would be apparent rather than the wt-13.6 kb band (Fig. 12A). There were 204 *Neo*^{r}-ES clones to screen for recombinant clones via Southern hybridization. Of these, 4 contained a targeted Bmp2 locus as verified by the presence of both the 13.6-kb wild-type band and the 6.1-kb targeted-allele band (Fig.12B). Since the 129/Bl6 G4-56 ES cells from Dr. Mario Capecchi's lab were from the same genetic background as the targeting vector (Bl6), much higher targeting efficiency was achieved: 17 out of 147 screen clones contained the targeted allele.

nBmp2-ko chimeras are successfully generated

The 1c-9 ES cells from the Capecchi lab were used for microinjection to generate chimeric mice. Fifteen chimeras were born, 10 of which appear to be over 90% and the remaining five appear to be over 80% composed of cells from the targeted ES cell line.

Zebrafish lacking nbmp4 have severe heart defects

To investigate the function of nBmp2 in development, we performed knockdown experiments in zebrafish embryos. Zebrafish have three different BMP proteins, bmp2a, bmp2b, and bmp4, which are all 60-62% homologous with rat Bmp2, complicating the determination of which zebrafish gene should be considered the homologue of mammalian Bmp2. Zebrafish bmp4 contains the conserved bipartite NLS overlapping the site of proteolytic cleavage, while bmp2a and bmp2b are both missing one of the first two basic amino acids (Fig. 13A). For this reason, we chose to design a morpholino antisense oligonucleotide (MO) against the alternative start codon in bmp4 to block translation of

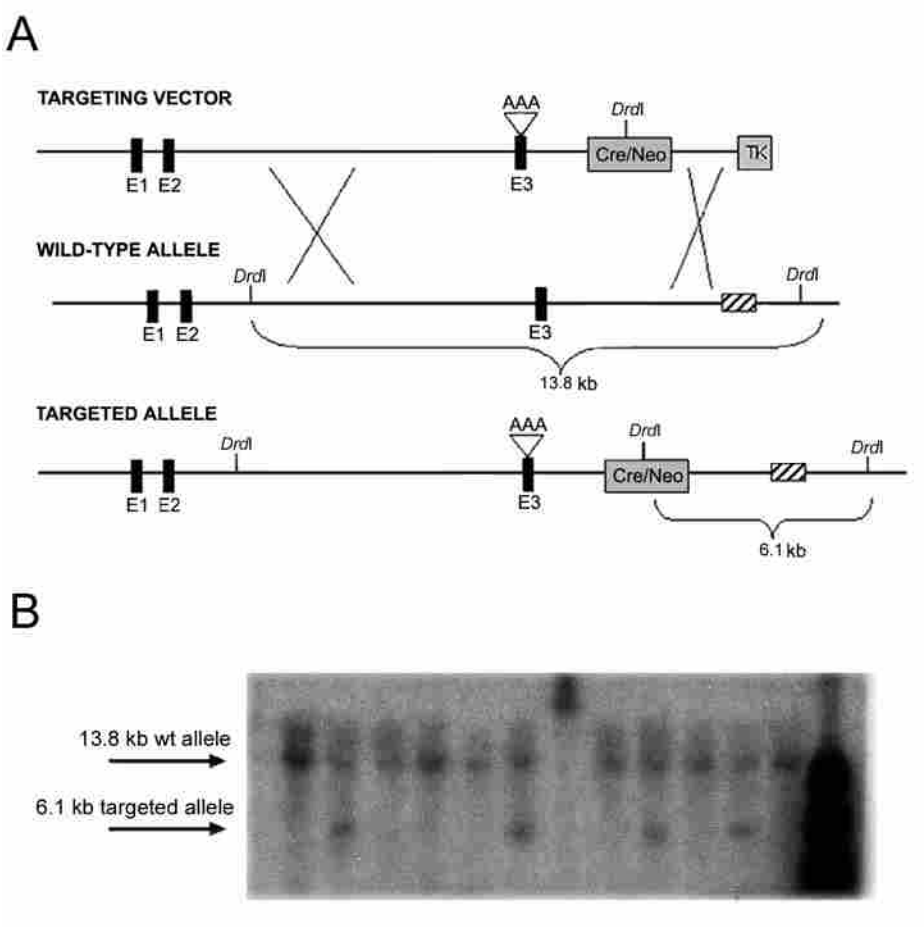

Figure 12. Southern analysis reveals ES cells targeted with the nBmp2-ko targeting vector. (A) Schematic of the nBmp2-ko targeting vector. The *Bmp2* exons are numbered and represented as black boxes while the *Neo* cassette and thymidine kinase (TK) gene are represented as grey boxes. Insertion of the *Neo* cassette introduces a *Drd*I restriction site as indicated. The mutation of NLSc (**KR**EKRQAKHKQ**RKR**L**K**S to **KR**EKRQAKHKQ**AAA**L**K**S) in exon 3 is denoted by AAA. After a *Drd*I digest and Southern hybridization using a 3′ flanking probe complementary to the region indicated with the striped box, the wild-type band was 13.8 kb, while a targeted allele resulted in a 6.1-kb band. **(B)** Southern blot analysis revealed targeted AV3 ES cells used for morulae aggregation here at BYU and targeted G4-56 ES cells used for microinjection at the University of Utah, as indicated by the presence of the 6.1-kb band.

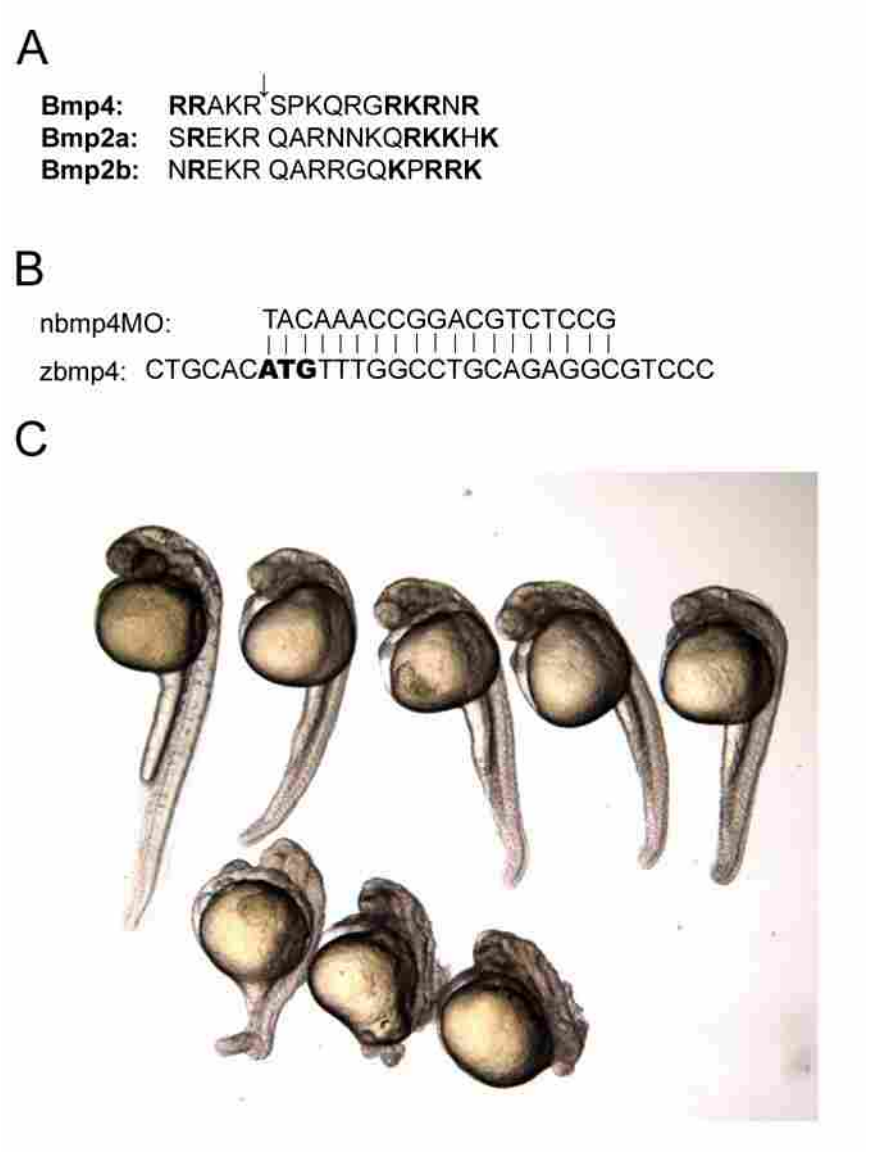

Figure 13. Elimination of nBmp4 in zebrafish results in defective heart development. To investigate the function of nBmp2 in development, we performed knock-down experiments in zebrafish embryos using morpholino antisense oligonucleotides to specifically inhibit translation from the downstream ATG in zebrafish bmp4. **(A)** Amino acid sequences surrounding the site of proteolytic processing (arrow) in zebrafish bmp4, bmp2a, and bmp2b. The predicted bmp4 bipartite NLS is shown in bold, and the equivalent amino acids in bmp2a and bmp2b are also bold. **(B)** Schematic of the nbmp4MO binding to the alternative start codon in zebrafish bmp4. **(C)** Injection of the nbmp4MO into zebrafish caused obvious cardiac defects in live embryos. The embryo on the left is a wild-type embryo while the remaining embryos represent varying degrees of the phenotype observed. By 24 hpf, most embryos had no visible heart. By 48 hpf, a beating heart was present although it was sluggish and failed to circulate blood. Embryos injected with the standard control MO had normal, beating hearts 24 hpf and normal blood circulation was visible at 48 hpf.

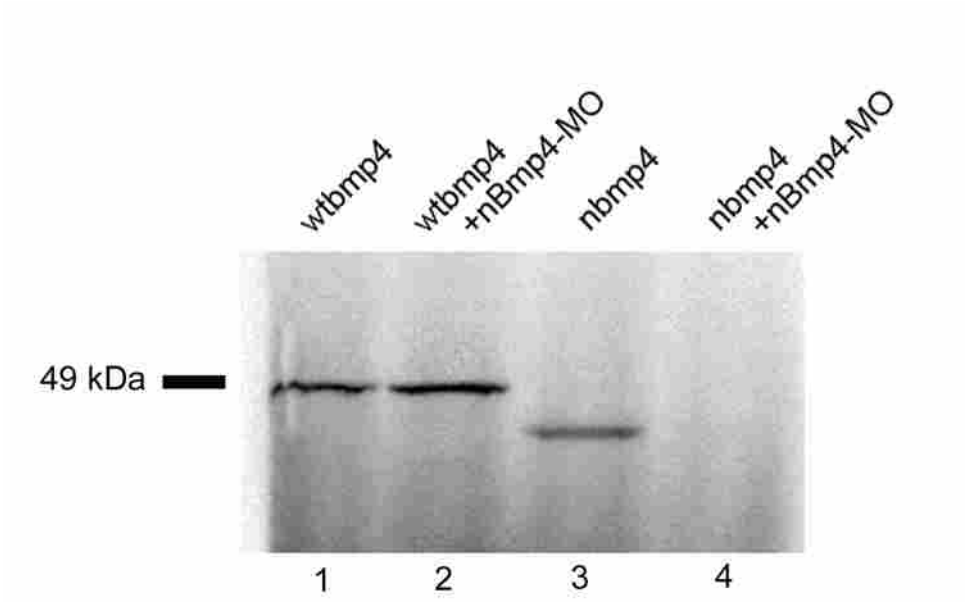

Figure 14. The morpholino nBmp4-MO blocks translation from the alternative, downstream ATG but does not block translation from the conventional start codon *in vitro.* To test the specificity of the nBmp4-MO, we made expression vectors for zebrafish full-length and nuclear bmp4 and used them for i*n vitro* transcription/translation experiments in the presence of [^{35}S]methionine. The expression vector for wild-type, full-length bmp4, wtbmp4, produced the expected ~46-kDa protein (lane 1). Including the morpholino nBmp4-MO in the reaction did not inhibit synthesis of this protein (lane 2). The expression vector for the nuclear version of zebrafish bmp4, nbmp4, produced the expected ~40-kDa protein (lane 3). Including nBmp4-MO in the reaction completely inhibited synthesis of this protein (lane 4).

zebrafish nbmp4 (Fig. 13B). Injection of the nBmp4-MO caused obvious cardiac defects in live embryos (Fig. 13C). By 30 hpf, most embryos had no visible heart. By 48 hpf, a beating heart was present although it was sluggish and failed to circulate blood. Embryos injected with the standard control MO had normal, beating hearts 30 hpf and normal blood circulation was visible at 48 hpf.

The morpholino nBmp4-MO blocks translation from the alternative, downstream ATG but does not block translation from the conventional start codon *in vitro*

To test the specificity of the nBmp4-MO *in vitro*, we synthesized zebrafish bmp4 in the presence of [^{35}S]methionine both with and without the morpholino present. *in vitro* transcription/translation of wild-type bmp4 produced a band of the expected size at ~46 kDa; *in vitro* transcription/translation of the nuclear form also produced a band of the expected size at ~40 kDa (Fig. 14). Addition of the nBmp4-MO to the full-length bmp4 *in vitro* transcription/translation reaction did not inhibit production of the ~46 kDa, as expected (Fig. 14). In contrast to this, addition of the nBmp4-MO to the nuclear bmp4 *in vitro* transcription/translation reaction inhibited production of the nuclear ~40 kDa (Fig. 14).

DISCUSSION

Our lab has shown for the first time that a Bmp family member is localized to the nucleus. When we first hypothesized that a form of Bmp2 may be localized to the nucleus, our initial step was to use the PSORT II prediction program to search the amino acid sequence of rat Bmp2 for potential NLSs. Three were identified. To test the

functionality of each putative NLS, we fused each to GFP. Only the bipartite NLS that overlaps the site of proteolytic cleavage was capable of localizing GFP to the nucleus. We later confirmed that this NLS is functional in the context of full-length Bmp2: a wtBmp2/GFP fusion construct clearly localized to the nucleus in a portion of transfected cells, but when the bipartite NLS was mutated, Bmp2 was no longer capable of directing GFP to the nucleus. Since the bipartite NLS is situated at the site for proteolytic cleavage, these results indicate that only an uncleaved version of Bmp2 could be localized to the nucleus, a premise that was later confirmed by western blotting.

Later experiments also verified that nuclear localization of Bmp2 is not an artifact of the GFP fusion constructs but that a form of endogenous Bmp2 is localized to the nucleus. Immunocytochemistry using two separate antibodies clearly showed endogenous Bmp2 in the nuclei of cultured cells. Additionally, western blots were used to show the presence of endogenous Bmp2 in nuclear extracts from cultured cells

Before verifying the size of nBmp2 with western blots and identifying the use of an alternative downstream start codon, we originally hypothesized that the uncleaved version of Bmp2 resulted from regulation of proteolytic processing. Elsewhere it has been shown that the proprotein convertase furin is responsible for processing Bmp4, and it has long been hypothesized that Bmp2 is also cleaved by furin due to the close homology of Bmp2 and Bmp4 and the presence of the furin recognition sequence upstream of the cleavage site in Bmp2 (Cui et al., 1998; Mishina, 2003). Further supporting this hypothesis, furin has been shown to modulate the activity of several of its substrates. The pro-β-NGF protein is a neurotropin that has opposing activities depending on whether or not it is cleaved by furin: cleaved β-NGF promotes cell survival, whereas

uncleaved β-NGF promotes apoptosis of neurons (Lee et al., 2001). The transmembrane receptor Notch is also cleaved by furin. When cleaved, the intracellular domain of Notch is released and activates genes involved in development and differentiation (Mumm et al., 2000). On the other hand, uncleaved Notch inhibits cell differentiation (Bush et al., 2001). Since opposing activities have been reported for Bmp2, particularly with cancer, we hypothesized that, like these proteins, Bmp2 could be regulated by furin activity.

With this information, we hypothesized that furin also modulated the activity of Bmp2. We were able to confirm that furin can indeed cleave Bmp2 *in vitro*, but regulating the activity of furin *in vivo* did not affect nuclear localization of Bmp2. We also mutated the cleavage recognition sequence to prevent proteolytic processing by any member of the proprotein convertase family. This mutation still did not affect the number of cells demonstrating nuclear localization Bmp2.

The results of these experiments led us to hypothesize that Bmp2 nuclear localization is achieved not through regulating Bmp2 proprotein processing but rather through the avoidance of the secretory pathway altogether by gaining access to the cytosol for translation. Alternative translational start sites play a significant role in altering the localization of a number of proteins (Kochetov et al., 2005). For example, the nuclear variant of PTHrP is translated from an alternative non-AUG start site downstream of the conventional initiator AUG, generating a protein with a truncated signal peptide (Nguyen et al., 2001). Similarly, the secreted growth factor bFGF can initiate at two upstream CUG codons to produce isoforms that include N-terminal extensions containing an NLS. These isoforms are localized to the nucleus. Spastin, a protein involved in microtubule dynamics and membrane trafficking, has two alternative translation start

sites. Both protein isoforms are targeted to the nucleus, but one of the isoforms also contains two nuclear export signals that efficiently drive export into the cytoplasm (Claudiani et al., 2005). Wnt13B and Wnt13C also have alternative translation start codons, the use of which determines whether they are localized to the nucleus or to the mitochondria (Struewing et al., 2006).

Our data indicate that, like these other growth factors, the nuclear version of Bmp2 results from the use of an alternative translational start site. We mutated the conventional start codon to force utilization of any downstream start codon within the Bmp2/GFP fusion construct. This mutation dramatically increased the amount of Bmp2 nuclear localization. Examination of the region downstream of the signal peptide led to the identification of an in-frame ATG that, when mutated, significantly decreaseds the frequency of nuclear localization. The protein produced by initiating translation at this site would lack the N-terminal signal peptide and would therefore bypass the rER and secretory pathway where the proteolytic cleavage would otherwise occur. Following cytoplasmic translation, the intact bipartite NLS could then direct translocation to the nucleus. The fact that some nuclear localization (10%) was still observed when this downstream ATG was mutated suggests utilization of one or more additional alternative start codons that also truncate the N-terminal signal peptide.

Further supporting our alternative start codon data are the results of our western blots. A band that corresponds to the predicted size of nBmp2 (calculated from the alternative downstream ATG to the end of the classical mature region at 38.6 kDa) was present in these blots. To confirm that this is in fact nBmp2, nuclear extracts from cells transfected with an HA-tagged version of Bmp2 were used for western blots, and again

the ~38.6 kDa band was present. This verification of the size of nBmp2 as ~38.6 kDa supports the hypothesis that nBmp2 is an uncleaved version that results from translation at the alternative start codon.

Having verified the existence of nBmp2 and identified the manner by which it escapes the secretory pathway, we were next interested in uncovering the function of nBmp2. We determined to generate mice that lack nBmp2 but still produce secreted Bmp2. To do this, we had two options: we could either mutate the alternative start codon or the NLS. Since mutating the alternative start codon decreased the amount of nuclear localization by half while mutating the NLS eliminated nuclear localization, we decided to mutate the NLS. Choosing how to mutate the NLS was complicated by the fact that the **RKR**-**K** portion of the NLS is within the mature region of Bmp2, and the **KR** portion of the NLS overlaps the recognition sequence for furin. Changing these amino acids had the potential to alter the function of the secreted Bmp2 or to prevent processing of Bmp2, in essence creating a Bmp2 knockout mouse.

Targeted mutagenesis experiments determined that mutating the **RKR** portion of the NLS would prevent nuclear localization. We performed additional experiments and verified that mutating the **RKR** portion of the NLS does not decrease secretion of Bmp2. Data reported by others suggested that this mutation would also have minimal affect on the function of the secreted Bmp2: Hillger et al. showed that Bmp2 species truncated N-terminally of either the R, K or R still had the capability to induce ectopic bone formation (Hillger et al., 2005). When the equivalent sequence in Bmp4 was deleted or substituted with three Ala residues and subjected to a battery of tests for receptor binding, antagonist binding, and target gene responsiveness, they showed that the mature Bmp4 homodimer

bearing the mutation was functionally indistinguishable from the wild-type Bmp4 (Ohkawara et al., 2002). However, animal cap conjugation experiments with *Xenopus* embryos demonstrated that these mutations reduced the ability of Bmp4 to bind heparin sulfate in the extracellular matrix with the result of increased diffusion range (Ohkawara et al., 2002). Because Bmp2 and Bmp4 are so highly related, these results strongly suggest that Bmp2 bearing the same mutations would also function normally, perhaps with a slightly increased diffusion range.

A similar increase in the diffusion range of Bmp2 growth factor produced in our mice could result in a phenotype that is not related to the loss of nBmp2. When evaluating the phenotype displayed in the nBmp2 null mouse, we will have to be aware of the possibility for an increased diffusion range of the secreted Bmp2 growth factor. Fortunately since the zebrafish morpholino experiments only block translation of the nuclear variant without producing any change in the amino acid sequence, the zebrafish results can be used to aid evaluation of the mouse phenotype. Any phenotype that appears in both zebrafish and in the nBmp2 null mouse can confidently be attributed to loss of nBmp2 rather than to a gain of growth factor diffusion range. If questions about the mouse phenotype arise that cannot be resolved by comparison to the zebrafish phenotype, nBmp2 transgene rescue experiments in the mouse can be performed to see if the mouse nBmp2-ko phenotype can be rescued by addition of nuclear-only Bmp2 in a tissue specific fashion.

The nBmp2-ko targeting vector was constructed using recombineering, a phage-based *E. coli* homologous recombination system pioneered by Dr. Neal G. Copeland of the National Cancer Institute. The targeting vector has a mutated and, therefore non-

functional, NLS, a Neo selection cassette, and a TK gene used for selection of homologous recombinants. Chimeric mice carrying the defective Bmp2 allele have been generated, and the process of breeding to homozygosity is underway.

While constructing the nBmp2-ko targeting vector and generating nBmp2-null mice, we investigated the function of nBmp2 by performing both a microarray and knockdown experiments in zebrafish. For the microarray experiments, we overexpressed nBmp2 in cell culture and compared the gene expression profile to that of cells transfected with the empty expression vector. The genes that had significant differences in expression largely clustered into genes involved with nervous system development and function, lipid metabolism, immune system functioning, and cancer. To collect more information from the microarray experiments, on-going work in the Bridgewater lab is focused on optimizing the real-time PCR parameters such as cDNA synthesis, primer design, and template concentration.

The zebrafish work has proved to be more promising in identifying a role of nBmp2. We chose to use morpholinos to block translation of nBmp2. When base paired at the translational start site, morpholinos prevent initiation of translation. When annealed to mRNA more than 30 bases downstream of the start site, however, the morpholinos are displaced by the ribosome and have no effect on translation (Gene Tools, LLC Targeting Guidelines, http://www.gene-tools.com/node/18). Therefore, morpholinos should work perfectly to block translation of nBmp2 and not secreted Bmp2, but to our knowledge this technology has never been used to block translation of a downstream alternative start codon. Our *in vitro* transcription/translation experiments verified that the nBmp4-MO did in fact block translation from the alternate, downstream start codon but did not affect

translation from the conventional start codon as expected. Also, as a control we injected zebrafish with a splice-blocking morpholino known to inhibit translation of bmp4. These fish exhibited a different phenotype than our nBmp4-MO injected fish.

In zebrafish, three different BMP proteins are all equally homologous with rat Bmp2: zebrafish bmp2a, bmp2b, and bmp4 proteins all have 60-62% sequence identity with rat Bmp2. bmp2a and bmp2b, however, may not contain functional bipartite NLSs. The characteristic pattern of bipartite NLS is two basic residues, nine or ten spacer residues, and another basic region consisting of four basic residues out of five (Cyert, 2001). Zebrafish bmp4 contains a characteristic bipartite NLS overlapping the site of proteolytic cleavage. bmp2a and bmp2b, on the other hand, are both missing one of the first two basic residues, unless the downstream KR residues just before the cleavage site serve the purpose, in which case the spacer is reduced to only six or seven residues. We therefore chose to knockdown zebrafish bmp4. Since bmp4 is as homologous to rat Bmp2 as bmp2a and bmp2b, a phenotype from knocking-down zebrafish nbmp4 would suggest the importance of nBmp2 for all vertebrates, including mammals.

Zebrafish embryos injected with a morpholino designed to block translation only of nbmp4, leaving secreted bmp4 intact, did indeed develop a significant phenotype: the majority of embryos developed severe heart defects. Interestingly, zebrafish embryos are not completely dependent on a functional cardiovascular system. Even without effective blood circulation, they receive enough oxygen by passive diffusion to survive for several days (Stainier, 2001). Additionally, their translucent skin facilitates visualizing the developing heart. Work is currently in progress to verify *in vivo* what we observed *in vitro*: that secreted bmp4 is present in normal amounts and that nbmp4 is, in fact, lacking.

This work includes western blot analysis on nuclear extracts as a means to visualize nbmp4 in wild-type fish but not in morphant fish. Also, rescue experiments are planned; these experiments will entail injecting nBmp4-MO and an excess of mRNA for nbmp4 into zebrafish embryos to determine if adding nbmp4 back into the morphant fish can rescue the phenotype. Since a phenotype for overexpression of nbmp4 is possible, the appropriate ratio of nBmp4-MO and nbmp4 mRNA to inject will need to be determined.

Several of the genes the microarray data indicated were regulated by nBmp2 are important in heart development. Neuregulin (Nrg1) morphant fish, for example, displayed inhibited conductive tissue development that resulted in slowed conduction throughout the heart (Milan et al., 2006). Blood vessel/epicardial substance (Bves/Pop1) is highly enriched in the developing heart and is the earliest known marker of cardiac vascular smooth muscle (Andree et al., 2000; Reese and Bader, 1999; Reese et al., 1999). Evidence suggests that Bves plays a role in cell adhesion and migration in the developing heart (Wada et al., 2001). Erythropoietin also had a significant change in expression in response to nBmp2. It plays a significant role in heart morphogenesis and differentiation of cardiac cells from embryonic stem cells (Sachinidis et al., 2002; Wu et al., 1999). Matrix metalloproteinase 2 (Mmp2) is another gene of interest: inhibition of Mmp2 in developing chick embryos produced severe heart tube defects (Linask et al., 2005). To better understand the heart defects in zebrafish, expression of these genes and others will be studied in future work involving *in situ* hybridization and real-time PCR on wild-type and morphant zebrafish.

In conclusion, this dissertation represents a body of work that points to a new paradigm for Bmp2 functioning. We have shown that a nuclear variant of Bmp2 does in

fact exist and that it is produced by translation from an alternative downstream start codon. We have also demonstrated that nBmp2 is critical for developing vertebrates; zebrafish lacking this protein have severe heart defects. To illuminate the role of nBmp2 in mammalian development, we have also designed a mouse model that will lack nBmp2 but retain the function of secreted Bmp2. Chimeric mice harboring this mutation have been generated, and, once breeding to homozygosity is complete, functional distinction between the nuclear and secreted forms of this protein will be possible. The original work detailed in this dissertation has opened new avenues of research that will make significant contributions toward understanding the full role BMP proteins play in development.

BOOK II

COORDINATE REGULATION OF *COL11A2* AND *COL27A1* BY THE TRANSCRIPTION FACTOR LC-MAF

INTRODUCTION

Maf proteins

Maf family proteins belong to the basic leucine zipper (bZIP) superfamily of transcription factors; they contain a leucine zipper dimerization interface adjacent to a basic DNA binding region (Motohashi et al., 1997). However, the basic regions of the Maf family of proteins contain non-conservative amino acid substitutions at positions that are highly conserved in other bZIP proteins. Maf proteins also contain an additional DNA-binding region on the N-terminal side of the bZIP domain that is highly conserved and required for specific DNA recognition (Kerppola and Curran, 1994). These differences result in a different tertiary structure and DNA contact interface than the canonical bZIP proteins (Dlakic et al., 2001). Until recently, Maf proteins have only been known to recognize longer DNA sequence elements (13-14 bp) that extend past the typical bZIP recognition element (Dlakic et al., 2001; Kataoka et al., 1994; Kerppola and Curran, 1994).

Individual Maf proteins can be widely expressed in diverse cell types and yet are involved in the expression of a variety of tissue-specific gene products both during and after development (de Crombrugghe et al., 2000; Ho et al., 1996; Huang et al., 2002; Kurschner and Morgan, 1995; Reza and Yasuda, 2004). This characteristic appears to be due, in part, to the ability of bZIP proteins to form heterodimers with a wide variety of other transcriptional regulatory proteins. Due to the nature of dimer formation among bZIP proteins, in which both proteins independently recognize one half of the DNA recognition sequence, Maf recognition elements frequently differ from each other

(Kerppola and Curran, 1994). It has been suggested that Maf proteins acquire their ability to regulate expression of such a diversity of genes through interacting with different transcriptional regulatory proteins in the developing tissues and thereby recognizing a variety of target-specific DNA elements (Dlakic et al., 2001; Hale et al., 2000; Ho et al., 1998; Kim et al., 1999; Motohashi et al., 1997).

Maf proteins may also play a role in carcinogenesis. c-*maf* is a cellular homologue of the avian viral oncogene v-Maf (MacLean et al., 2003). v-Maf was identified as the transforming gene of the avian retrovirus, musculoaponeurotic fibrosarcoma, which, when inoculated into newborn chickens, induces tumors (Kawai et al., 1992). v-Maf introduced into chicken embryo fibroblasts leads to cellular transformation (Kawai et al., 1992). c-Maf, without any structural modification in its protein-coding region, was shown to transform cells as efficiently as v-Maf when transduced by a retroviral vector into chicken embryo fibroblasts. Amino acid sequence analysis revealed few differences between v-Maf and chicken c-Maf. Further comparison revealed the chicken c-Maf to be highly conserved at the primary amino acid level with a number of mammals (Kataoka et al., 1993). Subsequent investigations revealed c-Maf as a human oncoprotein that was overexpressed in 25% of multiple myelomas that were tested (Chesi et al., 1998). Interestingly, both v-Maf and c-Maf are also shown to activate *p53* expression by binding to a Maf recognition sequence in the *p53* promoter, leading to p53-dependent cell death when overexpression of v-Maf exists in primary cells (Hale et al., 2000). Functional differences between c-Maf and a long form of c-Maf, Lc-Maf, are still unknown, but it has been suggested that they posses redundant functions since they share similar Northern and *in situ* hybridization patterns. It has also been suggested that v-Maf may be derived

from Lc-Maf rather than c-Maf since they both have a similar extra 10 amino acids (Huang et al., 2002).

A different form of c-Maf that includes a different 3′UTR region and an additional 10 amino acids at the carboxyl terminus, Lc-Maf, was identified in a yeast two-hybrid screen by its specific interaction with SOX9, a known transcriptional activator of a number of cartilage-specific genes, including those for the type II, IX, XI, and XXVII collagens (Bridgewater et al., 1998; Bridgewater et al., 2003; Huang et al., 2002; Jenkins et al., 2005; Zhang et al., 2003). Lc-Maf was shown to synergize with SOX9 to increase the expression of the cartilage-specific *Col2a1* gene in 10T1/2 cells and MC615 chondrocytes by binding within a *Col2a1* enhancer element to the short, 7-bp recognition element GGCTCTG (Huang et al., 2002). Lc-Maf appears to be a splice variant of c-Maf as it has a different 3′UTR region and an additional 10 amino acids at the carboxyl terminus (Huang et al., 2002). Using a probe from the 3′UTR of Lc-Maf, northern hybridizations revealed RNA expression in various mouse tissues, including cartilage (Huang et al., 2002). It has been demonstrated that the presence of Lc-Maf and c-Maf in cartilage plays a vital role for correct skeletal development: mice lacking these proteins exhibited decreased fetal bone length and had improper hypertrophic chondrocyte differentiation (MacLean et al., 2003).

Cartilage

Cartilage is an important tissue that serves a vital role as the template for many bones in the developing skeleton. During the process of endochondral ossification, long bones of the body develop from a cartilage intermediate that is progressively replaced by bone. During the first phase, the mesenchyme cells differentiate into chondrocytes.

Starting at the center of the cartilaginous template and progressing towards the epiphyses, these cells mature from resting to proliferating and on to hypertrophic chondrocytes, at which point mineralization begins (Fig. 1). At each stage of chondrocyte differentiation, the expression of extracellular matrix proteins are temporally and spatially coordinated due to a tight regulation via transcription factors, signaling molecules, hormones and local growth factors (Huang et al., 2002; Tchetina et al., 2003). Precise coordination of the expression of extracellular matrix proteins, such as the cartilage-specific collagens, is essential for correct skeletal development.

We investigated the role Lc-Maf might play in regulating enhancers of other cartilage specific collagen genes during development of the long bones, namely the B/C, D/E, and F/G enhancer elements of *Col11a2* and the 27D/E and 27F/G enhancer elements of *Col27a1* (Fig. 2A and B). Like *Col2a1*, these enhancer elements are also responsive to SOX9 (Bridgewater et al., 1998; Bridgewater et al., 2003; Jenkins et al., 2005; Liu et al., 2000; Pace et al., 2003). Our findings indicate that the transcription factor Lc-Maf can both positively and negatively regulate enhancer elements from these two different cartilage-specific collagen genes and may play an important role in the coordinated regulation of *Col11a2* and *Col27a1* during embryonic development of fetal limbs.

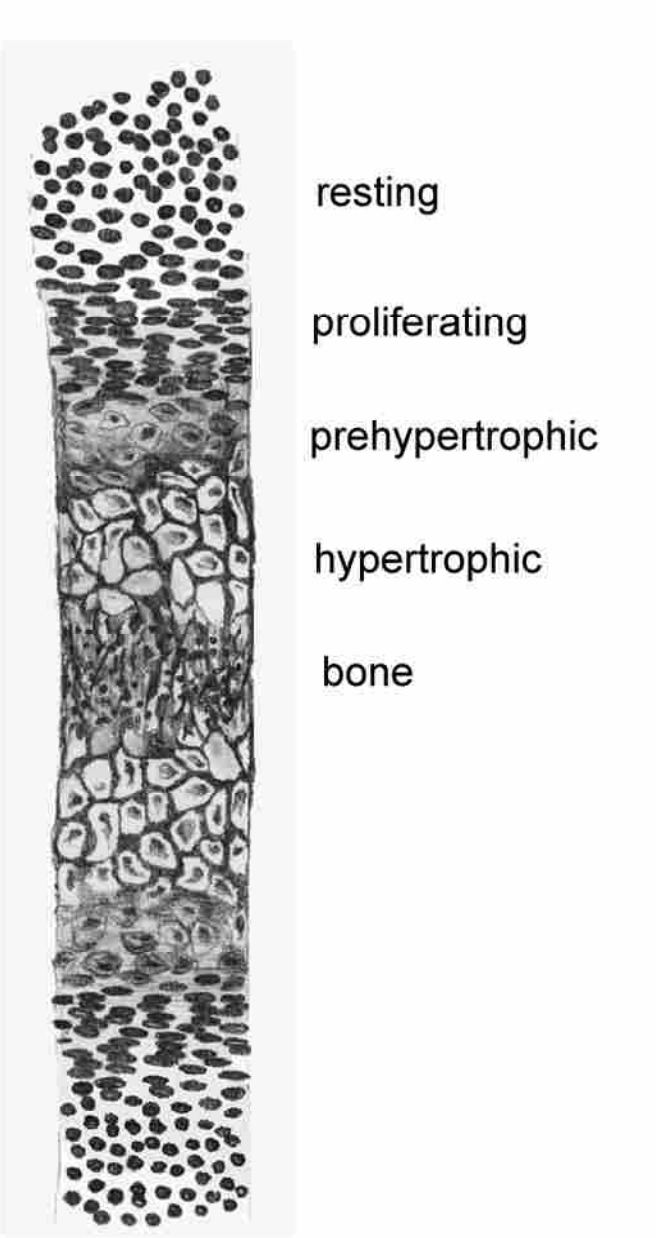

Figure 1. Model of endochondral ossification. During the process of endochondral ossification, long bones of the body develop from a cartilage intermediate that is progressively replaced by bone. The process of cellular maturation starts at the center of the cartilaginous template and progresses towards the epiphyses; the most mature cells are at the center of the diaphysis while the most immature are located at either epiphysis. This image depicts mineralized bone at the center of the diaphysis. These cells have already matured from resting, to proliferating and on to hypertrophic chondrocytes before ossification began, while the cells on either side of this center of ossification are still maturing.

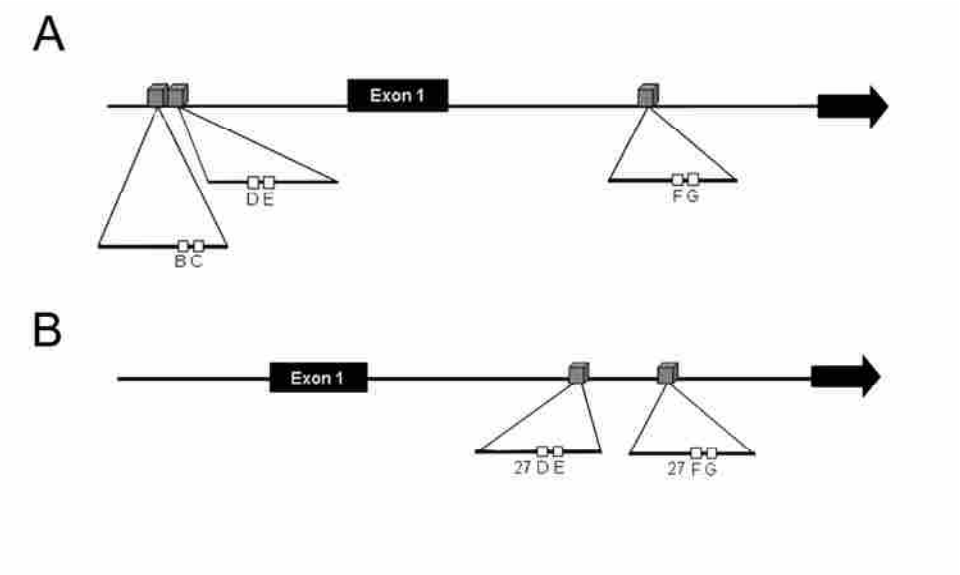

Figure 2. Schematic diagrams of the *Col11a2* and *COL27A1* cartilage-specific enhancer regions. (A) A schematic diagram of the 5′ region of *Col11a2* showing the B/C and D/E enhancer elements in the upstream promoter region and the F/G enhancer in the first intron, represented as boxes. **(B)** A schematic diagram of the 5′ region of *COL27A1* showing the 27D/E and the 27F/G enhancer elements in the first intron, represented as boxes. Expanded views of each enhancer element show approximate locations of the two Sox9-binding sequences (open boxes).

METHODS

Plasmids

Each of the experimental constructs used in transient transfections contained four tandem copies of an enhancer element, cloned upstream of the 95-bp *Col2a1* minimal promoter and a luciferase reporter gene. Enhancer elements tested in plasmids 4×(B/Cm1)p95Luc, 4×(B/Cm2)p95Luc, 4×(D/Em)p95Luc, 4×(27D/E)p95Luc, and 4×(27F/Gm)p95Luc were synthesized as complementary oligonucleotides purchased from Invitrogen (Carlsbad, CA). Oligonucleotides were purified by denaturing polyacrylamide gel electrophoresis before annealing. The plasmid p89Col2a1Bs was used to multimerize the enhancer elements before transferring them, along with the *Col2a1* minimal promoter, into the luciferase reporter vector pLuc4 as previously described (Bridgewater et al., 1998; Lefebvre et al., 1996). All other luciferase reporter plasmids were made previously (Bridgewater et al., 1998; Bridgewater et al., 2003; Jenkins et al., 2005). The SOX9 expression plasmid, SOX9-pcDNA-5′-UT, and p89Col2a1Bs were kind gifts from Dr. Veronique Lefebvre of the Cleveland Clinic in Cleveland, Ohio. The Lc-Maf expression vector was a kind gift from Dr. Wendong Huang of the Baylor College of Medicine in Houston, Texas.

Cell Types and Culture

Rat chondrosarcoma (RCS) cells and BALB/3T3 fibroblasts were maintained for use in transient transfection assays. Both cell lines were cultured at 37°C under 5% CO_2 in Dulbecco's modified Eagle's medium, supplemented with penicillin (50 units/ml),

streptomycin (50 μg/ml), L-glutamine (2mM) and 10% bovine growth serum. Every 3-4 days the cells were passaged using a 0.25% trypsin-1mM EDTA solution.

Transient Transfections

The transient transfections were performed in both RCS and BALB/3T3 cell lines. The enhancer/reporter gene constructs were cotransfected with Lc-Maf and SOX9 expression plasmids (pcDNA3.1-Lc-Maf and SOX9-pcDNA-5′-UT) to determine the effect of Lc-Maf on transcriptional activity, both alone and in conjunction with SOX9, a known transcriptional activator for the *Col2a1*, *Col11a2,* and *COL27A1* enhancer elements. All transfections were performed in triplicate and repeated at least three times. The plasmid pSV-β-galactosidase (Promega) was included in every reaction as an internal control for transfection efficiency.

Transfections were performed using LipofectAMINE PLUS reagent (Invitrogen) according to the manufacturer's protocol. A total of 2 μg of DNA was used to transfect each 10-cm^2 dish. For RCS cells, each reaction included 1.0 μg of the luciferase reporter plasmid, 0.5 μg of pSV-β-galactosidase as an internal control for transfection efficiency and 0.5 μg of either pcDNA3.1-Lc-Maf or the empty pcDNA3.1 vector. For BALB/3T3 fibroblasts, each reaction included 1.0 μg of the luciferase reporter plasmid, 0.4 μg of pSV-β-galactosidase as an internal control for transfection efficiency and 0.3 μg-combinations of either pcDNA3.1-Lc-Maf, SOX9-pcDNA-5′-UT, or the empty pcDNA3.1 vector for a total of 0.6 μg. β -galactosidase levels were measured using the Galacto-Light/Plus system (Tropix, Bedford, MA) following the manufacturer's protocol. Luciferase levels were measured using the Luciferase Assay Reagent (Promega.

Madison, WI) following the manufacturer's protocol. Transfection data is reported as Relative Luciferase Units (luciferase units per β-galactosidase unit) ± standard error (s.e.m.) and each graph represents at least three independent transfections, each performed in triplicate.

In Vitro Transcription/Translation

Lc-Maf protein was synthesized using the Single Tube Protein System 3, T7 kit (Novagen, San Diego, CA) according to manufacturer's instruction using the Lc-Maf expression plasmid, pcDNA3.1-Lc-Maf. To verify that both transcription and translation occurred as expected, [^{35}S]methionine-labeled Lc-Maf was visualized on SDS-PAGE.

Electrophoretic Mobility Shift Assay (EMSA)

Wild-type and mutant C*OL27A1* 27F/G probes were prepared by annealing complementary oligonucleotides synthesized by Invitrogen. The probes were labeled by end-filling with α-[^{32}P]dGTP using the Klenow fragment and purified using Amersham Biosciences NICK columns according to manufacturer's protocol (Amersham Biosciences, Piscataway, NJ). Labeled probes were adjusted with unlabeled probe to achieve equivalent specific activities. Lc-Maf protein was pre-incubated for 15 minutes in 20 µl buffer containing 20 mM HEPES, 100mM KCl, 10mM $MgCl_2$, 5% glycerol, 1 mM EDTA, 5 mM DTT, 0.1% NP-40, 0.5 mg ml^{-1} BSA, and 1 µg poly(dGdC)·poly(dGdC) (Amersham Biosciences, Piscataway, NJ). Addition of antibody, if included, took place at this incubation step. Since Lc-Maf differs from c-Maf by only an additional 10 amino acids at the carboxyl terminus, an antibody directed towards the amino terminus of c-Maf

was used (Santa Cruz Biotechnology, Santa Cruz, CA). Radiolabeled probe was added to the binding reaction and incubated at room temperature for an additional 15 minutes. The samples were then fractionated by electrophoresis through a non-denaturing 4% polyacrylamide gel in 0.5× TBE at 140 V and visualized by autoradiography.

Synthesis and labeling of *in situ* hybridization probes

In situ hybridization probes for the mouse *Col10a1, Col11a2*, *Col27a1,*and *Lc-Maf* genes were kind gifts from the following individuals: *Col10a1* from B. de Crumbrugghe, *Col11a2* from Y. Yamada, *Col27a1* from J. Pace and *Lc-Maf* from W. Huang. Additionally, a probe directed against the third exon of *Col27a1* was synthesized via PCR from mouse genomic DNA. The primer sequences we used were 5′-CATCCGCAGCAGGAAACAC and 5′-CAGCTGCGTTCAGAGACATC. The probe's specificity for *Col27a1* was verified by using the Basic Local Alignment Search Tool (BLAST). Single-strand RNA antisense probes were labeled with digoxigenin-11-UTP using the DIG RNA labeling kit (Roche, Indianapolis, IN) according to manufacturer's protocol.

***In situ* hybridizations and Immunohistochemistry**

Mouse embryos were collected at half-day intervals from embryonic day 15-17 (E15-E17). Forelimbs were removed, fixed overnight at 4°C in 4% paraformaldehyde/phosphate-buffered saline (PFA/PBS), embedded in paraffin wax, and sectioned (6-8 μm) before placing onto Superfrost/Plus microscope slides (Fisher) to make a series of slides with adjacent tissue sections.

In situ hybridization was performed following the protocol of Murtaugh (Murtaugh et al., 1999) with the following modifications: after incubation with 1 μg/mL proteinase K (Fisher) for 30 minutes at 37°C and washing with PBT (phosphate-buffered saline plus 0.1% Tween-20), sections were postfixed in 4% PFA/PBS and incubated 4 hours in a humid chamber with prehybridization buffer. Hybridization to digoxigenin-11-UTP-labeled probes for the *Col10a1, Col11a2, Col27a1*, and *Lc-Maf* genes was carried out in a humid chamber overnight in the same hybridization mixture. Following hybridization, sections were treated with RNAse A (Fisher) in TNE (10 mM Tris pH 7.5, 500mM NaCl, 1 mM EDTA) and washed in SSC (15 mM sodium citrate, 150 mM NaCl, pH 7.0). The sections were blocked using 10% serum/MABT (100 mM Maleic Acid, 150 mM NaCl, 0.1% Tween-20, pH 7.5) before visualizing the probes by staining with anti-DIG-alkaline phosphatase-conjugated antibody (Roche, Indianapolis, IN) and treating the slides with BM Purple (Fisher).

Immunohistochemistry was performed as described previously (Barrow et al., 2003) using primary antibody directed against mature type XXVII collagen. This antibody was designed, generated, and generously provided by J. Pace.

RESULTS

Lc-Maf interacts specifically with the *Col11a2* chondrocyte-specific B/C enhancer element to repress activity

The *Col11a2* wild-type luciferase reporter construct 4×(B/C)p95Luc was cotransfected with the Lc-Maf expression vector, pcDNA3.1-Lc-Maf, into both RCS and BALB/3T3 cells to determine whether Lc-Maf exerts any regulatory action on this

enhancer element, which contained a putative Lc-Maf binding sequence (Fig. 3E). The reporter construct was active in RCS cells but inactive in fibroblasts, demonstrating the expected cell-type specificity of the chondrocytic enhancer's activity (data not shown). The SOX9 expression plasmid activated the enhancer in fibroblasts as previously demonstrated (Bridgewater et al., 1998; Bridgewater et al., 2003).

When pcDNA3.1-Lc-Maf was cotransfected with 4×(B/C)p95Luc in RCS cells, a significant decrease in luciferase production was measured to 50% of the original B/C value ($p \leq 0.0001$) (Fig. 3A). Similar results were obtained when the reporter construct was cotransfected with pcDNA3.1-Lc-Maf and SOX9-pcDNA-5′-UT in BALB/3T3 fibroblasts: SOX9-induced luciferase production from 4×(B/C)p95Luc was significantly reduced by Lc-Maf to 79% ($p \leq 0.0004$) (data not shown).

Mutations were introduced into the *Col11a2* B/C enhancer element at the putative Lc-Maf binding sites to test for direct binding of Lc-Maf to these enhancers. Two separate sequences existed within the B/C enhancer element with similarity to the previously reported GGCTCTG binding sequences, so mutant enhancers B/Cm1 and B/Cm2 were designed to target these two putative binding sites (Fig. 3E). When the *Col11a2* mutant reporter construct 4×(B/Cm1)p95Luc was cotransfected with pcDNA3.1-Lc-Maf, the B/Cm1 mutant enhancer was not responsive to Lc-Maf (Fig. 3B). However, B/Cm2 responded similarly to Lc-Maf overexpression as the wild-type B/C enhancer (Fig. 3C). This suggests that Lc-Maf interacts specifically with the B/C enhancer element at the region mutated in B/Cm1. Interestingly, both mutant B/C enhancer elements were less active than the B/Cwt enhancer element, suggesting that the

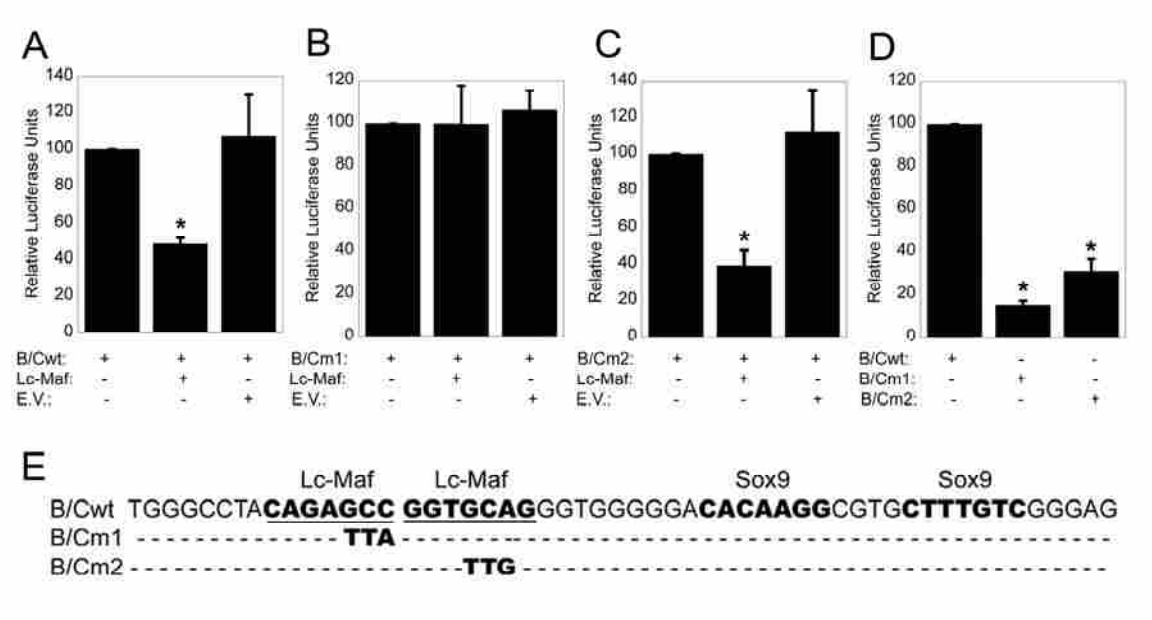

Figure 3. Lc-Maf interacts specifically with the *Col11a2* B/C enhancer element to inhibit enhancer activity. (A-D) RCS cells were transiently transfected with *Col11a2* B/C wild-type or mutant enhancer/reporter plasmids plus pcDNA3.1Lc-Maf (Lc-Maf) or the empty pcDNA3.1 vector (E.V.) as indicated. Enhancer activities that are significantly different from the corresponding wild-type enhancer activities are indicated with an asterisk ($p \leq 0.009$). **(E)** The wild-type *Col11a2* B/C sequence is shown with the Sox9 binding regions in bold and the putative Lc-Maf binding regions in bold and underlined. The nucleotide substitutions for the mutant enhancers are indicated below the wild-type sequences.

mutated region also binds a positive regulatory factor, perhaps one that competes with Lc-Maf for binding (Fig. 3D).

Lc-Maf interacts specifically with the *Col11a2* chondrocyte-specific D/E enhancer element to repress activity

The *Col11a2* wild-type luciferase reporter constructs 4×(D/E)p95Luc was cotransfected with the Lc-Maf expression vector, pcDNA3.1-Lc-Maf, into both RCS and BALB/3T3 cells to determine whether Lc-Maf exerts any regulatory action on this enhancer elements, which contained a putative Lc-Maf binding sequence (Fig. 4D). The reporter construct was active in RCS cells but inactive in fibroblasts, demonstrating the expected cell-type specificity of the chondrocytic enhancer's activity (data not shown). The SOX9 expression plasmid activated all the enhancer in fibroblasts as previously demonstrated (Bridgewater et al., 1998; Bridgewater et al., 2003).

When pcDNA3.1-Lc-Maf was cotransfected with 4×(D/E)p95Luc in RCS cells, a significant decrease in luciferase production was measured to 65% of the original D/E value ($p \leq 0.0002$) (Fig. 4A). Similar results were obtained when this reporter construct was cotransfected with pcDNA3.1-Lc-Maf and SOX9-pcDNA-5′-UT in BALB/3T3 fibroblasts: SOX9-induced luciferase production from 4×(D/E)p95Luc was significantly reduced by Lc-Maf to 64% ($p \leq 0.0004$).

For the *Col11a2* D/E enhancer element, the mutant enhancer D/Em targeted the putative Lc-Maf binding site (Fig. 4D). When the *Col11a2* mutant reporter construct 4×(D/Em)p95Luc was cotransfected with pcDNA3.1-Lc-Maf, the D/Em mutant enhancer was no longer responsive to Lc-Maf, suggesting that the specific interaction between Lc-

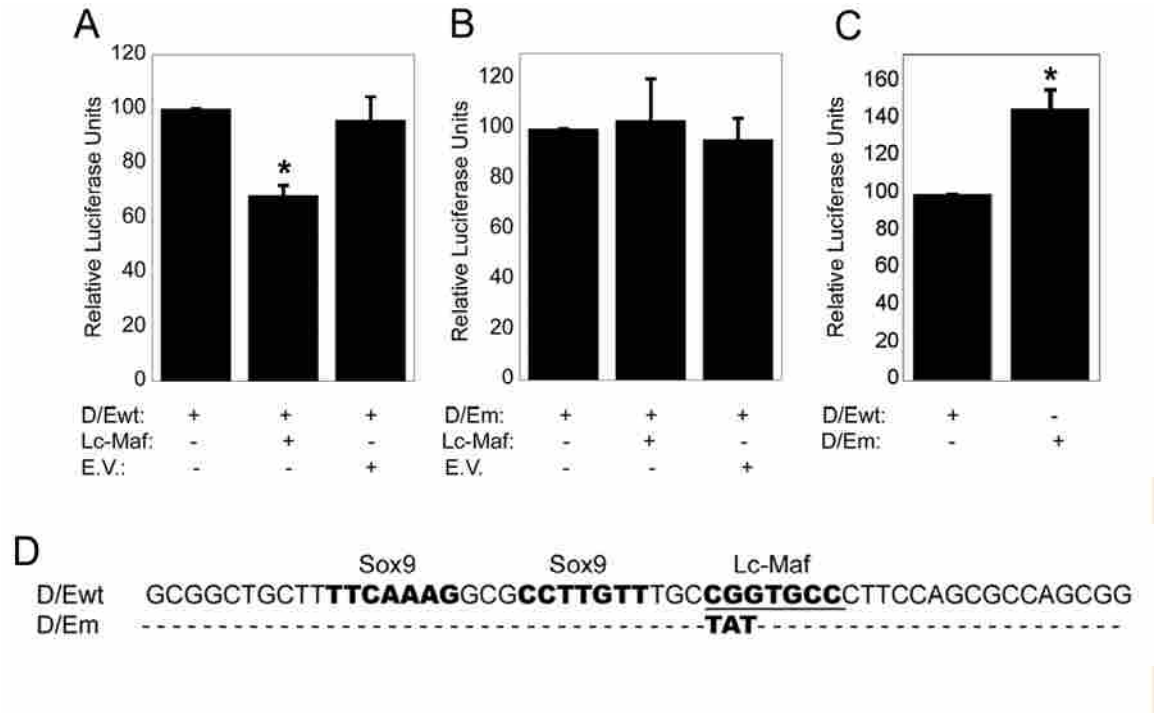

Figure 4. Lc-Maf interacts specifically with the *Col11a2* D/E enhancer element to inhibit enhancer activity. (A-C) RCS cells were transiently transfected with wild-type or mutant enhancer/reporter plasmids plus pcDNA3.1Lc-Maf (Lc-Maf) or the empty pcDNA3.1 vector (E.V.) as indicated. Enhancer activities that are significantly different from the corresponding wild-type enhancer activities are indicated with an asterisk ($p \leq 0.018$). **(D)** The wild-type *Col11a2* D/E sequence is shown with the Sox9 binding regions in bold and the putative Lc-Maf binding regions in bold and underlined. The nucleotide substitutions for the mutant enhancers are indicated below the wild-type sequences.

Maf and the D/E enhancer element occurs within the region mutated in D/Em (Fig. 4B). Comparison of the activities of the D/Ewt and the D/Em enhancers showed that D/Em was more active, consistent with the loss of a negative regulatory element (Fig. 4C).

Lc-Maf does not regulate the activity of the *Col11a2* F/G enhancer element

As with the other *Col11a2* enhancer elements, the *Col11a2* wild-type luciferase reporter construct 4×(F/G)p95Luc was cotransfected with pcDNA3.1-Lc-Maf into both RCS and BALB/3T3 cells to determine whether Lc-Maf exerts any regulatory action on this enhancer element, which contained a putative Lc-Maf binding sequence (Fig. 5B). No significant difference in luciferase production was detected, suggesting that Lc-Maf does not regulate this enhancer ($p= 0.38$) (Fig. 5A).

Similar results were obtained when this reporter construct was cotransfected with pcDNA3.1-Lc-Maf and SOX9-pcDNA-5′-UT in BALB/3T3 fibroblasts: Lc-Maf did not activate or inhibit 4×(F/G)p95Luc when compared to the SOX9-induced luciferase production ($p= 0.41$) (data not shown).

Lc-Maf does not regulate the *COL27A1* chondrocyte-specific 27D/E enhancer element

The *COL27A1* wild-type luciferase reporter construct 4×(27D/E)p95Luc was also cotransfected with the Lc-Maf expression vector, pcDNA3.1-Lc-Maf, into both RCS and BALB/3T3 cells to determine whether Lc-Maf exerts any regulatory action on this enhancer element, which contained a putative Lc-Maf binding sequence (Fig. 6B). This

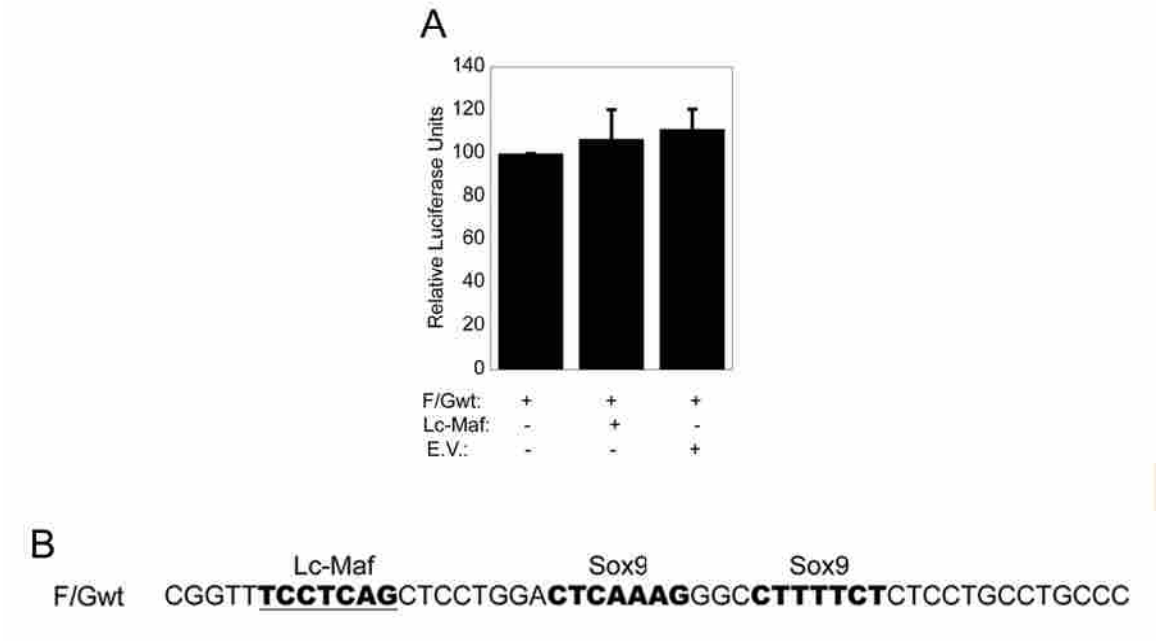

Figure 5. Lc-Maf does not modulate the activity of the *Col11a2* F/G enhancer element. (A) RCS cells were transiently transfected with wild-type *Col11a2* F/G enhancer/reporter plasmid plus pcDNA3.1Lc-Maf (Lc-Maf) or the empty pcDNA3.1 vector (E.V.) as indicated. **(B)** The wild-type *Col11a2* F/G sequence is shown with the Sox9 binding regions in bold and the putative Lc-Maf binding regions in bold and underlined.

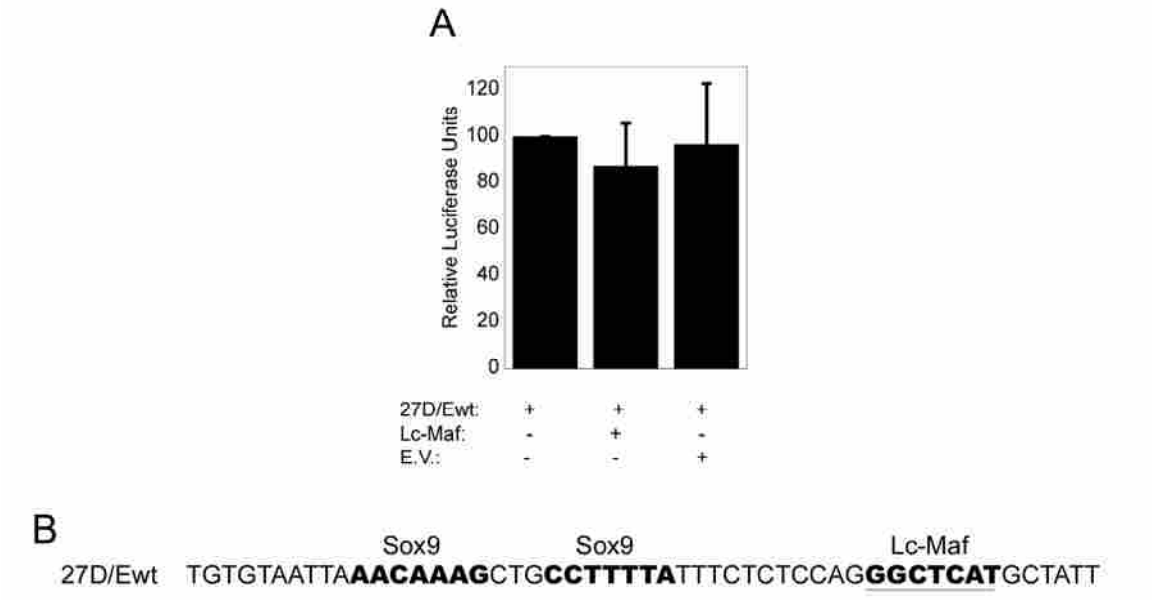

Figure 6. Lc-Maf does not modulate the activity of the *COL27A1* 27D/E enhancer element. (A) RCS cells were transiently transfected with wild-type *COL27A1* D/E enhancer/reporter plasmids plus pcDNA3.1-Lc-Maf (Lc-Maf) or the empty pcDNA3.1 vector (E.V.) as indicated. **(B)** The wild-type *COL27A1* 27D/E sequence is shown with the Sox9 binding regions in bold and the putative Lc-Maf binding region in bold and underlined.

reporter construct was active in RCS cells but inactive in fibroblasts, demonstrating the expected cell-type specificity of the chondrocytic enhancer's activity. The SOX9 expression plasmid activated the enhancer in fibroblasts as previously demonstrated (Jenkins et al., 2005). However, when pcDNA3.1-Lc-Maf was cotransfected with 4×(27D/E)p95Luc into RCS cells no regulatory action was detected, despite the existence of a sequence similar to the previously reported Lc-Maf binding sequence (Fig. 6A).

Lc-Maf interacts specifically to activate the *COL27A1* chondrocyte-specific 27F/G enhancer element

The *COL27A1* wild-type luciferase reporter construct 4×(27F/G)p95Luc was cotransfected with the Lc-Maf expression vector, pcDNA3.1-Lc-Maf, into both RCS and BALB/3T3 cells to determine whether Lc-Maf exerts any regulatory action on this enhancer element. The reporter construct was active in RCS cells but inactive in fibroblasts, demonstrating the expected cell-type specificity of the chondrocytic enhancer's activity. The SOX9 expression plasmid activated the enhancer element in fibroblasts as previously demonstrated (Jenkins et al., 2005).

Cotransfection of the *COL27A1* reporter plasmid 4×(27F/G)p95Luc with pcDNA3.1-Lc-Maf in RCS cells led to a 4.5-fold increase in reporter gene expression compared to the luciferase level from 4×(27F/G)p95Luc alone ($p= 0.0002$) (Fig. 7A). It was previously reported that cotransfection of Lc-Maf and SOX9, a known activator of the cartilage-specific collagen enhancer elements, led to a synergistic activation of the *Col2a1* 48-bp enhancer element (Huang et al., 2002). Such synergistic activation of the *COL27A1* 27F/G enhancer element was also evident in BALB/3T3 fibroblasts: forced

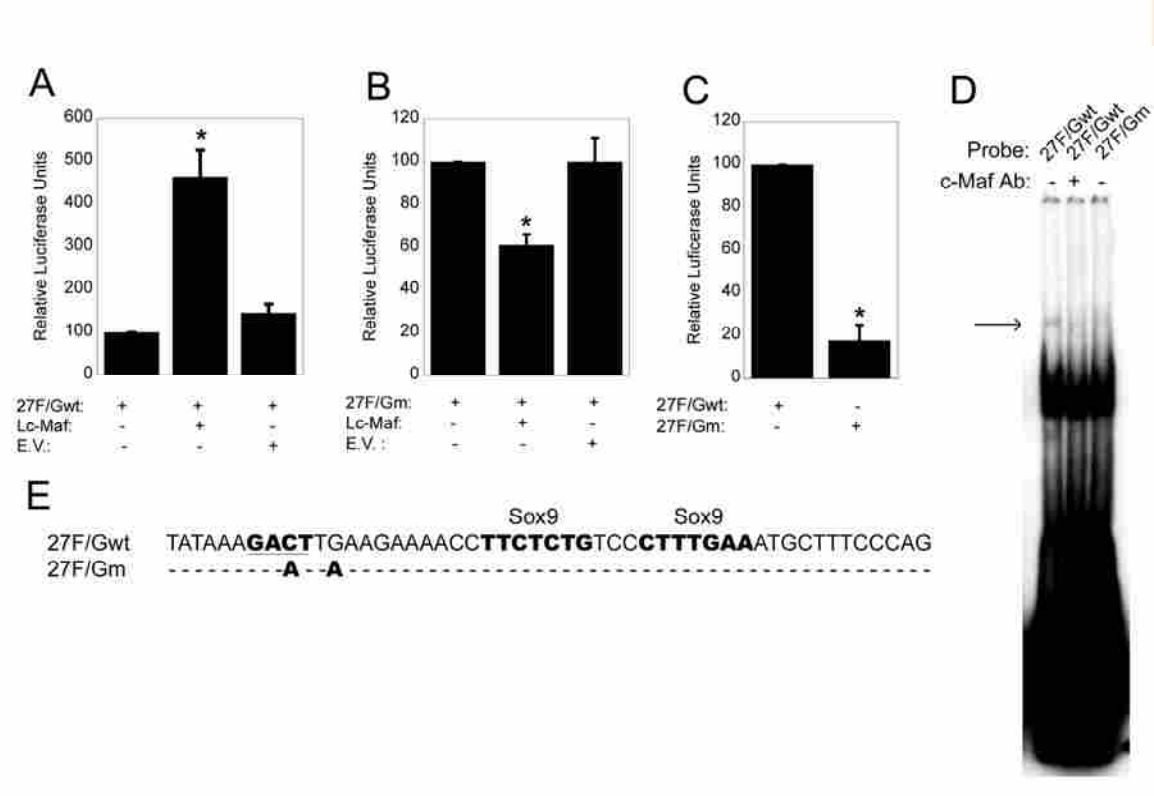

Figure 7. Lc-Maf activates the *COL27A1* 27F/G enhancer element by binding to a novel Maf binding sequence. (A-C) RCS cells were transiently transfected with wild-type or mutant enhancer/reporter plasmids plus pcDNA3.1-Lc-Maf (Lc-Maf) or the empty pcDNA3.1 vector (E.V.) as indicated. Enhancer activities that are significantly different from the corresponding wild-type enhancer activities are indicated with an asterisk ($p \leq 0.0004$). **(D)** Electrophoretic mobility shift assays were performed with the *COL27A1* 27F/Gwt and 27F/Gm enhancer elements as DNA probes with *in vitro* transcribed and translated Lc-Maf protein and c-Maf antibody as indicated. The arrow indicates the DNA-protein complex formed between the 27F/Gwt probe and *in vitro* made Lc-Maf. Addition of the c-Maf antibody in lane two interfered with formation of this complex. Lane 3 shows that the same 2-basepair mutation that prevented Lc-Maf from activating the 27F/Gwt enhancer in transient transfections also reduces Lc-Maf binding to the enhancer in EMSA. **(E)** The wild-type *COL27A1* 27F/G sequence is shown with the Sox9 binding regions in bold and the best-available Lc-Maf binding region in bold and underlined. The nucleotide substitutions for the mutant enhancer are indicated below the wild-type sequence.

expression of either SOX9 or Lc-Maf resulted in a 12.5-fold increase or a 6.5-fold increase in enhancer activity, respectively, while coexpression of both SOX9 and Lc-Maf resulted in a more-than-additive, 26-fold, activation of 27F/G enhancer activity (data not shown).

Neither an Lc-Maf consensus binding sequence nor any complete Maf-family consensus binding sequence could be identified within the *COL27A1* 27F/G enhancer element, but there appeared to be a half sequence (AAA**GACT**TGA) at the 5′ end of the probe. A 2-basepair mutation was introduced in this area (AAAGA**A**TT**A**A) (Fig. 7E). The activity of the mutant enhancer 27F/Gm, in which the 2-basepair mutation was introduced, was tested in transient transfections in both RCS and BALB/3T3 fibroblasts. When the *COL27A1* 27F/Gm mutant reporter construct 4×(27F/Gm)p95Luc was cotransfected with pcDNA3.1-Lc-Maf, the 27F/Gm mutant enhancer was no longer activated by Lc-Maf, suggesting that the mutation in 27F/Gm disrupts the interaction between the enhancer element and Lc-Maf (Fig. 7B). Comparison of the activities of the 27F/Gwt and the 27F/Gm enhancers showed that the mutant enhancer was only 20% as active as the wild-type, consistent with the loss of a positive regulatory element (Fig. 7C).

The 2-basepair mutation in the mutant enhancer 27F/Gm diminishes the ability of Lc-Maf to bind to the *COL27A1* 27F/G enhancer element.

Since the transfection experiments showed that Lc-Maf could only activate the wild-type *COL27A1* 27F/G enhancer and not the mutant enhancer 27F/Gm, EMSA experiments were performed with both the wild-type and mutant enhancers to verify that this activation was a result of Lc-Maf binding to the DNA. EMSAs showed that *in vitro*

transcribed and translated Lc-Maf bound to the wild-type 27F/G probe, producing a shifted complex indicated by the arrow (Fig. 7D). Formation of this complex was impaired by addition of the c-Maf antibody. The same 2-basepair mutation that eliminated the ability of the 27F/Gm enhancer to respond to Lc-Maf in the reporter assays also impaired Lc-Maf binding to the 27F/Gm enhancer element in EMSA, suggesting that Lc-Maf binds in this region despite the absence of a previously-identified consensus sequence (Fig. 7D).

Col11a2 and *Lc-Maf* exhibit expression patterns that are inversely related.

To observe the expression patterns of *Lc-Maf, Col11a2* and *Col27a1* during endochondral ossification of the developing limbs, we performed *in situ* hybridizations on the forelimbs of mouse embryos at half day intervals between embryonic days 15 and 17 (E15-E17), which represented a time interval directly before and after ossification began. A probe directed against *Col10a1,* a marker for prehypertrophic and hypertrophic chondrocytes, was included as a control. We found *Lc-Maf* to be weakly expressed. It is likely that the splice variant coding for Lc-Maf is of relatively low abundance. We did observe, however, that the most prominent *Lc-Maf* expression was in the prehypertrophic and hypertrophic zones, with only low levels of expression in the resting and proliferative zones (Fig. 8). The Lc-Maf transcript was consistently present at several time points in the prehypertrophic and hypertrophic zones both before and after mineralization at the diaphysis had begun. In contrast, *Col11a2* mRNA was most strongly expressed in the resting and proliferating zones as previously reported (Fig. 8). Together with our transfection data, this inverse pattern of expression supports the hypothesis that Lc-Maf

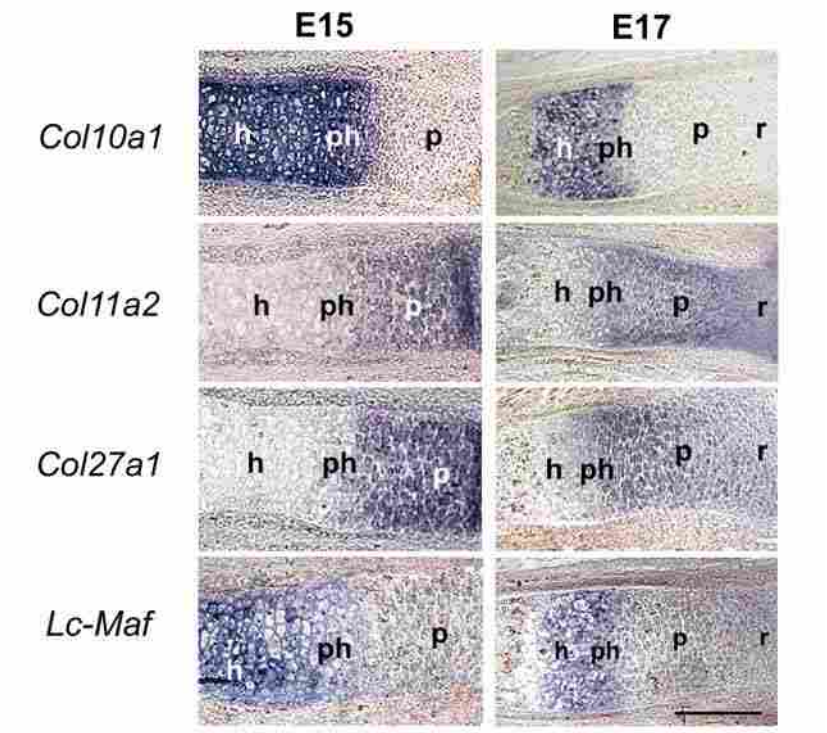

Figure 8. Expression patterns of *Col11a2, Col27a1*, and *Lc-Maf* during endochondral ossification in the murine forelimb. *In situ* hybridization on longitudinal sections of the radius of mouse embryos at E15, prior to the onset of mineralization, and E17, after the onset of mineralization. Panels are arranged with the diaphysis at the left. Expression of *Col10a1* was observed in hypertrophic and prehypertrophic chondrocytes as expected. *Lc-Maf* RNA was detected most strongly in the hypertrophic and prehypertrophic zones. *Col11a2* mRNA expression was detected in the resting and proliferative zones but declined through the prehypertrophic, until fully absent in the hypertrophic zone. *Col27a1* mRNA was detected in the resting, proliferating and prehypertrophic chondrocytes but not in the hypertrophic zone. Scale bar, 200 μm. h, hypertrophic; ph, prehypertrophic; p, proliferative; r, resting chondrocytes.

represses transcription of *Col11a2* as chondrocytes enter the prehypertrophic stage of their differentiation during limb development. Immunohistochemistry analyses performed by others have shown type XXVII collagen protein to be present only in hypertrophic chondrocytes (Hjorten, 2007). Our immunohistochemistry analyses gave similar results. In mouse forelimb growth plate sections from the same mice as those sections used for *in situ* hybridization, type XXVII collagen protein was detectable in both prehypertrophic and hypertrophic chondrocytes but not detected above background levels in the resting or proliferating zones of developing bone, similar to the expression pattern of Lc-Maf (Fig. 9).

To our surprise, *in situ* hybridization in mouse limb growth plates revealed that *Col27a1* mRNA was present in resting, proliferating and prehypertrophic chondrocytes but was not detectable in the hypertrophic zone (Fig. 8). To confirm this unexpected result, we generated a second probe directed against the third exon of *Col27a1* rather than the 3′UTR; again, *Col27a1* mRNA was detectable in the resting, proliferating and prehypertrophic chondrocytes but not in the hypertrophic zone (data not shown). These results have been further confirmed in human growth plate by R. Hjorten et al. using laser capture microdissection followed by quantitative RT-PCR: cells from the proliferative zone had 16 times more *COL27A1* transcript than cells in the hypertrophic zone (Hjorten, 2007).The expression patterns of Lc-Maf and *Col27a1* in mouse forelimb growth plate, therefore, overlap only in the prehypertrophic zone.

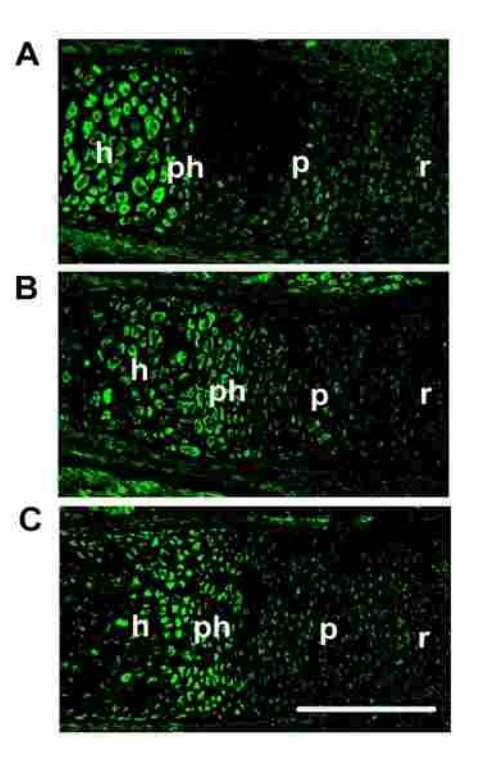

Figure 9. Murine type XXVII collagen protein is present in prehypertrophic and hypertrophic chondrocytes of bones undergoing endochondral ossification. (A) Longitudinal section of a digit at E16, prior to the onset of mineralization. **(B)** Longitudinal section of a radius at E16, showing the mineralized portion of the diaphysis at left. **(C)** Longitudinal section of an ulna at E17, showing the mineralized portion of the diaphysis at left. Immunohistochemistry was performed using a primary antibody directed against mature type XXVII collagen and a FITC-labeled secondary antibody. Scale bar, 200 μm. h, hypertrophic; ph, prehypertrophic; p, proliferative; r, resting chondrocytes.

DISCUSSION

The cell-type-specificity and timing of gene expression during chondrogenesis is largely managed by a delicate balance of positive and negative mediators of transcription. Proper expression of *Col11a2*, for example, is mediated in part by three cartilage-specific enhancer elements that Sox9 binds in order activate expression of the gene (Bridgewater et al., 1998; Bridgewater et al., 2003; Liu et al., 2000; Tsumaki et al., 1998). Interestingly, evidence suggests that one of the cartilage-specific elements has dual activities: it not only directs transcription of *Col11a2* in cartilage by binding positive regulators of transcription, but it also inactivates transcription of *Col11a2* in neural tissue by binding negative regulators of transcription (Tanaka et al., 2002; Tsumaki et al., 1998).

Individual transcription factors can also regulate in both a positive and a negative manner. Several bZIP family proteins, for example, have been shown to both activate and repress transcription at different promoters (Dhakshinamoorthy and Jaiswal, 2002; Li et al., 1999; Tone et al., 1999). c-Maf has been shown to activate the expression of genes such as L7, p53 and interleukin-4 and to repress expression of genes such as quinone oxidoreductase1 (NQO1) and glutathione S-transferase Ya subunit (GST Ya) (Dhakshinamoorthy and Jaiswal, 2002; Hale et al., 2000; Ho et al., 1996; Kurschner and Morgan, 1995). Here we demonstrate that the newest addition to the Maf family of transcription factors, Lc-Maf, is also capable of imposing both positive and negative regulation, as shown here with our work on several cartilage-specific collagen enhancers.

The primary goal of the research presented here was to determine whether Lc-Maf activated other developmentally important cartilage-specific enhancer elements in

addition to the *Col2a1* 48-bp enhancer that was previously demonstrated (Huang et al., 2002). Unexpectedly, we found that Lc-Maf may play a more complicated role in the transcriptional regulation of cartilage-specific collagen enhancers beyond simple activation. Despite having sequences similar to the Lc-Maf binding sequence reported for the *Col2a1* 48-bp enhancer, the *Col11a2* B/C and D/E enhancer elements were inhibited by Lc-Maf. The *Col11a2* F/G and *COL27A1* 27D/E enhancer elements also contained sequences similar to the reported Lc-Maf binding sequence and yet Lc-Maf had no regulatory effect on them. Most surprising was the *COL27A1* 27F/G enhancer element, which contains neither the consensus Lc-Maf binding sequence nor any known Maf recognition sequence, but was strongly activated by Lc-Maf. These unexpected results led us to examine the effect of Lc-Maf on the *Col2a1* 4x48 enhancer in our BALB/3T3 fibroblasts and RCS cells. While Lc-Maf has been shown to increase *Col2a1* expression in 10T1/2 cells and MC615 mouse immortalized chondrocytes (Huang et al., 2002), the results of our transient transfection experiments in BALB/3T3 and RCS cell lines showed that Lc-Maf either repressed the 4x48 enhancer or had no effect on the enhancer, respectively (data not shown). These results are consistent with the in vivo results from the *c-maf*-null mice that also lack Lc-Maf and had normal levels of *Col2a1* expression (MacLean et al., 2003). Taken together, these analyses demonstrate the variability between tissue culture lines and the importance of animal models

The ability of Lc-Maf to negatively regulate *Col11a2* cartilage-specific enhancer elements and positively regulate a *COL27A1* cartilage-specific enhancer element could have biological relevance in the context of a developing vertebrate by coordinating the expression of the cartilage-specific collagen genes during development of the long bones.

It has been reported that *Col11a2* mRNA and protein are primarily expressed by chondrocytes in the resting and proliferative zones of the cartilaginous bone templates undergoing endochondral ossification and not by chondrocytes in the hypertrophic zone (Swoboda et al., 1989; Tanaka et al., 2002). Our data support these findings. Mature type XXVII collagen, on the other hand, is strongly concentrated in regions preparing to go through mineralization such as the hypertrophic zones and the diaphisial perichondrium (Hjorten, 2007) (Fig. 9). These differential expression patterns not only suggest a functional difference between the two gene products but also the need for a strict transcriptional control of when and where these collagen genes are expressed. We hypothesized that Lc-Maf could play a role in activating the expression of *Col27a1* in the hypertrophic chondrocytes while serving the dual role of repressing the expression of *Col11a2* in those cells. Indeed, our *in situ* hybridization results show *Lc-Maf* mRNA in the prehypertrophic and hypertrophic zones of the developing limb where it likely plays a role in repressing the expression of *Col11a2*.

We expected to see *Col27a1* mRNA restricted to the prehypertrophic and hypertrophic zones since that is where the mature protein is localized and where Lc-Maf is present to activate its expression in the developing limb. Unexpectedly, the *Col27a1* probe directed against the 3′UTR revealed mRNA throughout the resting, proliferative and into the prehypertrophic zones but not in the hypertrophic zone. We constructed a second *Col27a1* probe directed against the translated third exon and again observed the same pattern of expression. Consistent with these results, laser capture microdissection followed by quantitative RT-PCR on human growth plate cells revealed 16-fold more *COL27A1* transcript in proliferative chondrocytes than in hypertrophic chondrocytes

(Hjorten, 2007). Previous work demonstrated that several splice variants of the *Col27a1* gene exist (all of the major variants contained the third exon, to which our second *in situ* hybridization probe anneals). Interestingly, the authors reported that one of the splice variants "was retained in the nucleus, and therefore would not be translated into protein" (Pace et al., 2003). It is possible that the *Col27a1* transcript we identified in the resting and proliferative zones is a splice variant of a non-translated variety, either nuclear or cytoplasmic. The data presented here, together with the prior work of others (Pace et al., 2003) is consistent with the following model: as cells enter the prehypertrophic stage and begin expressing the transcription factor Lc-Maf, it binds to the *Col27a1* 27F/G enhancer and triggers transcription of a short-lived, translatable *Col27a1* mRNA. The resulting mature type XXVII collagen protein remains present and detectable in cells as they progress from prehypertrophic to hypertrophic chondrocytes, even though the short-lived transcript is quickly degraded and is therefore not detectable by *in situ* hybridization in hypertrophic chondrocytes.

It is likely that a unique binding partner for Lc-Maf is expressed in prehypertrophic chondrocytes. The expression of this binding partner would allow Lc-Maf to recognize and activate the *Col27a1* 27F/G enhancer element, triggering expression of the translatable transcript. The fact that no previously recognized consensus binding sequence for Maf transcription factors could be identified within the 27F/G enhancer implies that this protein has not previously been identified as a Maf binding partner.

Proper expression of the chondrocyte-specific collagens during endochondral ossification is necessary for correct skeletal development (Farquharson and Jefferies,

2000; Huang et al., 2002; Okazaki and Sandell, 2004; Velleman, 2000). In 2003, MacLean et al. demonstrated that *c-maf*-null mice, which lack both c-Maf and Lc-Maf, have abnormal chondrocyte development. These mice demonstrated delayed hypertrophic chondrocyte differentiation and reduced fetal bone length (MacLean et al., 2003). These results complement and are consistent with the data presented here, which suggest that the transcription factor Lc-Maf coordinates *Col11a2* and *Col27a1* collagen gene expression during the developmental transition from proliferating to hypertrophic chondrocytes.

APPENDIX

M9 medium (1 Liter)

1× 11.33 g $Na_2HPO_4 \cdot 7H_2O$
3 g KH_2PO_4
1 g NH4Cl
0.5 g NaCl

Autoclave

M63 minimal plates

1L 5× 10 g $(NH_4)_2SO_4$
68 g KH_2PO_4
2.5 mg $FeSO_4 \cdot 7H_2O$
adjust to pH 7 with KOH

Autoclave

Other: 0.2 mg/mL d-biotin (sterile filtered) (1:5000)
0.2 mg/mL d-biotin (sterile filtered) (1:5000)
20% galactose (autoclaved) (1:100)
20% 2-deoxy-galactose (autoclaved) (1:100)
20% glycerol (autoclaved) (1:100)
10 mg/mL L-leucine (1%, heated, then cooled and sterile filtered)
25 mg/mL Chloramphenicol in EtOH (1:2000)
1 M MgSO4·7H2O (1:1000)

Autoclave 15 g agar in 800 mL H2O in a 2 liter flask; let cool a little. Add 200 mL autoclaved 5× M63 medium and 1 mL 1 M MgSO4·7H2O. Adjust volume to 1 L with H2O if necessary. When cooled to 50°C, add 10 mL carbon source (final conc. 0.2%), 5 mL biotin (1 mg), 4.5 mL leucine (45 mg), and 500 mL Chloramphenicol (final conc. 12.5 mg/ml). Pour the plates.

MacConkey indicator plates

Prepare MacConkey agar plus galactose according to manufacturer's instructions. After autoclaving and cooling to 50°C, add 500 mL Chloramphenicol (final conc. 12.5 mg/mL) to one L, and pour the plates.

Maintenance of ES cells and aggregation:

MEF Media:

10% FBS
10 mL FBS (do not refreeze)
1 mL 10mM MEM Non Essential amino acids (store at 4°C)

1 mL 10mM β-Mercaptoethanol (store at 4°C, good for 1 week)
1 mL 200mM L-Glutamine (store at -20°C)
1 mL 5mg/mL Pen/Strep (store at -20°C)
85 mL DMEM, Gibco, High Glucose

ES Media:
15% FBS
15 mL FBS (do not refreeze)
1 mL 10mM MEM Non Essential amino acids (store at 4°C)
1 mL 10mM β-Mercaptoethanol (store at 4°C, good for 1 week)
1 mL 200mM L-Glutamine (store at -20°C)
1 mL 5mg/mL Pen/Strep (store at -20°C)
100 μL LIF 10E6 (store at 4°C)
80.9 mL DMEM, Gibco, High Glucose

M2 media:
15% FBS
15 mL FBS (do not refreeze)
1 mL 10mM MEM Non Essential amino acids (store at 4°C)
1 mL 10mM β-Mercaptoethanol (store at 4°C, good for 1 week)
1 mL 200mM L-Glutamine (store at -20°C)
1 mL 5mg/mL Pen/Strep (store at -20°C)
90 mL HEPES-buffered DMEM, Gibco, High Glucose

Freezing media:
2X: 2 mL FBS
2 mL DMSO
6 mL MEF Media

Stock Solutions
FBS: thaw, heat inactivate 30 minutes at 55°C, aliquot (store at -20°C until use)
1000X solutions: 200 mg/mL active G418 in PBS, filtered (store at -20°C)
0.1 mM FIAU in PBS, filtered (store at -20°C)
10E7 units LIF (Gibco) resuspended in 10 mL DMEM (store at 4°C)
100X solutions 10 mM MEM Non Essential A.A., aliquot (store at 4C)
10mM β-Mercaptoethanol (3.5 μL into 5 mL PBS, filter, store at 4°C, good for 1 week)
200 mM L-Glutamine, aliquot (store -20°C)
5 mg/mL Pen/Strep, aliquot (store -20°C)

LITERATURE CITED

Adam, S.A. (2001). The nuclear pore complex. Genome Biol *2*, REVIEWS0007.

Amalric, F., Baldin, V., Bosc-Bierne, I., Bugler, B., Couderc, B., Guyader, M., Patry, V., Prats, H., Roman, A.M., and Bouche, G. (1991). Nuclear translocation of basic fibroblast growth factor. Ann N Y Acad Sci *638*, 127-138.

Anderson, E.D., Thomas, L., Hayflick, J.S., and Thomas, G. (1993). Inhibition of HIV-1 gp160-dependent membrane fusion by a furin-directed alpha 1-antitrypsin variant. J Biol Chem *268*, 24887-24891.

Andree, B., Hillemann, T., Kessler-Icekson, G., Schmitt-John, T., Jockusch, H., Arnold, H.H., and Brand, T. (2000). Isolation and characterization of the novel popeye gene family expressed in skeletal muscle and heart. Dev Biol *223*, 371-382.

Antoine, M., Reimers, K., Dickson, C., and Kiefer, P. (1997). Fibroblast growth factor 3, a protein with dual subcellular localization, is targeted to the nucleus and nucleolus by the concerted action of two nuclear localization signals and a nucleolar retention signal. J Biol Chem *272*, 29475-29481.

Arnold, M., Nath, A., Hauber, J., and Kehlenbach, R.H. (2006). Multiple importins function as nuclear transport receptors for the Rev protein of the human immunodeficiency virus type I. J Biol Chem.

Arnold, S.F., Tims, E., and McGrath, B.E. (1999). Identification of bone morphogenetic proteins and their receptors in human breast cancer cell lines: importance of BMP2. Cytokine *11*, 1031-1037.

Barrow, J.R., Thomas, K.R., Boussadia-Zahui, O., Moore, R., Kemler, R., Capecchi, M.R., and McMahon, A.P. (2003). Ectodermal Wnt3/beta-catenin signaling is required for the establishment and maintenance of the apical ectodermal ridge. Genes Dev *17*, 394-409.

Bridgewater, L.C., Lefebvre, V., and de Crombrugghe, B. (1998). Chondrocyte-specific enhancer elements in the Col11a2 gene resemble the Col2a1 tissue-specific enhancer. J Biol Chem *273*, 14998-15006.

Bridgewater, L.C., Walker, M.D., Miller, G.C., Ellison, T.A., Holsinger, L.D., Potter, J.L., Jackson, T.L., Chen, R.K., Winkel, V.L., Zhang, Z., *et al.* (2003). Adjacent DNA sequences modulate Sox9 transcriptional activation at paired Sox sites in three chondrocyte-specific enhancer elements. Nucleic Acids Res *31*, 1541-1553.

Bugler, B., Amalric, F., and Prats, H. (1991). Alternative initiation of translation determines cytoplasmic or nuclear localization of basic fibroblast growth factor. Mol Cell Biol *11*, 573-577.

Bush, G., diSibio, G., Miyamoto, A., Denault, J.B., Leduc, R., and Weinmaster, G. (2001). Ligand-induced signaling in the absence of furin processing of Notch1. Dev Biol *229*, 494-502.

Chen, D., Zhao, M., Harris, S.E., and Mi, Z. (2004). Signal transduction and biological functions of bone morphogenetic proteins. Front Biosci *9*, 349-358.

Chesi, M., Bergsagel, P.L., Shonukan, O.O., Martelli, M.L., Brents, L.A., Chen, T., Schrock, E., Ried, T., and Kuehl, W.M. (1998). Frequent dysregulation of the c-maf proto-oncogene at 16q23 by translocation to an Ig locus in multiple myeloma. Blood *91*, 4457-4463.

Claudiani, P., Riano, E., Errico, A., Andolfi, G., and Rugarli, E.I. (2005). Spastin subcellular localization is regulated through usage of different translation start sites and active export from the nucleus. Exp Cell Res *309*, 358-369.

Constam, D.B., and Robertson, E.J. (1999). Regulation of bone morphogenetic protein activity by pro domains and proprotein convertases. J Cell Biol *144*, 139-149.

Copeland, N.G., Jenkins, N.A., and Court, D.L. (2001). Recombineering: a powerful new tool for mouse functional genomics. Nat Rev Genet *2*, 769-779.

Corbett, A.H., and Silver, P.A. (1997). Nucleocytoplasmic transport of macromolecules. Microbiol Mol Biol Rev *61*, 193-211.

Cubitt, A.B., Heim, R., Adams, S.R., Boyd, A.E., Gross, L.A., and Tsien, R.Y. (1995). Understanding, improving and using green fluorescent proteins. Trends Biochem Sci *20*, 448-455.

Cui, Y., Jean, F., Thomas, G., and Christian, J.L. (1998). BMP-4 is proteolytically activated by furin and/or PC6 during vertebrate embryonic development. Embo J *17*, 4735-4743.

Cyert, M.S. (2001). Regulation of nuclear localization during signaling. J Biol Chem *276*, 20805-20808.

de Crombrugghe, B., Lefebvre, V., Behringer, R.R., Bi, W., Murakami, S., and Huang, W. (2000). Transcriptional mechanisms of chondrocyte differentiation. Matrix Biol *19*, 389-394.

Dhakshinamoorthy, S., and Jaiswal, A.K. (2002). c-Maf negatively regulates ARE-mediated detoxifying enzyme genes expression and anti-oxidant induction. Oncogene *21*, 5301-5312.

Dlakic, M., Grinberg, A.V., Leonard, D.A., and Kerppola, T.K. (2001). DNA sequence-dependent folding determines the divergence in binding specificities between Maf and other bZIP proteins. Embo J *20*, 828-840.

Drossopoulou, G., Lewis, K.E., Sanz-Ezquerro, J.J., Nikbakht, N., McMahon, A.P., Hofmann, C., and Tickle, C. (2000). A model for anteroposterior patterning of the vertebrate limb based on sequential long- and short-range Shh signalling and Bmp signalling. Development *127*, 1337-1348.

Dudley, A.T., and Robertson, E.J. (1997). Overlapping expression domains of bone morphogenetic protein family members potentially account for limited tissue defects in BMP7 deficient embryos. Dev Dyn *208*, 349-362.

Farquharson, C., and Jefferies, D. (2000). Chondrocytes and longitudinal bone growth: the development of tibial dyschondroplasia. Poult Sci *79*, 994-1004.

Forwood, J.K., Lam, M.H., and Jans, D.A. (2001). Nuclear import of Creb and AP-1 transcription factors requires importin-beta 1 and Ran but is independent of importin-alpha. Biochemistry *40*, 5208-5217.

Fried, H., and Kutay, U. (2003). Nucleocytoplasmic transport: taking an inventory. Cell Mol Life Sci *60*, 1659-1688.

Fritz, D.T., Jiang, S., Xu, J., and Rogers, M.B. (2006). A polymorphism in a conserved posttranscriptional regulatory motif alters bone morphogenetic protein 2 (BMP2) RNA:protein interactions. Mol Endocrinol *20*, 1574-1586.

Fritz, D.T., Liu, D., Xu, J., Jiang, S., and Rogers, M.B. (2004). Conservation of Bmp2 post-transcriptional regulatory mechanisms. J Biol Chem *279*, 48950-48958.

Furuta, Y., Piston, D.W., and Hogan, B.L. (1997). Bone morphogenetic proteins (BMPs) as regulators of dorsal forebrain development. Development *124*, 2203-2212.

Gallea, S., Lallemand, F., Atfi, A., Rawadi, G., Ramez, V., Spinella-Jaegle, S., Kawai, S., Faucheu, C., Huet, L., Baron, R., *et al.* (2001). Activation of mitogen-activated protein kinase cascades is involved in regulation of bone morphogenetic protein-2-induced osteoblast differentiation in pluripotent C2C12 cells. Bone *28*, 491-498.

Granjeiro, J.M., Oliveira, R.C., Bustos-Valenzuela, J.C., Sogayar, M.C., and Taga, R. (2005). Bone morphogenetic proteins: from structure to clinical use. Braz J Med Biol Res *38*, 1463-1473.

Guicheux, J., Lemonnier, J., Ghayor, C., Suzuki, A., Palmer, G., and Caverzasio, J. (2003). Activation of p38 mitogen-activated protein kinase and c-Jun-NH2-terminal kinase by BMP-2 and their implication in the stimulation of osteoblastic cell differentiation. J Bone Miner Res *18*, 2060-2068.

Hale, T.K., Myers, C., Maitra, R., Kolzau, T., Nishizawa, M., and Braithwaite, A.W. (2000). Maf transcriptionally activates the mouse p53 promoter and causes a p53-dependent cell death. J Biol Chem *275*, 17991-17999.

Hillger, F., Herr, G., Rudolph, R., and Schwarz, E. (2005). Biophysical comparison of BMP-2, ProBMP-2, and the free pro-peptide reveals stabilization of the pro-peptide by the mature growth factor. J Biol Chem *280*, 14974-14980.

Hjorten, R., Hansen, Uwe, Underwood, Robert A., Telfer, Helena E., Fernandes, Russell J., Krakow, Deborah, Selbald, Eiman, Wachsmann-Hogiu, Sebastian, Bruckner, Peter, Jacquet, Robin, Landis, William J., Byers, Peter H., Pace, James M. (2007). Type XXVII collagen at the transition of cartilage to bone during skeletogenesis. Bone.

Ho, I.C., Hodge, M.R., Rooney, J.W., and Glimcher, L.H. (1996). The proto-oncogene c-maf is responsible for tissue-specific expression of interleukin-4. Cell *85*, 973-983.

Ho, I.C., Lo, D., and Glimcher, L.H. (1998). c-maf promotes T helper cell type 2 (Th2) and attenuates Th1 differentiation by both interleukin 4-dependent and -independent mechanisms. J Exp Med *188*, 1859-1866.

Hogan, B.L. (1996). Bone morphogenetic proteins in development. Curr Opin Genet Dev *6*, 432-438.

Horvath, L.G., Henshall, S.M., Kench, J.G., Turner, J.J., Golovsky, D., Brenner, P.C., O'Neill, G.F., Kooner, R., Stricker, P.D., Grygiel, J.J., *et al.* (2004). Loss of BMP2, Smad8, and Smad4 expression in prostate cancer progression. Prostate *59*, 234-242.

Huang, W., Lu, N., Eberspaecher, H., and De Crombrugghe, B. (2002). A new long form of c-Maf cooperates with Sox9 to activate the type II collagen gene. J Biol Chem *277*, 50668-50675.

Jean, F., Stella, K., Thomas, L., Liu, G., Xiang, Y., Reason, A.J., and Thomas, G. (1998). alpha1-Antitrypsin Portland, a bioengineered serpin highly selective for furin: application as an antipathogenic agent. Proc Natl Acad Sci U S A *95*, 7293-7298.

Jenkins, E., Moss, J.B., Pace, J.M., and Bridgewater, L.C. (2005). The new collagen gene COL27A1 contains SOX9-responsive enhancer elements. Matrix Biol *24*, 177-184.

Kalderon, D., Richardson, W.D., Markham, A.F., and Smith, A.E. (1984a). Sequence requirements for nuclear location of simian virus 40 large-T antigen. Nature *311*, 33-38.

Kalderon, D., Roberts, B.L., Richardson, W.D., and Smith, A.E. (1984b). A short amino acid sequence able to specify nuclear location. Cell *39*, 499-509.

Kanzler, B., Foreman, R.K., Labosky, P.A., and Mallo, M. (2000). BMP signaling is essential for development of skeletogenic and neurogenic cranial neural crest. Development *127*, 1095-1104.

Kataoka, K., Nishizawa, M., and Kawai, S. (1993). Structure-function analysis of the maf oncogene product, a member of the b-Zip protein family. J Virol *67*, 2133-2141.

Kataoka, K., Noda, M., and Nishizawa, M. (1994). Maf nuclear oncoprotein recognizes sequences related to an AP-1 site and forms heterodimers with both Fos and Jun. Mol Cell Biol *14*, 700-712.

Kawai, S., Goto, N., Kataoka, K., Saegusa, T., Shinno-Kohno, H., and Nishizawa, M. (1992). Isolation of the avian transforming retrovirus, AS42, carrying the v-maf oncogene and initial characterization of its gene product. Virology *188*, 778-784.

Kawamura, C., Kizaki, M., Yamato, K., Uchida, H., Fukuchi, Y., Hattori, Y., Koseki, T., Nishihara, T., and Ikeda, Y. (2000). Bone morphogenetic protein-2 induces apoptosis in human myeloma cells with modulation of STAT3. Blood *96*, 2005-2011.

Kerppola, T.K., and Curran, T. (1994). A conserved region adjacent to the basic domain is required for recognition of an extended DNA binding site by Maf/Nrl family proteins. Oncogene *9*, 3149-3158.

Kiefer, P., Acland, P., Pappin, D., Peters, G., and Dickson, C. (1994). Competition between nuclear localization and secretory signals determines the subcellular fate of a single CUG-initiated form of FGF3. Embo J *13*, 4126-4136.

Kim, D.G., Kang, H.M., Jang, S.K., and Shin, H.S. (1992). Construction of a bifunctional mRNA in the mouse by using the internal ribosomal entry site of the encephalomyocarditis virus. Mol Cell Biol *12*, 3636-3643.

Kim, H.J., Rice, D.P., Kettunen, P.J., and Thesleff, I. (1998). FGF-, BMP- and Shh-mediated signalling pathways in the regulation of cranial suture morphogenesis and calvarial bone development. Development *125*, 1241-1251.

Kim, J.I., Li, T., Ho, I.C., Grusby, M.J., and Glimcher, L.H. (1999). Requirement for the c-Maf transcription factor in crystallin gene regulation and lens development. Proc Natl Acad Sci U S A *96*, 3781-3785.

Kochetov, A.V., Sarai, A., Rogozin, I.B., Shumny, V.K., and Kolchanov, N.A. (2005). The role of alternative translation start sites in the generation of human protein diversity. Mol Genet Genomics *273*, 491-496.

Kurschner, C., and Morgan, J.I. (1995). The maf proto-oncogene stimulates transcription from multiple sites in a promoter that directs Purkinje neuron-specific gene expression. Mol Cell Biol *15*, 246-254.

Lam, M.H., Thomas, R.J., Loveland, K.L., Schilders, S., Gu, M., Martin, T.J., Gillespie, M.T., and Jans, D.A. (2002). Nuclear transport of parathyroid hormone (PTH)-related protein is dependent on microtubules. Mol Endocrinol *16*, 390-401.

Langenfeld, E.M., Bojnowski, J., Perone, J., and Langenfeld, J. (2005). Expression of bone morphogenetic proteins in human lung carcinomas. Ann Thorac Surg *80*, 1028-1032.

Langenfeld, E.M., Calvano, S.E., Abou-Nukta, F., Lowry, S.F., Amenta, P., and Langenfeld, J. (2003). The mature bone morphogenetic protein-2 is aberrantly expressed in non-small cell lung carcinomas and stimulates tumor growth of A549 cells. Carcinogenesis *24*, 1445-1454.

Langenfeld, E.M., and Langenfeld, J. (2004). Bone morphogenetic protein-2 stimulates angiogenesis in developing tumors. Mol Cancer Res *2*, 141-149.

Lee, R., Kermani, P., Teng, K.K., and Hempstead, B.L. (2001). Regulation of cell survival by secreted proneurotrophins. Science *294*, 1945-1948.

Lefebvre, V., Zhou, G., Mukhopadhyay, K., Smith, C.N., Zhang, Z., Eberspaecher, H., Zhou, X., Sinha, S., Maity, S.N., and de Crombrugghe, B. (1996). An 18-base-pair sequence in the mouse proalpha1(II) collagen gene is sufficient for expression in cartilage and binds nuclear proteins that are selectively expressed in chondrocytes. Mol Cell Biol *16*, 4512-4523.

Lemonnier, J., Ghayor, C., Guicheux, J., and Caverzasio, J. (2004). Protein kinase C-independent activation of protein kinase D is involved in BMP-2-induced activation of stress mitogen-activated protein kinases JNK and p38 and osteoblastic cell differentiation. J Biol Chem *279*, 259-264.

Li, B., Tournier, C., Davis, R.J., and Flavell, R.A. (1999). Regulation of IL-4 expression by the transcription factor JunB during T helper cell differentiation. Embo J *18*, 420-432.

Linask, K.K., Han, M., Cai, D.H., Brauer, P.R., and Maisastry, S.M. (2005). Cardiac morphogenesis: matrix metalloproteinase coordination of cellular mechanisms underlying heart tube formation and directionality of looping. Dev Dyn *233*, 739-753.

Liu, P., Jenkins, N.A., and Copeland, N.G. (2003). A highly efficient recombineering-based method for generating conditional knockout mutations. Genome Res *13*, 476-484.

Liu, Y., Li, H., Tanaka, K., Tsumaki, N., and Yamada, Y. (2000). Identification of an enhancer sequence within the first intron required for cartilage-specific transcription of the alpha2(XI) collagen gene. J Biol Chem *275*, 12712-12718.

Luyten, F.P., Cunningham, N.S., Ma, S., Muthukumaran, N., Hammonds, R.G., Nevins, W.B., Woods, W.I., and Reddi, A.H. (1989). Purification and partial amino acid sequence of osteogenin, a protein initiating bone differentiation. J Biol Chem *264*, 13377-13380.

Lyons, K.M., Hogan, B.L., and Robertson, E.J. (1995). Colocalization of BMP 7 and BMP 2 RNAs suggests that these factors cooperatively mediate tissue interactions during murine development. Mech Dev *50*, 71-83.

Lyons, K.M., Pelton, R.W., and Hogan, B.L. (1990). Organogenesis and pattern formation in the mouse: RNA distribution patterns suggest a role for bone morphogenetic protein-2A (BMP-2A). Development *109*, 833-844.

Macara, I.G. (2001). Transport into and out of the nucleus. Microbiol Mol Biol Rev *65*, 570-594, table of contents.

MacLean, H.E., Kim, J.I., Glimcher, M.J., Wang, J., Kronenberg, H.M., and Glimcher, L.H. (2003). Absence of transcription factor c-maf causes abnormal terminal differentiation of hypertrophic chondrocytes during endochondral bone development. Dev Biol *262*, 51-63.

Milan, D.J., Giokas, A.C., Serluca, F.C., Peterson, R.T., and MacRae, C.A. (2006). Notch1b and neuregulin are required for specification of central cardiac conduction tissue. Development *133*, 1125-1132.

Mishina, Y. (2003). Function of bone morphogenetic protein signaling during mouse development. Front Biosci *8*, d855-869.

Moore, J.D., Yang, J., Truant, R., and Kornbluth, S. (1999). Nuclear import of Cdk/cyclin complexes: identification of distinct mechanisms for import of Cdk2/cyclin E and Cdc2/cyclin B1. J Cell Biol *144*, 213-224.

Motohashi, H., Shavit, J.A., Igarashi, K., Yamamoto, M., and Engel, J.D. (1997). The world according to Maf. Nucleic Acids Res *25*, 2953-2959.

Moustakas, A., and Heldin, C.H. (2002). From mono- to oligo-Smads: the heart of the matter in TGF-beta signal transduction. Genes Dev *16*, 1867-1871.

Mumm, J.S., Schroeter, E.H., Saxena, M.T., Griesemer, A., Tian, X., Pan, D.J., Ray, W.J., and Kopan, R. (2000). A ligand-induced extracellular cleavage regulates gamma-secretase-like proteolytic activation of Notch1. Mol Cell *5*, 197-206.

Murtaugh, L.C., Chyung, J.H., and Lassar, A.B. (1999). Sonic hedgehog promotes somitic chondrogenesis by altering the cellular response to BMP signaling. Genes Dev *13*, 225-237.

Nguyen, M., He, B., and Karaplis, A. (2001). Nuclear forms of parathyroid hormone-related peptide are translated from non-AUG start sites downstream from the initiator methionine. Endocrinology *142*, 694-703.

Ohkawara, B., Iemura, S., ten Dijke, P., and Ueno, N. (2002). Action range of BMP is defined by its N-terminal basic amino acid core. Curr Biol *12*, 205-209.

Okazaki, K., and Sandell, L.J. (2004). Extracellular matrix gene regulation. Clin Orthop Relat Res, S123-128.

Pace, J.M., Corrado, M., Missero, C., and Byers, P.H. (2003). Identification, characterization and expression analysis of a new fibrillar collagen gene, COL27A1. Matrix Biol *22*, 3-14.

Pemberton, L.F., and Paschal, B.M. (2005). Mechanisms of receptor-mediated nuclear import and nuclear export. Traffic *6*, 187-198.

Puglisi, R., Montanari, M., Chiarella, P., Stefanini, M., and Boitani, C. (2004). Regulatory role of BMP2 and BMP7 in spermatogonia and Sertoli cell proliferation in the immature mouse. Eur J Endocrinol *151*, 511-520.

Raftery, L.A., and Sutherland, D.J. (1999). TGF-beta family signal transduction in Drosophila development: from Mad to Smads. Dev Biol *210*, 251-268.

Raida, M., Clement, J.H., Leek, R.D., Ameri, K., Bicknell, R., Niederwieser, D., and Harris, A.L. (2005). Bone morphogenetic protein 2 (BMP-2) and induction of tumor angiogenesis. J Cancer Res Clin Oncol, 1-10.

Reese, D.E., and Bader, D.M. (1999). Cloning and expression of hbves, a novel and highly conserved mRNA expressed in the developing and adult heart and skeletal muscle in the human. Mamm Genome *10*, 913-915.

Reese, D.E., Zavaljevski, M., Streiff, N.L., and Bader, D. (1999). bves: A novel gene expressed during coronary blood vessel development. Dev Biol *209*, 159-171.

Reza, H.M., and Yasuda, K. (2004). Roles of Maf family proteins in lens development. Dev Dyn *229*, 440-448.

Sachinidis, A., Kolossov, E., Fleischmann, B.K., and Hescheler, J. (2002). Generation of cardiomyocytes from embryonic stem cells experimental studies. Herz *27*, 589-597.

Schlange, T., Arnold, H.H., and Brand, T. (2002). BMP2 is a positive regulator of Nodal signaling during left-right axis formation in the chicken embryo. Development *129*, 3421-3429.

St-Jacques, B., Dassule, H.R., Karavanova, I., Botchkarev, V.A., Li, J., Danielian, P.S., McMahon, J.A., Lewis, P.M., Paus, R., and McMahon, A.P. (1998). Sonic hedgehog signaling is essential for hair development. Curr Biol *8*, 1058-1068.

Stainier, D.Y. (2001). Zebrafish genetics and vertebrate heart formation. Nat Rev Genet *2*, 39-48.

Struewing, I.T., Toborek, A., and Mao, C.D. (2006). Mitochondrial and nuclear forms of Wnt13 are generated via alternative promoters, alternative RNA splicing, and alternative translation start sites. J Biol Chem *281*, 7282-7293.

Swoboda, B., Holmdahl, R., Stoss, H., and von der Mark, K. (1989). Cellular heterogeneity in cultured human chondrocytes identified by antibodies specific for alpha 2(XI) collagen chains. J Cell Biol *109*, 1363-1369.

Tanaka, K., Tsumaki, N., Kozak, C.A., Matsumoto, Y., Nakatani, F., Iwamoto, Y., and Yamada, Y. (2002). A Kruppel-associated box-zinc finger protein, NT2, represses cell-type-specific promoter activity of the alpha 2(XI) collagen gene. Mol Cell Biol *22*, 4256-4267.

Tchetina, E., Mwale, F., and Poole, A.R. (2003). Distinct phases of coordinated early and late gene expression in growth plate chondrocytes in relationship to cell proliferation, matrix assembly, remodeling, and cell differentiation. J Bone Miner Res *18*, 844-851.

Thomas, G. (2002). Furin at the cutting edge: from protein traffic to embryogenesis and disease. Nat Rev Mol Cell Biol *3*, 753-766.

Tomari, K., Kumagai, T., Shimizu, T., and Takeda, K. (2005). Bone morphogenetic protein-2 induces hypophosphorylation of Rb protein and repression of E2F in androgen-treated LNCaP human prostate cancer cells. Int J Mol Med *15*, 253-258.

Tone, M., Diamond, L.E., Walsh, L.A., Tone, Y., Thompson, S.A., Shanahan, E.M., Logan, J.S., and Waldmann, H. (1999). High level transcription of the complement regulatory protein CD59 requires an enhancer located in intron 1. J Biol Chem *274*, 710-716.

Tsumaki, N., Kimura, T., Tanaka, K., Kimura, J.H., Ochi, T., and Yamada, Y. (1998). Modular arrangement of cartilage- and neural tissue-specific cis-elements in the mouse alpha2(XI) collagen promoter. J Biol Chem *273*, 22861-22864.

Urist, M.R. (1965). Bone: formation by autoinduction. Science *150*, 893-899.

Usami, N., Yoshioka, H., Mori, S., Imaizumi, M., Nagasaka, T., and Ueda, Y. (2005). Primary lung adenocarcinoma with heterotopic bone formation. Jpn J Thorac Cardiovasc Surg *53*, 102-105.

Velleman, S.G. (2000). The role of the extracellular matrix in skeletal development. Poult Sci *79*, 985-989.

Wada, A.M., Reese, D.E., and Bader, D.M. (2001). Bves: prototype of a new class of cell adhesion molecules expressed during coronary artery development. Development *128*, 2085-2093.

Wang, E.A., Rosen, V., D'Alessandro, J.S., Bauduy, M., Cordes, P., Harada, T., Israel, D.I., Hewick, R.M., Kerns, K.M., LaPan, P., *et al.* (1990). Recombinant human bone morphogenetic protein induces bone formation. Proc Natl Acad Sci U S A *87*, 2220-2224.

Warming, S., Costantino, N., Court, D.L., Jenkins, N.A., and Copeland, N.G. (2005). Simple and highly efficient BAC recombineering using galK selection. Nucleic Acids Res *33*, e36.

Wen, X.Z., Miyake, S., Akiyama, Y., and Yuasa, Y. (2004). BMP-2 modulates the proliferation and differentiation of normal and cancerous gastric cells. Biochem Biophys Res Commun *316*, 100-106.

Wozney, J.M. (1989). Bone morphogenetic proteins. Prog Growth Factor Res *1*, 267-280.

Wozney, J.M. (1992). The bone morphogenetic protein family and osteogenesis. Molecular reproduction and development *32*, 160-167.

Wozney, J.M., Rosen, V., Celeste, A.J., Mitsock, L.M., Whitters, M.J., Kriz, R.W., Hewick, R.M., and Wang, E.A. (1988). Novel regulators of bone formation: molecular clones and activities. Science *242*, 1528-1534.

Wu, H., Lee, S.H., Gao, J., Liu, X., and Iruela-Arispe, M.L. (1999). Inactivation of erythropoietin leads to defects in cardiac morphogenesis. Development *126*, 3597-3605.

Yamasaki, H., Sekimoto, T., Ohkubo, T., Douchi, T., Nagata, Y., Ozawa, M., and Yoneda, Y. (2005). Zinc finger domain of Snail functions as a nuclear localization signal for importin beta-mediated nuclear import pathway. Genes Cells *10*, 455-464.

Zhang, H., and Bradley, A. (1996). Mice deficient for BMP2 are nonviable and have defects in amnion/chorion and cardiac development. Development *122*, 2977-2986.

Zhang, P., Jimenez, S.A., and Stokes, D.G. (2003). Regulation of human COL9A1 gene expression. Activation of the proximal promoter region by SOX9. J Biol Chem *278*, 117-123.